WATER BENEFIT ANALYSIS FOR BAHR EL-GABEL

DEVELOPMENT PROJECTS

BY

M. Halim Salem, Hassan T. Dorrah, and M. Yousef Seood

Cairo, October 1981

جامعة القاهرة - معهد ماساتشوستس للتكنولوجيا
برنامج التخطيط التكنولوجي
CAIRO UNIVERSITY - MASSACHUSETTS INSTITUTE OF TECHNOLOGY
TECHNOLOGICAL PLANNING PROGRAM

E6

PREFACE

Because Egypt's water resources are limited, the national development program has emphasized the discovery and development of new water resources. This can be attained by reducing the tremendous water losses experienced by the Nile system. A first step to achieve this goal, is to model the hydrologic behaviour of the potential areas and to study the effect of possible drainage, channelization and agricultural projects upon the contribution from these regions to the flow of the Nile.

Among the water saving proposed projects over the Nile are those to be constructed in Bahr El-Gabel region in the White Nile, named by the Jonglei project. This project will be implemented in two phases. The first comprises the construction of a canal to take part of the discharge of Bahr El-Gabel and Bahr El-Zaraf with a capacity of 20 million m^3/day with a head and tail regulators. As for the second phase of the Jonglei project, it includes the enlargement and remodeling of the first phase canal to carry 43 million m^3/day, together with the regulation of the Equatorial lakes.

This report complements previous work of the project in investigating the water benefit of the Upper Nile developments. It concentrates on the Bahr El-Gabel region and studies the impact of different scenarios of the Jonglei project upon the total yield of the area. A full hydrological analysis of Bahr El-Gabel region is also presented.

ACKNOWLEDGEMENTS

The authors would like to express their appreciation to Professor Rafael Bras and Professor Peter S. Eagleson, of the Ralph M. Parsons Laboratory of Water Resources and Hydrodynamics of the M.I.T., for commenting on the original manuscript. Special thanks are extended to Professor M.F. Sakr of Cairo University, Dr. Hassan Ibrahim, Director of the Water Resources Development Institute, Ministry of Irrigation, and to Eng. A. Afifi of the Nile Control Department, Cairo, for all the help they provided.

This study was completely sponsored by the Cairo University/ M.I.T. Technological Planning Program which is funded by a contract between the Agency for International Development, United States Department of State and the M.I.T. Technology Adaptation Program. The views and opinions expressed in this report, however, are those of the authors and do not necessarily reflect those of the sponsors.

Many thanks are extended to the staff members of the Cairo University Program Office for their unlimited services and typing the report.

LIST OF CONTENTS

Page

CHAPTER I

INTRODUCTION

CHAPTER I

INTRODUCTION

One of the important reaches of the River Nile is Bahr El-Gabel. It functions as a critical link between the water resources projects of the Lake Plateau, upstream, and the different development projects downstream, see Fig. (1.1).

This reach is considered as one of the complicated reaches along the River Nile. It conveys the yield from the Lake Plateau to the White Nile through the Sudd Region. The water courses in this region are not well defined, but are formed generally of many immature side channels surrounded with wide swampy areas. The existence of such swamps and channel systems in a flat basin increases the chances for water losses through spilling, evaporation and evapotranspiration, ref. (5). In order to save some of this water losses, a new canal is designed to carry some of Bahr El-Gabel water, starting from Bor and ending near the mouth of Sobat River. This canal is known as the Jonglei canal, see Fig. (1.2).

In this work, both statistical and hydrological techniques will be applied in order to attain a full understanding of the potentialities of the reach. Simple hydrological analysis for the guage levels and the corresponding discharges will be invoked to determine the capabilities of the different cross-sections to convey the flow. From the same analysis, the spilling levels at the different sections are obtained. Accordingly, the possibility of strengthening or elevating the river banks in some parts of this

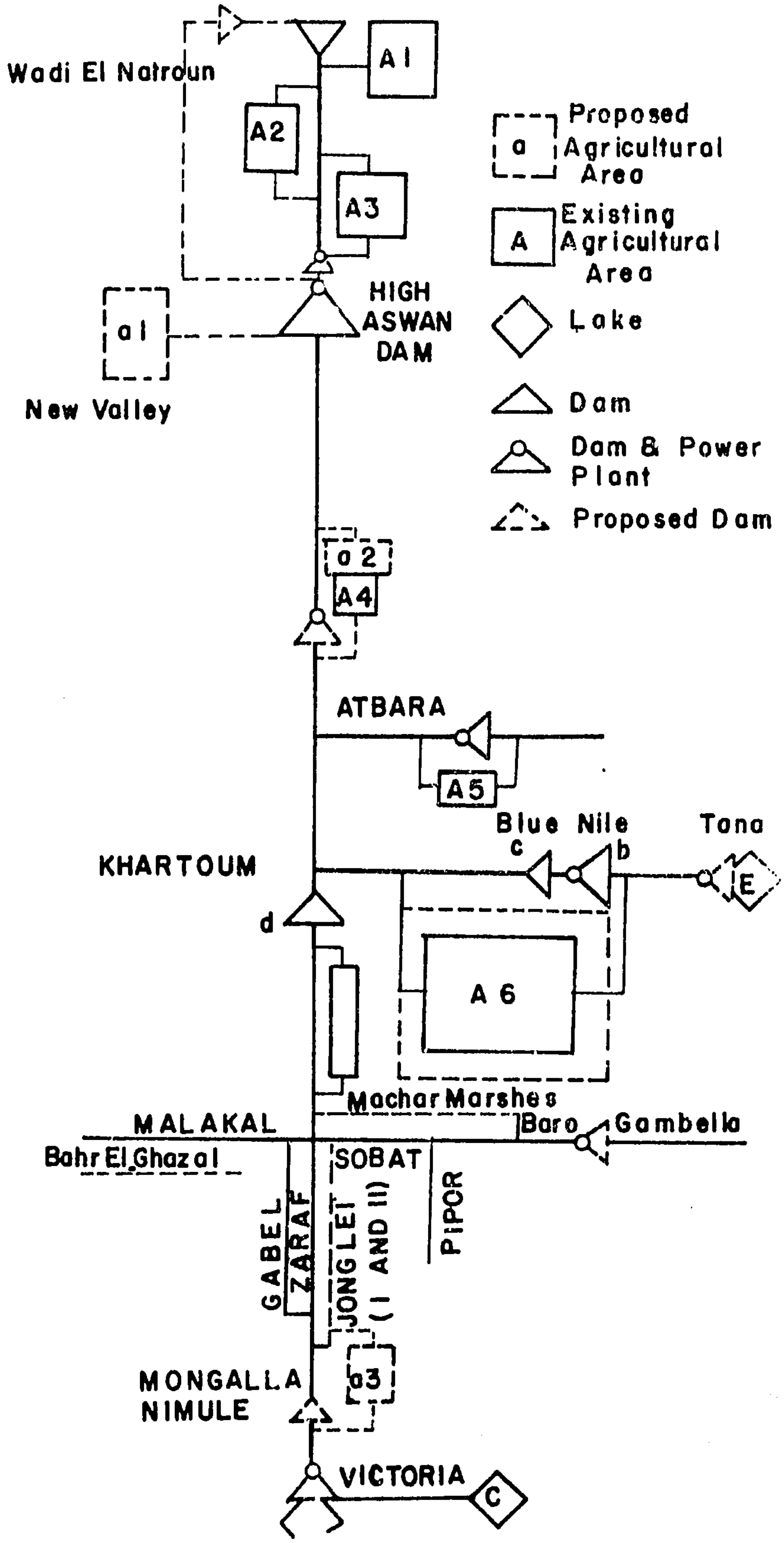

Fig.(1.1) SCHEMATIC REPRESENTATION OF THE NIL BASIN INDICATING FUTURE DEVELOPMENT PROJECTS.

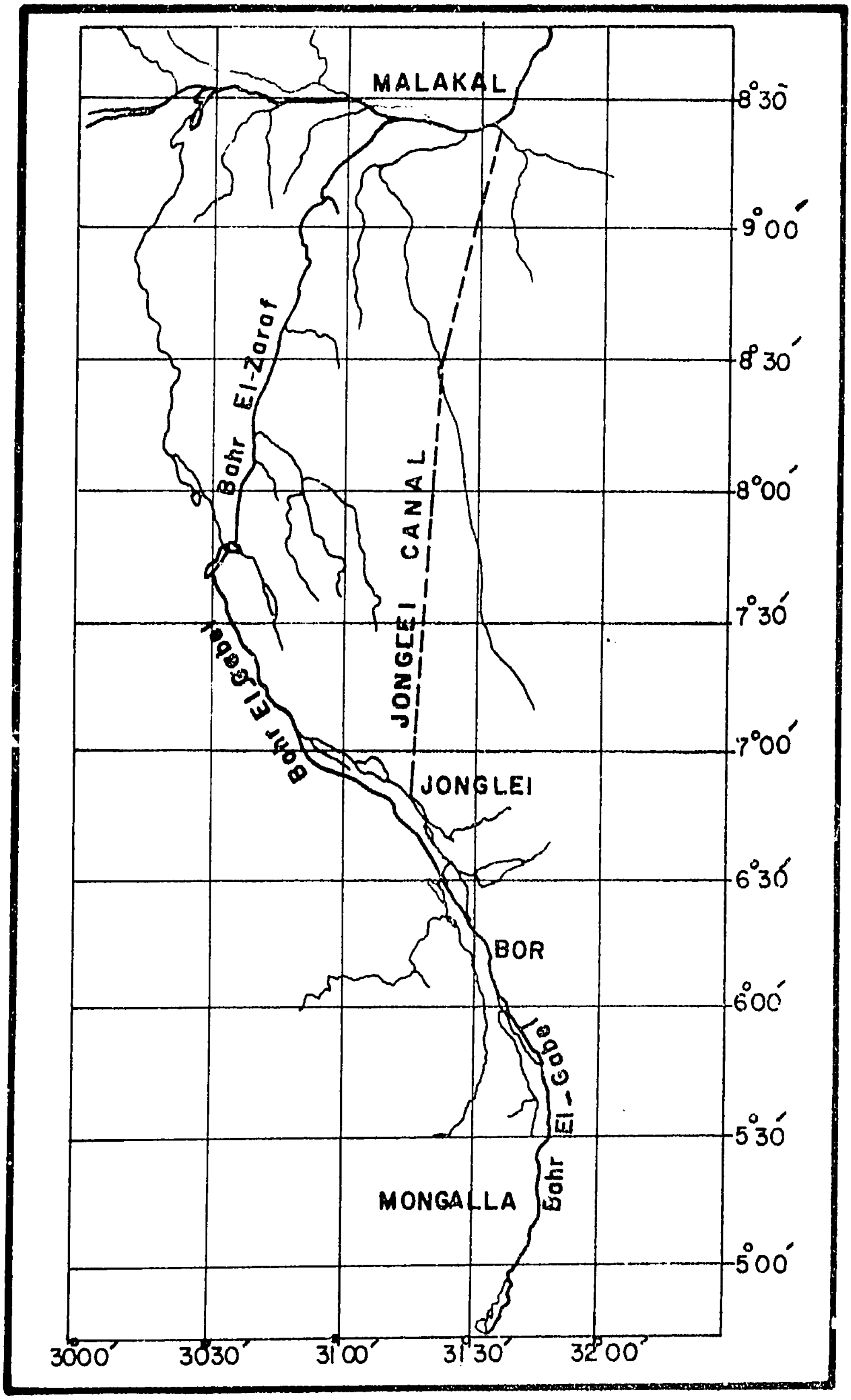

Fig. (1.2) A MAP SHOWING THE LOCATION OF THE JONGLEI PROJECT.

reach can thus be studied. This step is mandatory to analyze the water benefit obtained from the construction of the Jonglei canal in the area.

A routing scheme is suggested to correlate the flow passing from one section to another as well as to estimate the monthly losses or gains along this reach. Another alternate routing scheme is also proposed to estimate the expected flow downstream Bahr El-Gabel as a result of executing any of the development projects in the area. The regulated outflow from the Equatorial Lakes Plateau, the diverted flow to Jonglei canal at its different phases and the expected gain from the southern collecting canal at Bahr El-Ghazal catchment are then applied as new constraints for the generated routing scheme, see Fig. (1.3). The output of the routing scheme will thus represent the flow expected to arrive at Malakal under these new constraints.

The organization of this study can be summarized as follows: Chapter II gives a general description of the main hydrological features of Bahr El-Gabel area. Data availability and consistency are presented in Chapter III, as well as the spilling characteristics of Bahr El-Gabel Area. Routing schemes are suggested in Chapter IV, to estimate the monthly flow at Malakal as a response of known input flow at Mongalla. The expected water benefits from the proposed Jonglei project are investigated in Chapter V using a probabilistic approach. Chapter VI then furnishes the main findings and summary of the work.

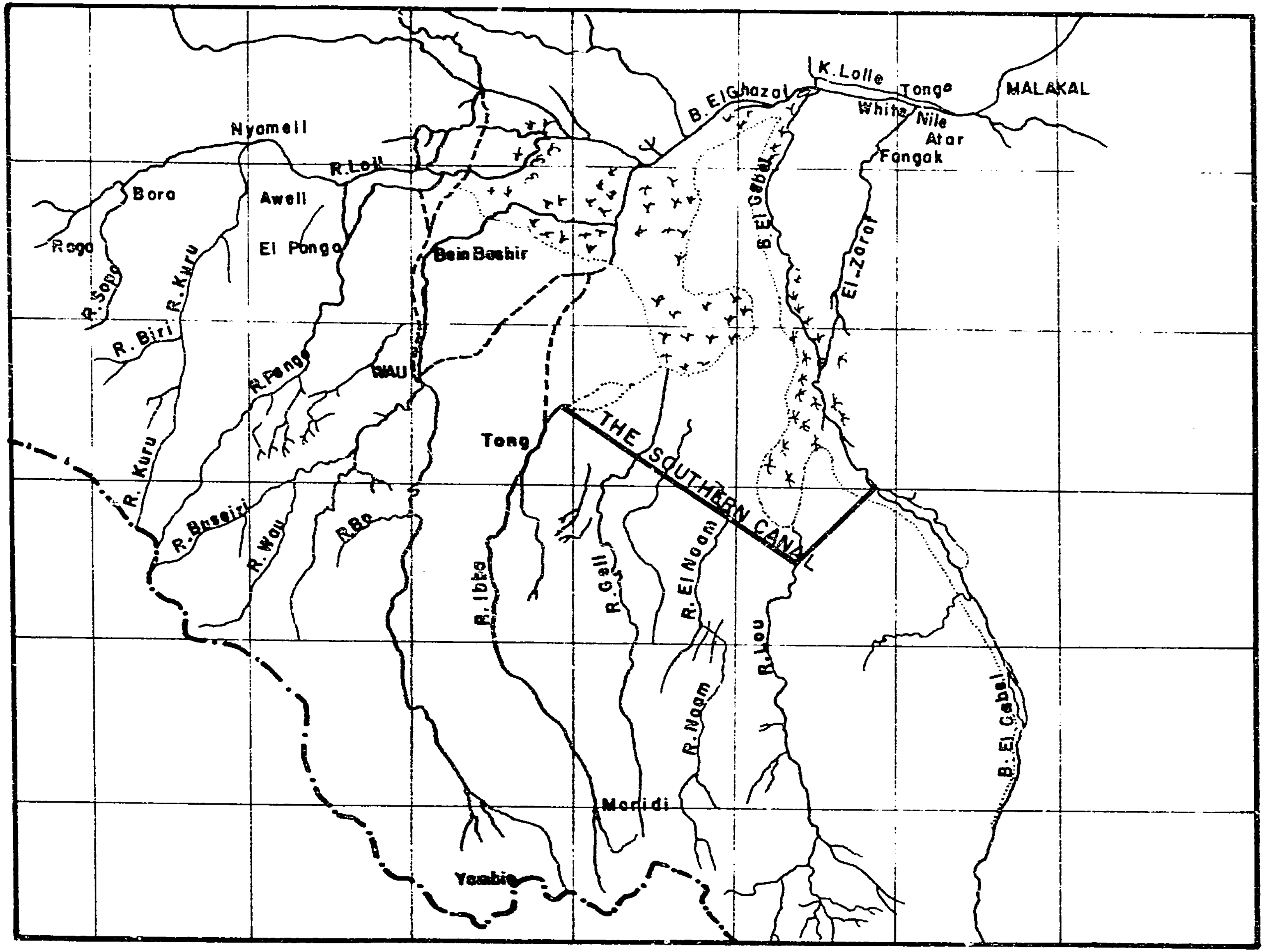

Fig.(1.3) A MAP SHOWING THE LOCATION OF THE SOUTHERN BAHR EL-GHAZAL CANAL.

CHAPTER II

HYDROLOGY OF BAHR EL_GABEL AREA

CHAPTER II

HYDROLOGY OF BAHR EL-GABEL AREA

2.1 GENERAL DESCRIPTION OF THE REGION

Bahr El-Gabel is situated in southern Sudan, extending from latitudes 4° to 9° north. It flows in general northward adjacent to longtitude 31°. This reach of Bahr El-Gabel can be considered as a conveyer stream between the Equatorial lakes and the White Nile, in addition to that, it has some of its own sources, Fig. (2.1). The course of Bahr El-Gabel can be divided into three main portions, ref. (6), these are:

1) From lake Albert to Nimule.
2) From Nimule to Rejaf.
3) From Rejaf to lake No.

2.1.1 The Reach From Lake Albert to Nimule

This portion from lake Albert to Nimule is a placid stream from 100 to 300 meters wide and is not very deep. This reach is navigable by lake streamers except in years when lake Albert is very low. The flood plain forms the bed of a well defined valley which at its maximum is about 6.0 kilometers wide. There are many small streams that join the main channel along this reach. These contribute practically no water during the dry season, but during the flood they have considerable contributions. In general, little is known about these streams.

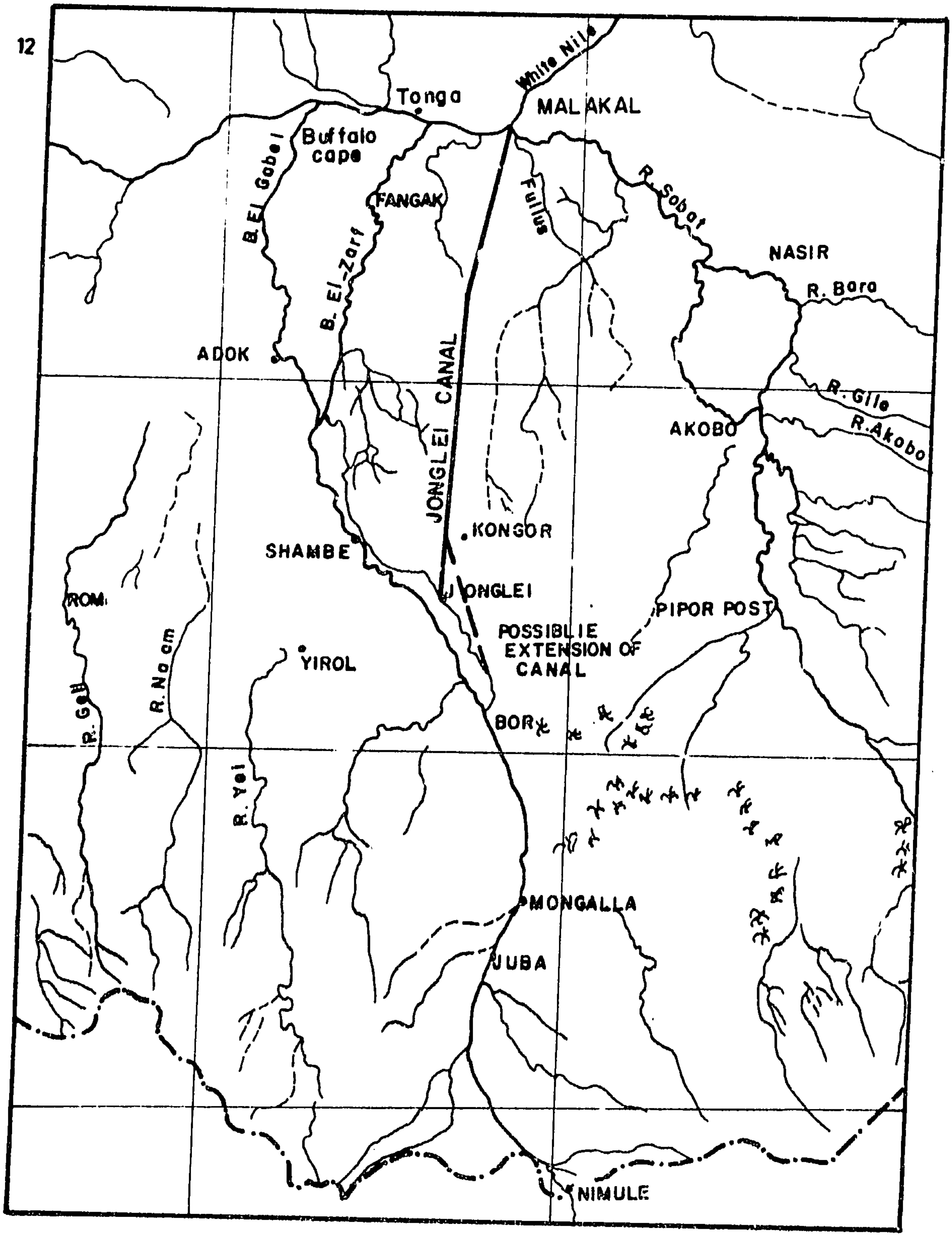

Fig (2.1) A MAP SHOWING BAHR EL-GABEL AND THE JONGLEI CANAL.

2.1.2 The Reach From Nimule to Rejaf

When Bahr El-Gabel approaches Nimule it makes a sharp bend and changes its character. Through 160 kilometers the river descends about 150 meters and flows in a narrow valley through hilly lands. The river course is broken by many rapids in this reach. Also, some tributaries join the main river. They are torrential in type and rise and fall very rapidly. The river Aswa is the most important one among these torrents, because it drains a large area and collects considerable amounts of water during the flood season. Most of the other torrents have practically no flow most of the year.

2.1.3 The Reach From Rejaf to Lake No

From Rejaf for some distance northwards the valley is well-defined, and the river winds about in the plain forming the valley floor, sometimes touching the high ground on one side and sometimes on the other side of the valley. The valley floor is flooded when the river is high and gets more swampy as one travels north. It is for the most part covered with tall grass known as Elephant grass which reaches 4.0 meters high and is of a bamboo-like nature similar to the grass called "Ghab Ralady". The higher land at the edge of the valley is covered with thin Savannah and Scattered trees. Downstream Mongalla, the river flows in many channels. The western channels, which are called Aliab system has many intakes from the main river south of the Bor. An effective erosion is taking place for that, the navigable channel changes from time to time. North of Bor, the valley widens and becomes more swampy, while the sides are less defined. Extensive and immense swamps spread out on either side of the river and continue down to lake No. This region is known as the Sudd Region. Another side channels system is existing in the eastern side downstream Reference Pole 114 (R.P. 114). This channels system changes occasionally as some of channels become blocked with vegetation from time to time.

Further north, occasional isolated spots of higher ground can be observed from the air, as at Hillet Nuer and Bufflo Cape on the east bank. Northeast of this reach there is Bahr El-Zaraf which has its origin in the swamps to the east of Bahr El-Gabel, and is then joined by two artificial cuts. In this lower course it flows between well-defined banks, but its upper course is swampy.

2.2 HYDROLOGY OF BAHR EL-GABEL REGION

The main feature of this reach from Mongalla up to lake No are the wide swampy areas. These swamps can be considered as wide basins which are filled with water during the high flows of Bahr El-Gabel. These swamps with its shallow depth permit considerable evaporation and evapotranspiration to take place. The efficiency of Bahr El-Gabel to convey the water flow from lake Albert to the White Nile varies considerably from the high flow to the low flow cases. For instance in cases of high flow, the losses through the reach from Mongalla up to Bufflo Cape may be over 50%. In the other cases of very low flow, gain may occur between the two sites. This gain may be attributed to the fact that in cases of low flow the main stream works as a drain for the swamps.

The increase in losses with increasing flow above the swamps is mainly due to the additional flow causing the water to spill over a larger area than the permanent swamps. Fig. (2.2) illustrates this phenomena. For the dry season the river level is at "a" and little spilling take place. When the river rises to "b", it will spill on the left bank only. Rising further to "c", it will spill on both banks. Although vegetation impedes the spilling, the spread is considerable and evaporation is high. To reduce the losses the level must always be kept below "b".

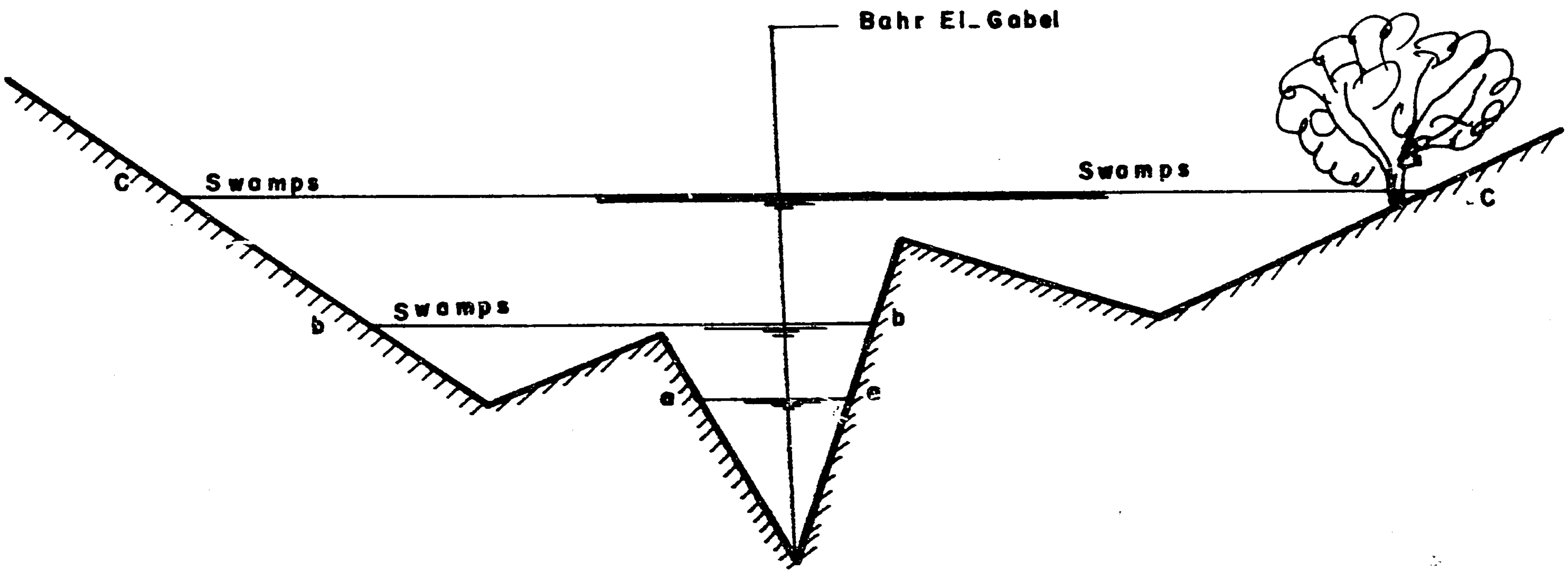

Fig.(2.2) THE SPILLING CHARACTERISTICS OF BAHR EL-GABEL (NOT TO SCALE).

In order to get full understanding of the hydrology of Bahr El-Gabel, detailed hydrological analysis will be carried out at many gauging stations along its reach in Chapter IV. Although, it is postulated that there is a shortage in the hydrological information for this region, attempts were done in order to get the atmost out of the available data.

2.3 MORPHOLOGY OF BAHR EL-GABEL REGION

From the begining of the ninteenth century, many exploration trips had investigated the area of Bahr El-Gabel. Many reports described the morphology of this area were then published from time to time. In April 1981, the Academy of Scientific Research and Technology, Cairo, Egypt, published a valuable report about this region, ref. (13). This report came out as a result of the interpretation of the LANDSAT satellite imagery pictures.

In the following paragraphs the morphology of Bahr El-Gabel will be discussed based on the report mentioned above.

The study area is part of large sedimentary basin complex. The southern portion is hilly and mountainous, Fig. (2.3). Elevations range from 3188 m in the Lolibai Mountains to 640 m at Nimule. The general slope is north towards the Sudd Region where elevations range from 484 m at Juba to 387 m at Malakal. The slope in the Sudd is toward the north. The elevation of the northern edge of the study area is as large as 592 m. Drainage in the area generally follows the regional slopes. This area was found to be composed of five general soil landscape units. They are flat sedimentary deposits, swampy areas, recent alluvial deposits, sloping upland areas and mountainous areas. Each unit has unique surface morphometry and soils.

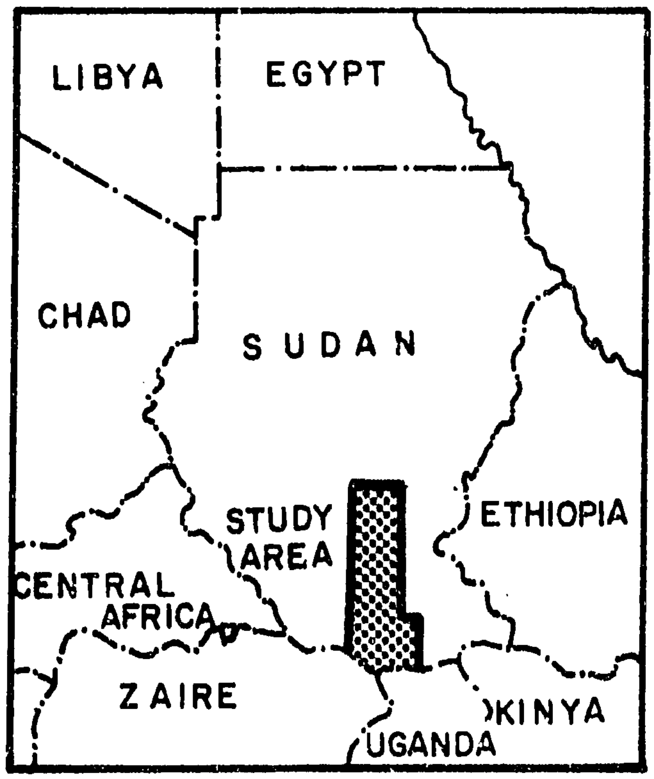

THE STUDY AREA IS PART OF A LARGE SEDIMENTARY BASIN COMPLEX. THE SOUTHERN PORTION IS HILLY AND MOUNTAINOUS, (REF. 13).

Fig. (2.3) GENERAL LOCATION OF THE AREA STUDIED BY LANDSAT SATELLITE PICTURES.

The flat sedimentary deposits occupy the central and northern portions of the study area. This was most likely an area of down sinking in the geologic past between the mountainous areas to the north and south. The sediments are derived from upland areas north and south with the majority of the sediments coming from the south. The surface of the area is very flat with slopes from 0 to 2 percent. The sediment is deep and fine-textured. The drainage pattern is not deeply incised. Some well defined drainage ways do exist such as Khor Fullus and Khor Atar. The majority of surface drainage occurs seasonally through linear depressional areas. The margins of these areas are poorly defined and incision rarely exceeds one or two meters. Very low stream gradients and flow velocities could account for these features. In addition, some of the drainage ways appear to meander and change location annually with the runoff of flood water.

The swampy areas are closely associated with Bahr El-Gabel, Bahr El-Ghazal and Bahr El-Zaraf. There are permanently or semi-permanently flooded areas of open water lakes and streams and dense growths of water hyacinth and papyrus. Occasional topographically higher areas of alluvium occur within the swampy areas.

Recent alluvial deposits occur in association with the drainage ways in sedimentary deposits and less frequently in the swampy areas. These deposits are, by their nature of deposition, coarser-textured than the surrounding areas. They are normally topographic high areas. Large areas of sandy textured alluvium occur as natural levees along Bahr El-Gabel. The materials are most extensively deposited along the west bank between the Juba and Kongor. The deposits are thickest close to Juba and thin northward. The pattern distribution indicates that the sands are derived from the sloping upland areas to the south and are deposited during flood stages of Bahr El-Gabel.

The sands are gray near Bor and Kongor but become increasingly redder to the south. The soils in the southern upland area are reddish. This also, indicates that it is the parent source for this area. From Nimule to Juba, the gradient of the river is approximately 0.98 m/km, while from Juba to Bor, the gradient decreases to 0.54 m/km. This sudden decrease could be sufficient to account for the deposition of sands to form the natural levee. From Bor to Malakai, the gradient is 0.06 m/km. This is insufficient to transport sand-size particles. Whereas the levee is a continuous feature on the landscape, it is interrupted at regular intervals by incised drainage ways running from east to west. The bottom of these channels expose the underlying, fine-textured sedimentary clays. These drains are thought to have been formed by floodwater draining from swamp areas back into the river channel.

The rolling upland areas occupy the southern and western portion of the study area. They are severely eroded with deeply incised drainage. Soil development in gently sloping areas indicates that this area is geologically much older than the areas previously discussed. Numerous bedrock outcrops occur throughout this area. The flat sedimentary deposits, swampy areas and recent alluvium are principally constructional topography and have thick soils developed on them. The upland areas are destructional topography and have generally thin soil developed on them. Extremely steep mountainous areas are associated with rolling uplands. They are the major bedrock outcrops in the area of Bahr El-Gabel. There are occasional, deep valley with gently sloping surfaces.

2.4 CLIMATIC ZONES IN BAHR EL-GABEL AREA

In this section we investigate the general climatology of Bahr El-Gabel, ref. (13). According to the classification of above report, the area of Bahr El-Gabel has been divided into six classes, as delineated in Fig. (2.4).

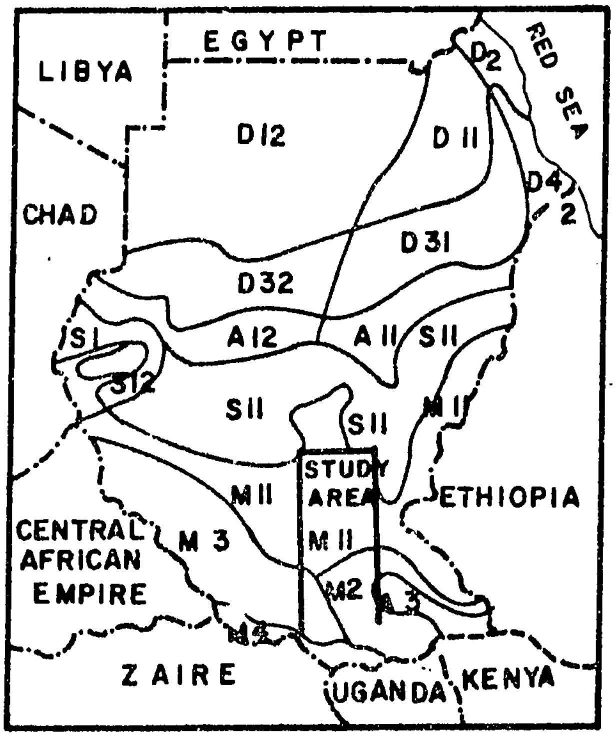

SYMBOL	CLIMATIC ZONE	HUMID MONTHS	DRY MONTHS	MEAN MAX. TEMP. IN HOTTEST MONTH	MEAN MIN. TEMP. IN COLDEST MONTH
S11	SEMI_ARID, SUMMER RAIN, WARM WINTER	1	9	39_40	13 _ 17
M11	DRY MONSOON, LONG DRY SEASON WARM WINTER	3- 5	5 _ 7	36_41	17 _ 20
M 2	DRY MONSOON MEDIUM DRY SEASON	2_ 3	4_ 6	36_38	18_21
M 3	WET MONSOON MEDIUM WET SEASON	5_7	3_5	34_39	12_ 20
M 4	WET MONSOON LONG WET SEASON	7_ 8	1_ 2	34_35	14_19
H 2	HIGHLAND MEDIUM WET SEASON COLD WINTER	5_ 6	3_4	23_33	10_ 17

Fig.(2.4) CLIMATIC ZONES IN SUDAN AND IN THE STUDY AREA (REF. 13).

2.5 RAINFALL DATA IN BAHR EL-GABEL AREA

Around the reach of Bahr El-Gabel there are ten rainfall stations. They are shown in Fig. (2.5). Also, the location of each station and the recorded period up to 1967 are indicated in Table (2.1). The records of these mentioned stations are available in the Nile Basin series up to 1967. However, four of these stations have regular records up to 1975. These records were published year by year in the Annual Meteorological Reports, ref. (7). These four stations are Rumbek, Juba, Bor and Malakal.

The distribution of the rainfall during the year and the number of days with rainfall of 1.0 mm or more is shown in Fig. (2.6). Table (2.2) gives the normals of monthly and annual totals of rainfall in millimeters and number of rainy days. Also, Fig. (2.7) shows the isohytal lines for the normal yearly rainfall depth in millimeters.

2.6 EVAPORATION AND EVAPOTRANSPIRATION RATES IN BAHR EL-GABEL

Generally, little is known about the attempts of measuring the actual evaporation and evapotranspiration in the studied area by using the tanks or the lysimeters. Also, there is no information about the measurements of the few experimental lysimeters which have been allocated in the last few years around Bahr El-Gabel area. Therefore, we had to depend on the old information of either the measured evapotranspiration or the piche evaporation. The potential evaporation can be calculated from the meteorological data available in reference (7). It includes the recorded data for the mean atmospheric pressure, air temperature, wet bulb temperature, vapour pressure and mean relative humidity on a monthly basis for the period 1960-1975. These records are available for four stations located in the area of Bahr El-Gabel, namely Rumbek, Juba, Bor and Malakal.

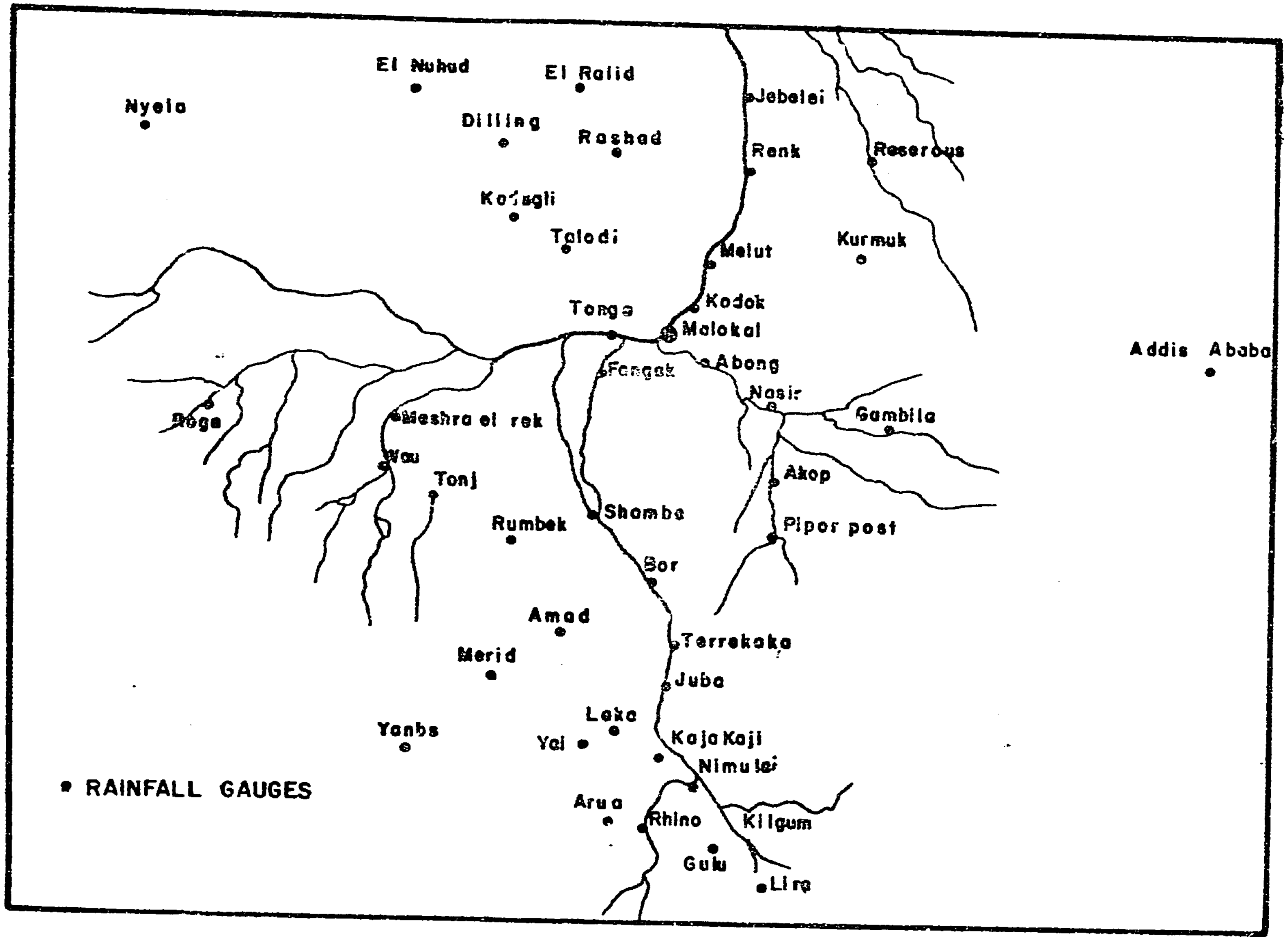

Fig.(2.5) AVAILABLE RAINFALL STATIONS IN BAHR EL-GABEL AREA.

Table (2.1) DIFFERNT METEOROLOGICAL STATIONS OF BAHR EL-GABEL AREA.

STATIONS	YEARS OF OBSERVATION UP TO 1967	LATITUDE N	LONGITUDE E	ALTITUDE In metres
JUBA	11924 _ 1967	04° 51′	31° 37′	462
TERREKAKA	1925 _ 1967	05° 27′	31° 45′	437
AMADI	1924 _ 1964	05° 31′	30° 20′	500
BOR	1905 _ 1967	06° 12′	31 33′	422
RUMBEK	1907 _ 1967	06° 48′	29 42′	420
SHAMBE	1903 _ 1935	07° 07′	30° 46′	406
FANGAK	1922 _ 1967	09° 04′	30° 53′	388
TONGA	1903 _ 1967	09° 28′	31° 03′	390
Malakal	1915 _ 1967	09° 32′	31° 39′	389
ABWONG	1919 _ 1964	09° 07′	32° 12′	389

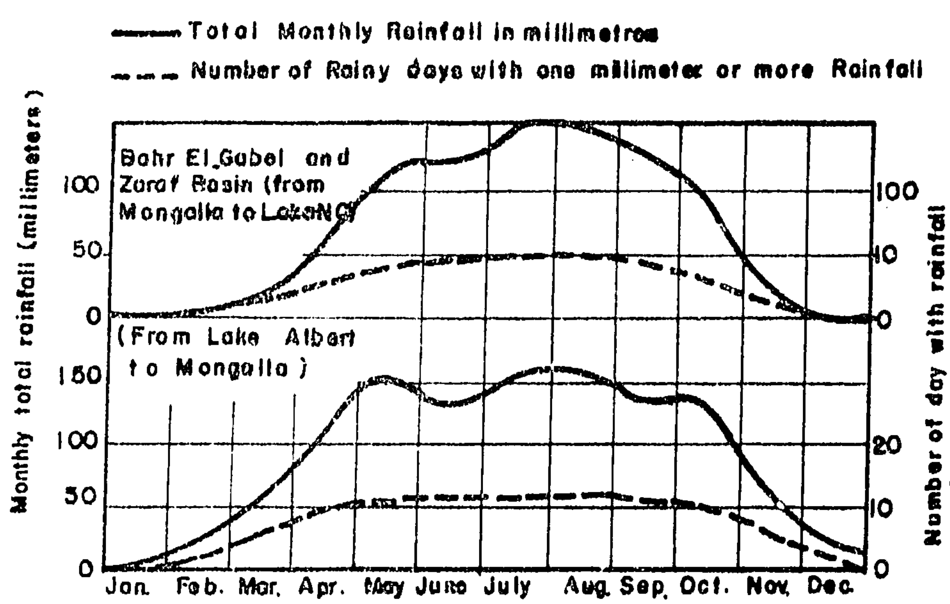

Fig. (2.6) NORMAL MONTHLY RAINFALL AND NUMBER OF RAINY DAYS IN VARIOUS DISTRICTS UP TO 1967.

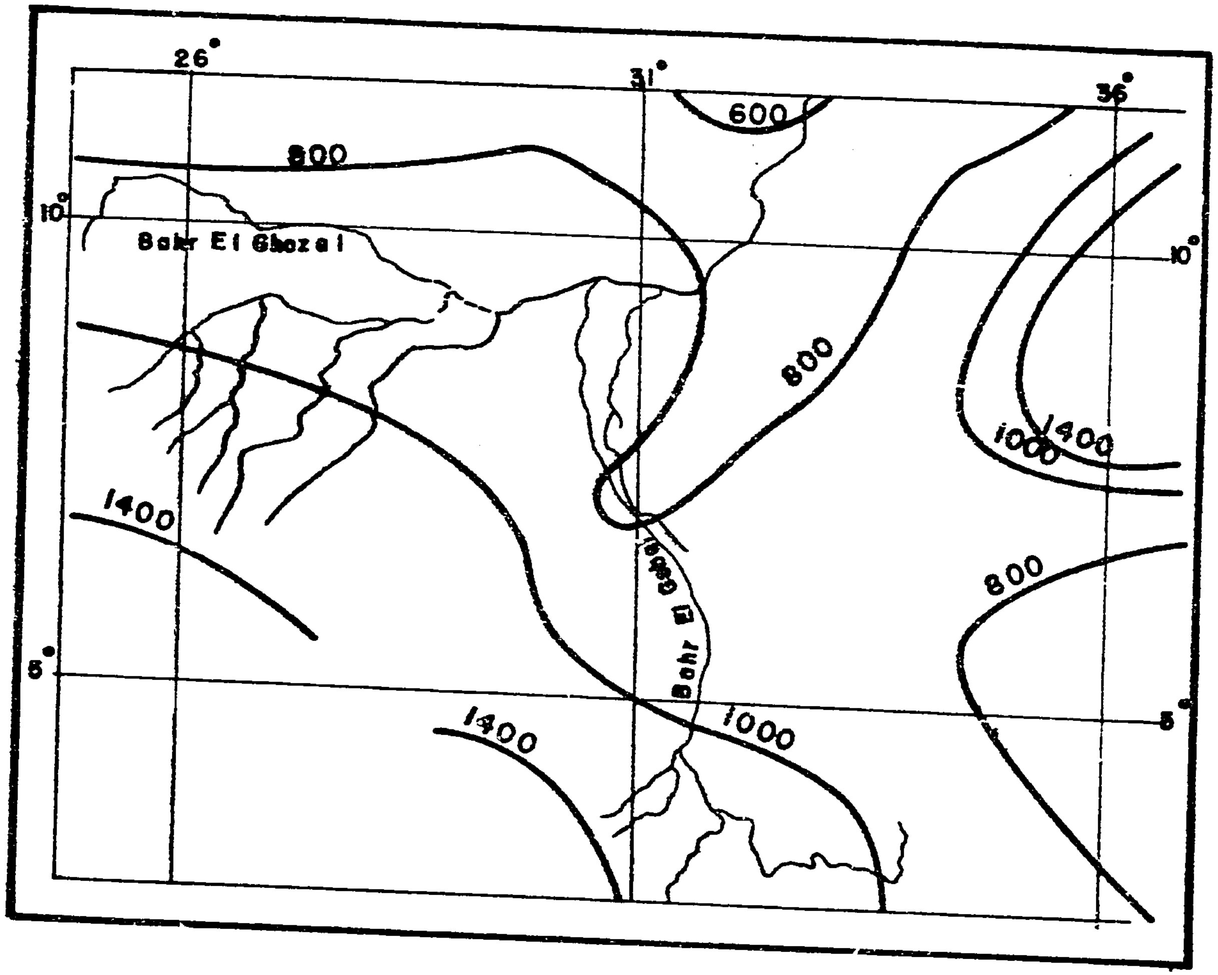

Fig(2.7) ANNUAL TOTAL RAINFAL NORMAL UP TO 1967
(THE NUMBERS REPRESENT MILLIMETRES OF RAIN).

Table (2.2)

Normals of the Monthly and Annual Rainfall Totals and Normal Number of Rainy Days, (up to 1967)*.

Station	Jan.	Feb.	Mar.	Apr.	May	June	July	Aug.	Sep.	Oct.	Nov.	Dec.	Year
Malakal	Tr. 0.0	Tr. 0.1	6 0.9	26 2.7	92 7.5	120 8.9	163 12.7	177 14.3	141 10.2	79 6.7	8 0.9	1 0.1	813 65.0
Tonga	Tr. 0.0	1 0.1	6 0.6	26 2.4	91 6.3	133 8.9	170 11.1	207 13.4	155 10.3	89 6.6	5 0.5	Tr. 0.0	883 60.2
Abwong	0 0.0	Tr. 0.0	6 0.5	24 2.3	77 5.4	116 7.4	158 9.4	177 10.9	90 7.5	73 5.1	8 0.7	Tr. 0.0	738 49.2
Fangak	Tr. 0.0	1 0.1	7 1.1	31 3.1	101 7.1	138 8.1	210 12.0	219 13.3	104 10.1	96 6.5	8 0.8	Tr. 0.0	975 62.2
Bor	2 0.4	8 1.2	31 3.3	84 6.9	119 8.2	118 7.7	140 8.5	134 8.6	130 7.8	108 6.6	27 2.5	6 0.8	907 62.5
Amadi	3 0.6	16 1.7	48 4.8	124 8.9	171 10.4	144 10.0	179 10.5	174 12.0	157 9.5	125 8.3	37 3.5	5 0.9	1183 81.1
Terrekaka	5 0.6	12 1.4	37 3.8	90 6.8	151 8.5	114 6.8	140 7.9	135 7.9	115 6.3	92 5.4	33 3.6	10 1.0	934 60.0
Rumbek	Tr. 0.1	6 0.6	26 2.7	85 6.3	140 8.4	153 9.2	169 10.4	194 11.5	135 8.4	73 5.5	15 1.3	1 0.1	997 64.5
Shambe	Tr. 0.2	4 0.4	16 1.5	48 3.4	86 5.2	120 7.0	151 8.7	157 9.0	120 6.7	66 7.7	9 0.9	1 0.3	778 51.0
Juba	4 0.7	9 1.8	43 6.0	104 9.8	155 11.5	119 9.9	132 10.8	143 10.9	113 9.2	106 9.4	38 4.9	12 2.0	978 86.9

* The upper figures are the Normal Rainfall Totals in millimeters; while the lower figures are the Normals of the Number of Days with Rainfall of one millimeter or more.

Tr. = Traces.

In 1926 a meteorological station commenced near Gabel El-Zaraf Cuts, with special observations of evaporation, as well as the usual measurements of temperature, humidity, wind, rainfall, cloud and etc. The station was in the middle of papyrus at a point mid-way between lake No and Bor, where the swamps are 10 to 15 kilometers wide. It should therefore be fairly representative of the climate in the swamps of Bahr El-Gabel.

A tank 10 meters square by 2.5 meters deep was sunk in the swamp and planted with papyrus. The water in this tank was kept approximately at the same level as the water outside, and regular measurements were made. The loss of water due to evaporation and transpiration was corrected for any rain which might had fallen. The papyrus in the tank was not always as luxuriant in growth as the free vegetation outside as there is great difficulty with this type of experiment in getting a representative sample of vegetation to grow in the tank. Table (2.3) gives the results of the observations from the papyrus tank together with the evaporation from a piche tube and the rainfall. The mean rainfall for the period from all stations near the swamps is 2.4 mms. per day, so that as far as rainfall is concerned the Cuts station with 2.2 mms. is representative of the district. Tables (2.3) and (2.4) give the evaporation and rainfall in the Sudd Region and the normal evaporation from the piche evapometer in, or near the Sudd Region. Also, Fig. (2.8) shows the evaporation and rainfall in the Sudd Region in one graph.

Table (2.3)

Evaporation and Rainfall in the Sudd Region. (Monthly and annual means in millimeteres per day, Annual totals in mms.).

Months	1926			1927			1928			1929			1930			1931			1932			Mean		
	Piche	Tank	Rain	Piche	Tank	Rain	Piche	Tank	Rain	Piche	Tank	Rain	Piche	Tank	Rain	Piche	Tank	Rain	Piche	Tank	Rain	Piche	Tank	Rain
January				4.1	4.3	0	3.3	4.2	0.1	3.6	3.9	0	3.2	3.2	0	4.2	4.2	0	3.7	2.0	0	3.7	3.6	0
February				4.7	4.3	0	4.8	5.4	0	3.2	4.0	0.2	3.5	3.2	0	4.7	4.1	0	4.7	2.0	0	4.3	3.8	0
March				4.2	4.4	0	4.3	5.4	0.3	3.6	4.8	0	3.4	3.3	1.3	4.8	3.9	0.1	4.2	2.2	0.2	4.1	4.0	0.3
April				3.8	5.4	1.2	3.5	5.4	1.7	2.3	4.1	0.7	3.6	3.2	0.6	4.6	4.0	1.2	3.7	2.4	1.0	3.6	4.1	1.1
May				3.3	4.8	1.2	2.3	4.7	3.6	1.7	3.6	6.2	4.0	3.0	1.7	2.8	2.7	2.7	2.6	3.0	6.9	2.8	3.6	3.7
June				2.4	4.0	3.6	2.3	4.2	6.2	1.8	3.8	5.9	2.[illegible]	3.0	6.0	2.1	2.4	3.1				2.2	3.5	5.0
July				1.7	3.7	1.5	1.9	3.6	4.3	1.7	3.2	3.1	2.5	3.5	5.6	2.2	2.9	5.7				2.0	3.4	4.0
August				1.7	3.7	4.7	1.7	3.6	4.0	1.6	3.5	4.8	2.2	3.0	2.2	1.9	2.5	2.8				1.8	3.3	3.7
September				2.1	3.8	1.6	1.8	3.7	6.3	1.6	3.2	2.6	2.5	3.5	3.8	2.0	3.6	9.8				2.0	3.6	4.8
October				2.8	4.1	1.3	1.9	3.9	3.0	1.6	3.2	3.2	2.4	3.2	2.4	2.1	2.9	3.6				2.2	3.5	2.7
November	2.9	4.5	0.2	3.1	3.8	0.1	2.7	4.1	0	2.0	3.1	0	3.2	3.1	0.5	2.7	2.3	0				2.8	3.5	0.1
December	3.8	4.6	0	3.1	3.5	0.2	3.3	4.1	0	2.9	3.1	0	4.0	3.4	0	3.4	2.5	0				3.4	3.5	0
Mean				3.1	4.2	1.3	2.8	4.4	2.5	2.3	3.6	2.2	3.1	3.2	2.0	3.1	3.2	2.4				2.9	3.6	2.1
Ratio Tank/Piche					1.4			1.6			1.6			1.0			1.0						1.25	
Annual				1118	1513	474	1024	1597	902	840	1322	822	1118	1169	736	1137	1157	883				1053	1318	781

Table (2.4)

Normal Evaporation from Piche Evaporometer (mms), in or near the Sudd Region.

STATION	January	February	March	April	May	June	July	August	September	October	November	December	Year
<u>Period</u>													
Malakal.(1915-1937)	16.45	18.24	15.73	10.89	7.01	4.36	2.93	2.46	2.87	3.66	8.30	13.56	8.87
Aweil...(1932-1937)	12.20	14.10	14.69	12.92	6.84	4.76	3.28	2.71	3.25	4.60	6.41	8.61	7.86
Akobo...(1932-1937)	12.31	13.77	12.83	9.23	5.45	3.87	2.94	2.77	3.32	4.04	5.69	8.46	7.06
Wau.....(1906-1937)	11.85	12.55	12.02	9.38	6.42	4.73	3.71	3.50	3.94	4.70	7.70	10.21	7.56
Shambe..(1931-1937)	7.67	8.25	7.91	6.39	4.69	3.64	2.79	2.64	2.82	3.43	4.77	6.37	5.11
Malek...(1932-1937)	10.92	10.04	8.95	6.92	4.36	3.31	2.72	2.57	3.26	4.44	7.13	3.30	6.08
Juba....(1925-1928, 1931-1937)	12.28	12.00	9.70	7.38	4.89	4.30	3.26	3.44	4.41	5.36	7.08	9.22	6.94
Torit...(1922-1937)	12.73	12.09	10.74	6.70	4.75	4.47	3.63	3.64	4.55	5.36	7.27	9.62	7.13
Mean	12.05	12.63	11.57	8.73	5.55	4.18	3.16	2.97	3.55	4.45	6.79	9.29	7.08

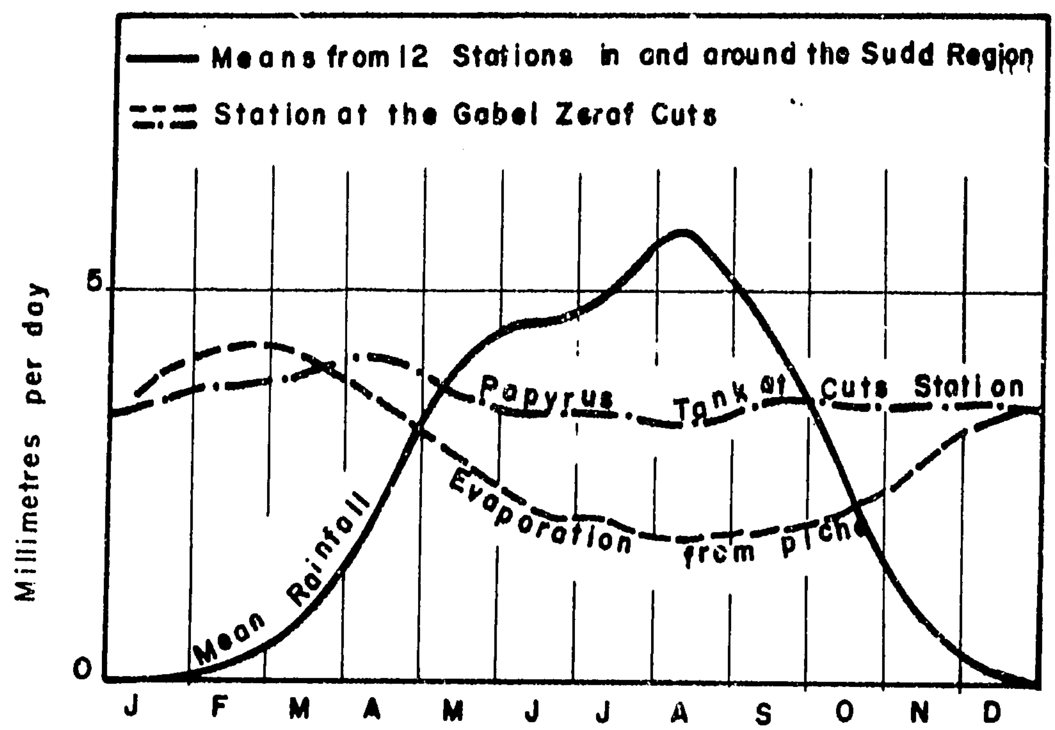

Fig.(2.8) EVAPORATION AND RAINFALL IN THE SUDD REGION.

CHAPTER III

DATA ANALYSIS AND CHARACTERISTIC OF MEASURING LOCATIONS

CHAPTER III

DATA ANALYSIS AND CHARACTERISTICS OF MEASURING LOCATIONS

3.1 STREAMFLOW DATA

The available hydrological data that is invoked to carry out the different analysis is the monthly and yearly discharges. We have to deal with this kind of data because of the following reasons and constraints:

i) Using the monthly or yearly records in the different analysis provides reasonable numbers of points to deal with, either in plotting the relationships or in modeling.

ii) It is the most regularly recorded data. For instance, the monthly data "gauge or discharge" are dated for all the stations in the same manner. This dating helps to correlate each reading with the corresponding one.

Tables (3.1) and (3.2) furnish the period of the 10-day mean records and the zero gauge for measuring stations of Bahr El-Gabel respectively.

3.2 THE DOUBLE MASS ANALYSIS OF STREAMFLOW DATA

The theory of the double mass curve is based on the fact that a graph of the accumulation of one quantity against the accumulation of another quantity for the same period will plot as a straight line so long as the data are

Table (3.1)
Available 10-day mean data for Bahr El-Gabel, ref. (6).

Station	Gauge	Discharge
Mongalla	1905-1967	1905-1967
Terrekaka	1927-1967	1931-1942
Gigging	1908-1967	1931-1959,1963-1967
Gemmeiza	1931-1967	1931-1967
Malek	1920-1964	1950-1966
Bor	1906-1967	1906-1942
R.P.114	1936-1964	1936-1964
U.S.Papiu	1936-1964	1936-1964
D.S.Papiu	1936-1964	1936-1964
Kenisa	1926-1964	1936-1964
Jonglei (3)	1924-1967	1933-1964
Jonglei (4)	1924-1967	1933-1964
D.S.Awai (1)	1936-1964	1936-1964
U.S.Awai (1)	1936-1964	1936-1964
D.S.Awai (3)	1924-1964	1936-1963
Bufflo Cape	1927-1964	1936-1964
Zaraf Kilo (3)	1908-1964	1908-1964
R.P.104	1937-1963	1937-1963
Hillet Nuer	1927-1963	1937-1962

Table (3.2)

The zero gauge level and the distance from the gauging stations to Lake No.

Station	Distance in Kms from Lake No	Zero gauge level in meter refered to Khartoum.
Mongalla	765	428.23
Terrekaka	735	420.59
Gigging	701	398.91
Gemmeiza	704	0.00
Malek	648	400.75
Bor	628	408.52
R.P. 114	584	400.56
Papiu	569	403.08
Kenisa	504	399.03
Jonglei	581	402.19
Awai Tail (1)	440	not fixed
Awai Tail (3)	380	391.12
Bufflo Cape	52	376.58
Zaraf Kilo (3)	77	372.51
Hillet Nuer	222	383.4

proportional; the slope of the line will represent the constant of proportionality between the quantities. A break in the slope of the double mass curve means that a change in the constant of proportionality between the two variables has occured, or perhaps that the proportionality is not a constant at all rates of accumulation. The break in the slope of the graphed line indicates the time at which a change occurs. The difference in the slope of the line before and after the break reveals the degree of change in the relation between the two variables.

In the hydrological studies, definite results cannot be obtained by using two variables only (e.g. two gauging stations), because we can not say which of the variables caused the break in slope. Therefore, to get more accurate results, the accumulation of one of the variables can be plotted against the accumulation of the pattern composed of all similar records in a given area. The method of using the double mass curve to check the consistency is only applied here for streamflow. The stations that form the pattern are:

1) Mongalla.
2) Gemmeiza.
3) Reference Pole 114.
4) Upstream Papiu.
5) Downstream Papiu.
6) Kenisa.
7) Jonglei (3).
8) Jonglei (4).
9) Downstream Awai Tail (1).
10) Upstream Awai Tail (1).
11) Zaraf Kilometer (3).
12) Bufflo Cape.
13) Reference Pole 104.
14) Hillet Nuer.

The data of the total yearly flow for the stations mentioned above is available for the period 1936-1962. There are two missing readings (not recorded), these are:

i) Year 1940 for Upstream Awai Tail (1).
ii) Year 1952 for Zaraf Kilo (3).

The two missing readings were completed using the mean yearly flow of each station during the period 1936-1962. The results of the double mass analysis is given in Appendix A. It may be concluded from Appendix A that the pattern formed by these fourteen stations is not consistent for all the stations and all the studied period (1936-1962). Some curves show that few stations had new trends in the last years. Generally, these changes can be attributed to human factors such as the measuring instruments or the method of calculation. Another reason for causing such inconsistency is the major changes in the gauging stations characteristics or in the regime of the pattern.

3.3 CHARACTERISTICS OF MEASURING LOCATIONS

The following analysis mainly depends on the available gauge and discharge data. In some locations the historical events help in the interpretation of some hydrological changes.

1. MONGALLA:

The gauge-discharge relationship at Mongalla, Fig. (3.1), is not a stable relationship for all the recorded period. Two rating curves can be graphed, each represents the gauge-discharge relationship for a certain period. The first one represents the period 1912-1962, while the second represents the

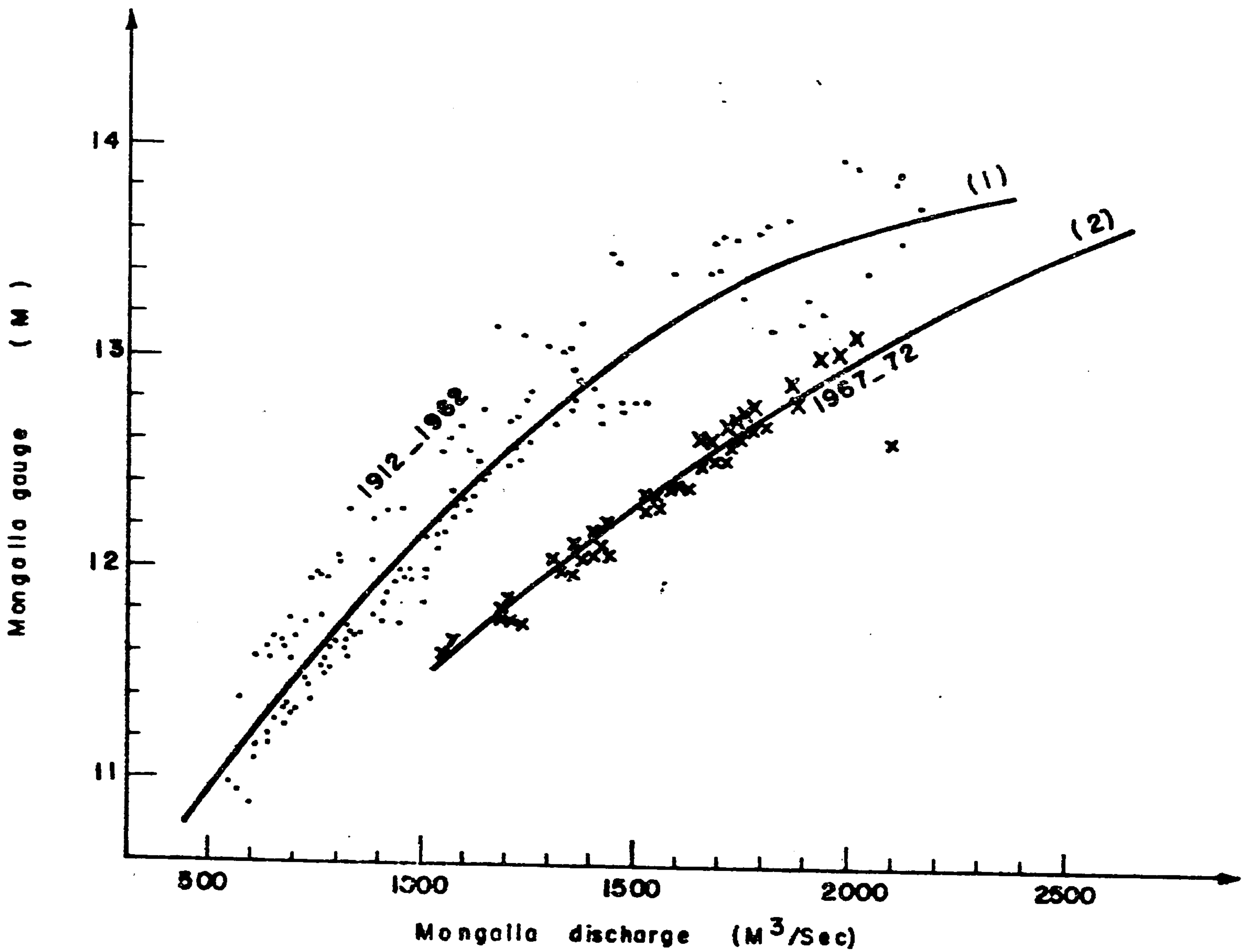

Fig(3.1) MONGALLA GAUGE-DISCHARGE RELATIONSHIP.

period 1967-1972. This change in the rating curve at Mongalla is attributed to the change in the geometry of the cross-section, especially during the high flood of 1964. From this rating curve of Mongalla, it can be inferred that the cross-section of the stream is a confined section up to 1600 m^3 per second discharge and 13.4 m gauge. For discharges and gauge readings greater than these values, spilling may occur. In both rating curves, increasing the discharge over 1600 m^3 per second has no remarkable increase in the gauge height.

The relationship between Mongalla and Malek gauges, Fig. (3.2), was then plotted to illustrate the correlation between the gauge level at Mongalla and the corresponding gauge level at Malek for the different stages of the river. This relation was represented by two linear equations. The first equation was $Y = 0.769\ X-4.08$, valid for the different values of X up to 21.14 meter. The second was $Y = 4X - 72.3$ and is valid for the values of X greater than 21.14 meter (Y as Mongalla gauge and X as Malek gauge). The second stage showed that the gauge readings over 12.18 m at Mongalla do not give considerable response at Malek. For instance, for the first stage an increment of 1.3 m at Mongalla gave 1.0 m at Malek, in the second stage an increment of 1.5 m at Mongalla gave 0.4 m only at Malek. This change in this relationship could be attributed to the fact that for the gauge readings higher than 12.18 m at Mongalla the Aliab System starts to play an active part in conveying a considerable portion of Bahr El-Gabel flow.

The gauge level 12.18 m at Mongalla corresponds to a discharge of 900 m^3 per second which is 78 million m^3/day. It is clear from Mongalla-Malek discharges relationship, Fig. (3.3), that for 78 million m^3/day at Mongalla the discharge at Malek tends to be constant, and any amount of discharge over 78 million m^3/day has practically no response at Malek. Again, it can be said that the rest of the discharge is either lost by spilling or being discharged through the Aliab System. From Mongalla-Malek relationships, it

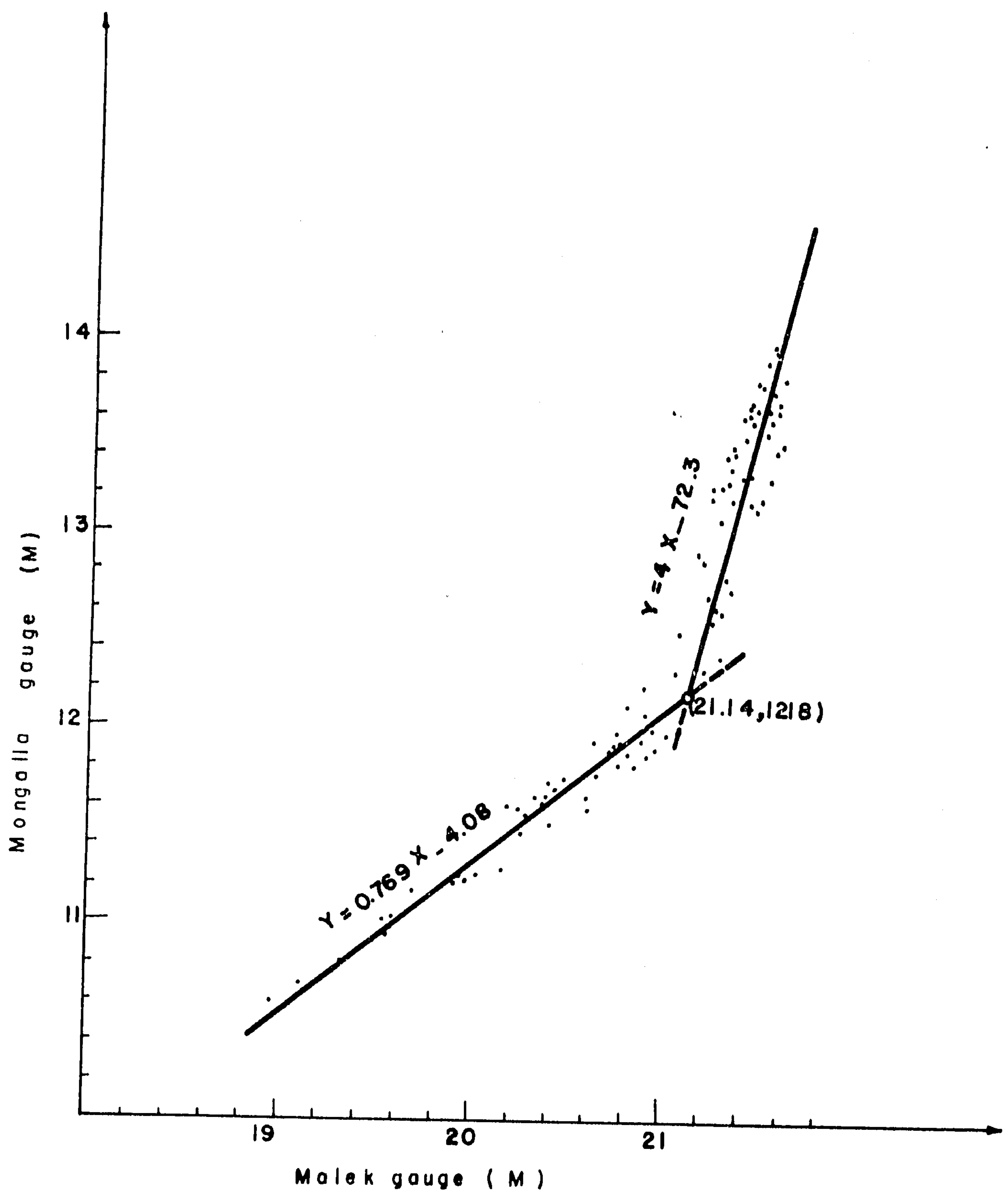

Fig.(3.2) MONGALLA_MALEK GAUGES RELATIONSHIP.

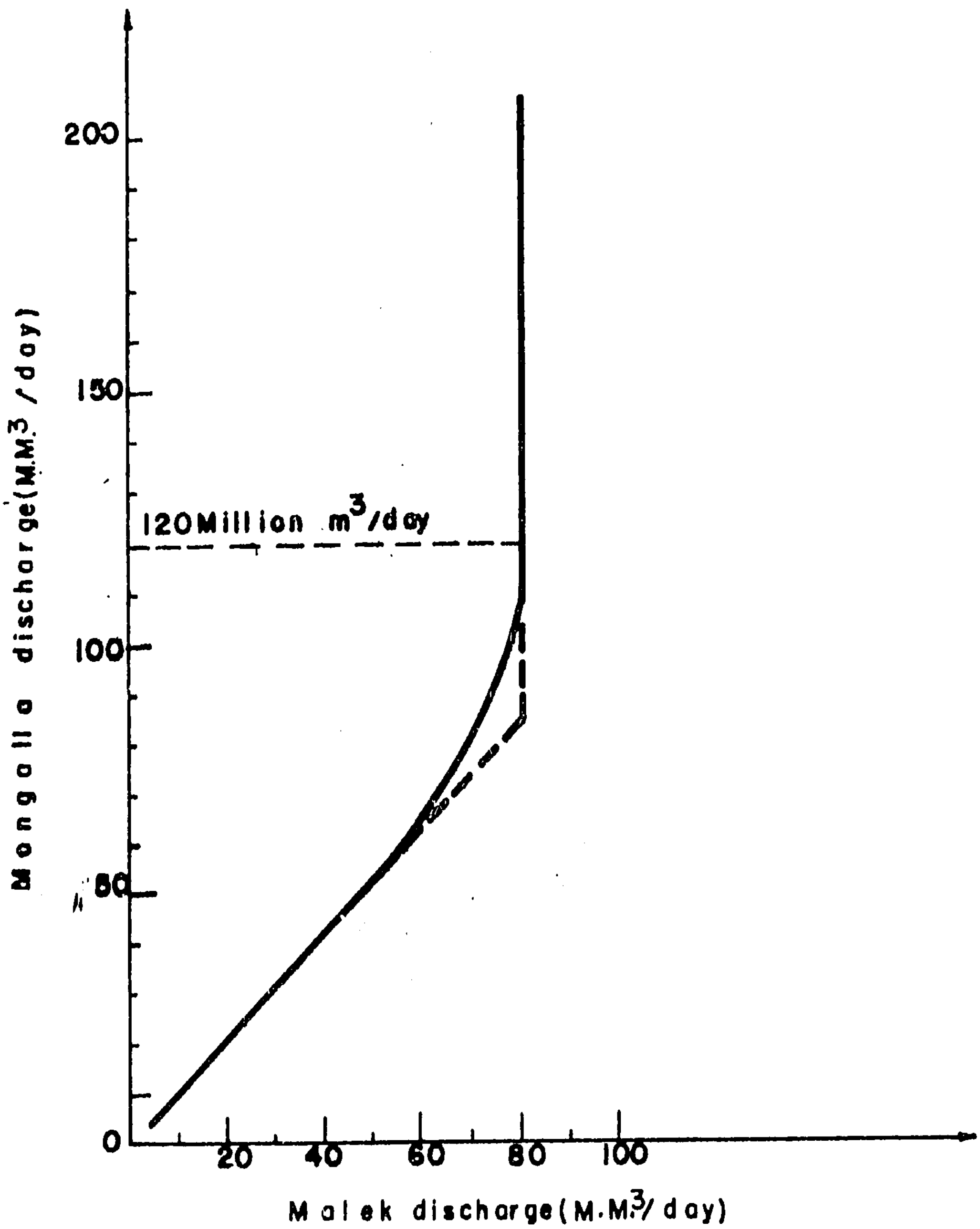

Fig. (3.3) MONGALLA_MALEK DISCHARGES RELATIONSHIP.

can be observed that the cross-sections of Bahr El-Gabel from Mongalla up to Malek has the capability to convey only about 80 million m^3/day. Mongalla-Bor gauges relationship could be represented by three linear equations, Fig. (3.4), each covering certain gauges intervals.

2. TERREKAKA:

There was no recorded measured discharge at this site. However, its gauge level could be related to the summation of the discharges of Gigging and Gemmeiza, assuming that the losses between Terrekaka and Gigging-Gemmeiza latitude is almost negligible. Theis relationship could be represented by the three curves given in Fig. (3.5). Each of these curves represents a certain period. Curve (1) represents the period 1948-1962, curve (2) indicates the period 1963-1966 and curve (3) represents the year 1970. The change of the general slope of the three curves demonstrates that the cross-section at Terrekaka was too much affected during the peak flood of 1962. It was clear from the figure that for the same gauge level, the discharge in 1970 was more than twice the discharge in the period 1948-1962. The relationship between Terrekaka-Malek and Downstream Papiu gauge levels was plotted in Fig. (3.6) together with the regression equations obtained. This represented the records up to 1970.

3. GIGGING:

The gauge-discharge relationship at Gigging is illustrated by the relationship shown in Fig. (3.7). This curve indicates that for gauge levels exceeding 30.0 meters, the discharge increased rapidly without any appreciable increase in the gauge level. Accordingly, it can be concluded that the cross-section at Gigging is not confined for stages higher than 30.0 m. For this case the flow behaves as sheet flow in an unconfined section.

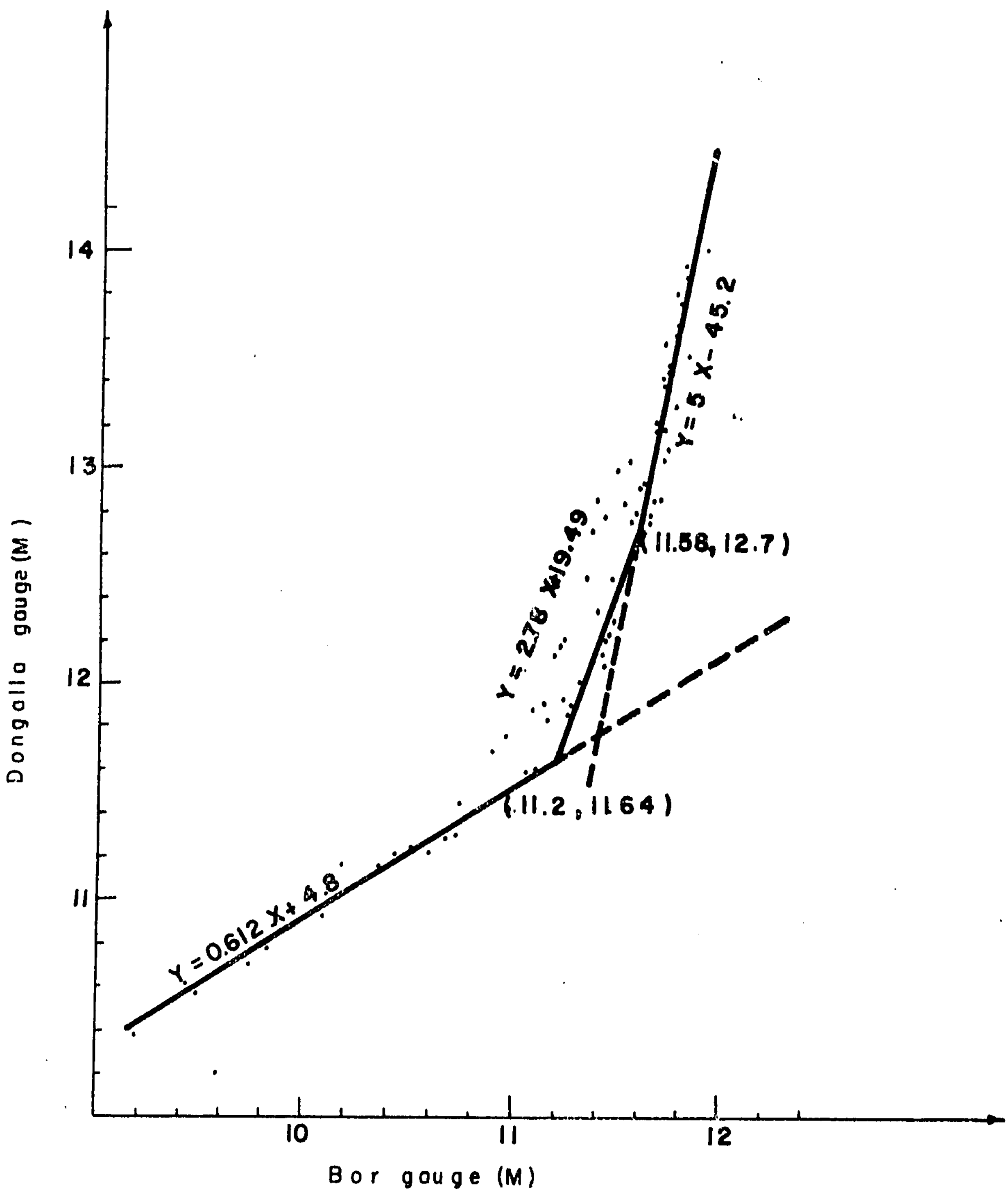

Fig.(3.4) MONGALLA_BOR GAUGES RELATIONSHIP.

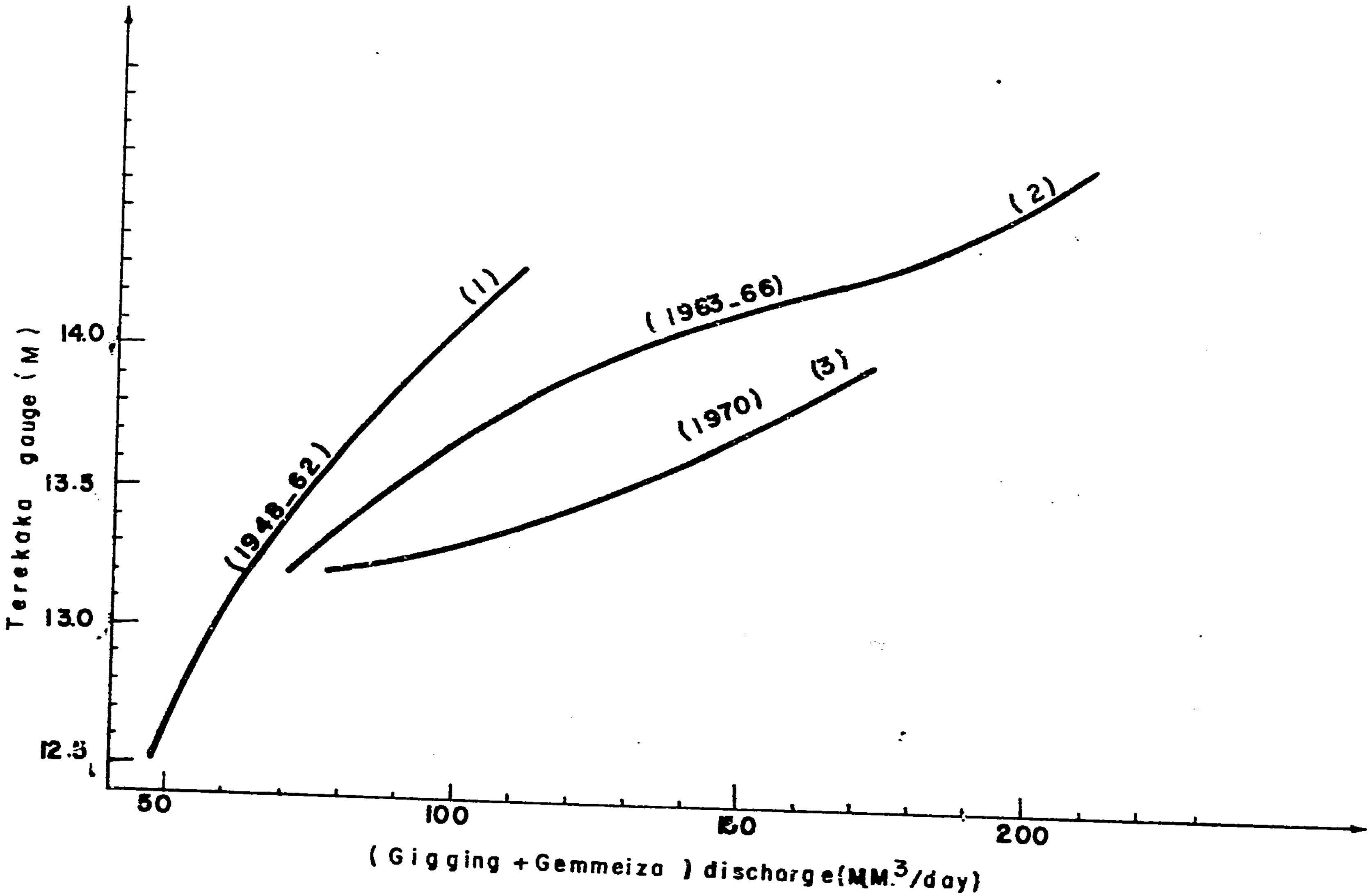

Fig. (3.5) RELATIONSHIP BETWEEN TEREKAKA GAUGE AND GIGGING GEMMEIZA DISCHARGE FOR VARIOUS PERIODS.

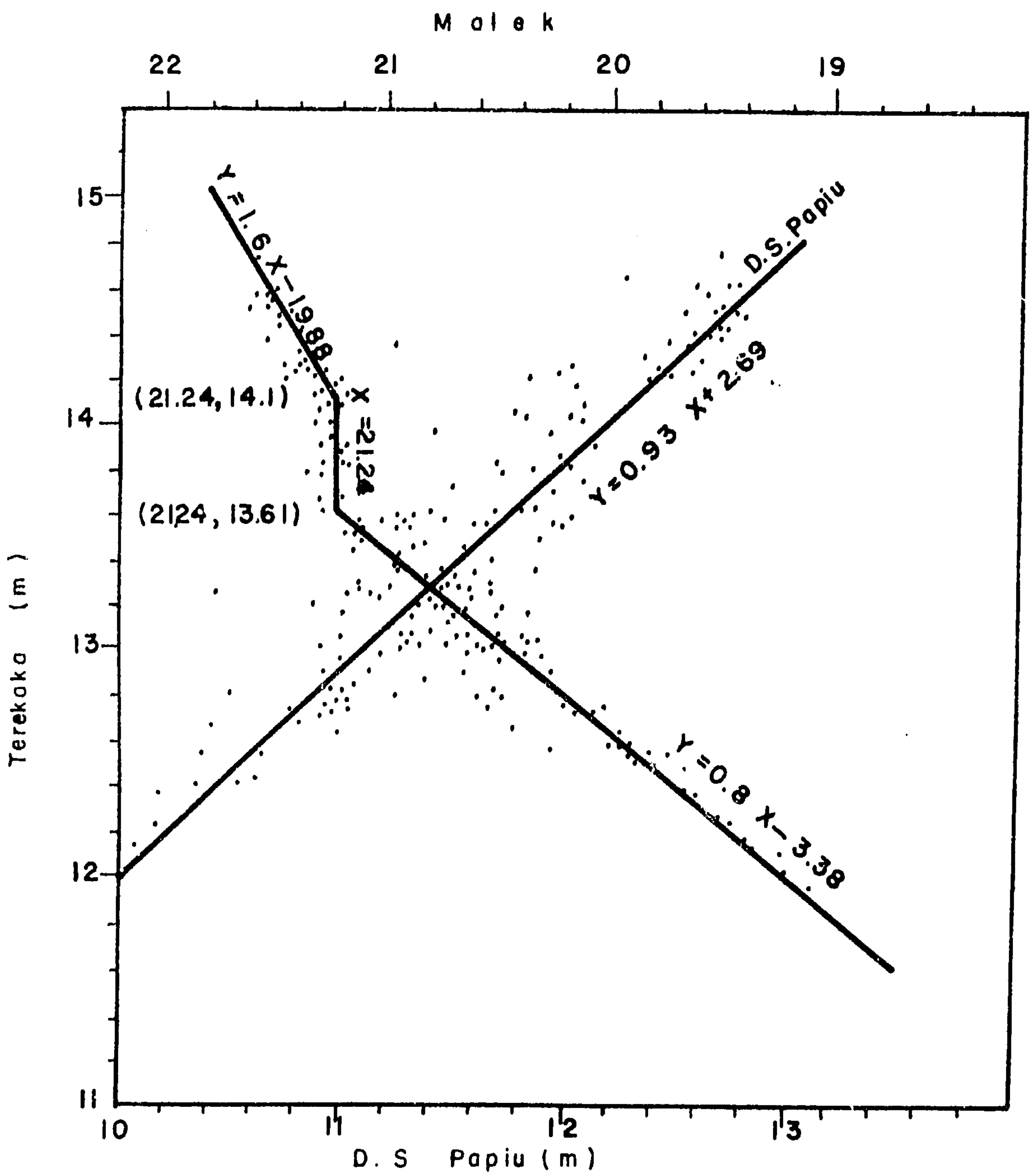

Fig.(3.6)TEREKAKA_ D.S.PAPIU TEREKAKA_ MALEK GAUGES RELATIONSHIPS.

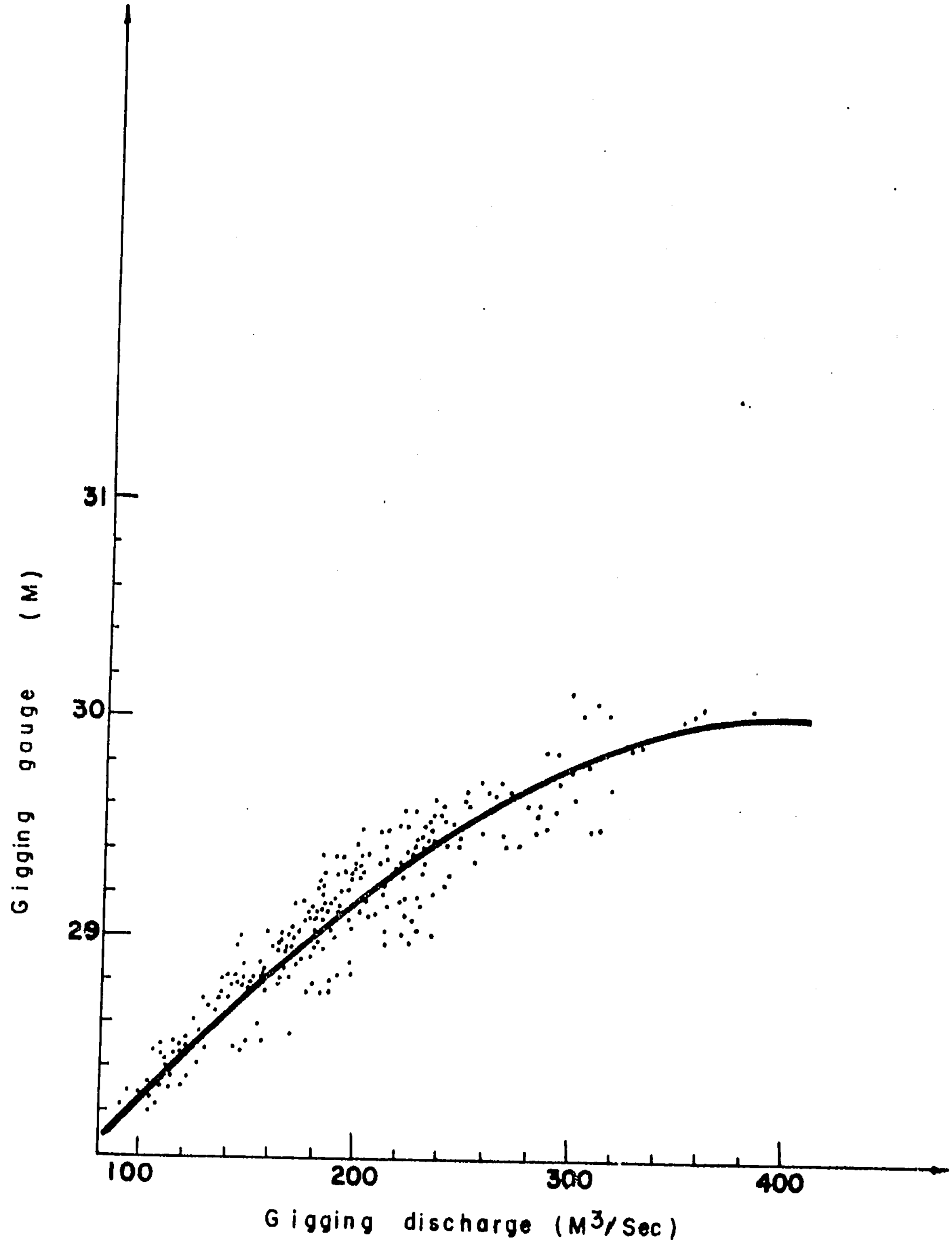

Fig. (3.7) GIGGING GAUGE_DISCHARGE RELATIONSHIP UP TO 1957.

Gigging-Gemmeiza gauges relationship is delineated in Fig. (3.8) for the period 1938-1967. The first part of the relationship is expressed by the linear equation $Y = 1.06X + 397.97$ and is valid up to $X = 29.60$ m, while the second part is represented by the linear equation $Y = 1.975X + 370.89$ and is valid for $X > 29.60$m, (X as Gigging gauge and Y as Gemmeiza gauge). In the first relation, 0.5 meter increment at Gemmeiza reflects about 0.5 meter increment at Gigging, but in the second part the same increment at Gemmeiza reflects 0.25 meters increment at Gigging. This shows that Gigging gauge is not too much affected as Gemmeiza gauge in cases of high water levels.

4. <u>GEMMEIZA</u>:

Up to 1962 the gauge-discharge relationship at Gemmeiza is shown by curve (1) in Fig. (3.9). Plotting of the available measurements during the period 1963-1969 demonstrates wide scatter and it is difficult to fit any regression line to them. Although the available data during the period 1970-1972 were few, one could reach a reasonable relationship for this period. However, it is obvious that the characteristics of the cross-section at Gemmeiza has completely changed during the period 1963-1970. Therefore, it is expected that the cross-section will be stable but forming another gauge-discharge relationship and one could assure that the relationship of curve (2) has attained stability.

5. <u>MALEK</u>:

The gauge discharge relationship at Malek shown in Fig. (3.10) follows the equation $\text{Log } Y = 0.125 \text{ Log } X + 0.957$ (where Y designates the gauge level in meters and X denotes the discharge in m^3 per second). From the rating curve of Malek, it is difficult to determine which level spilling or overtoping begins.

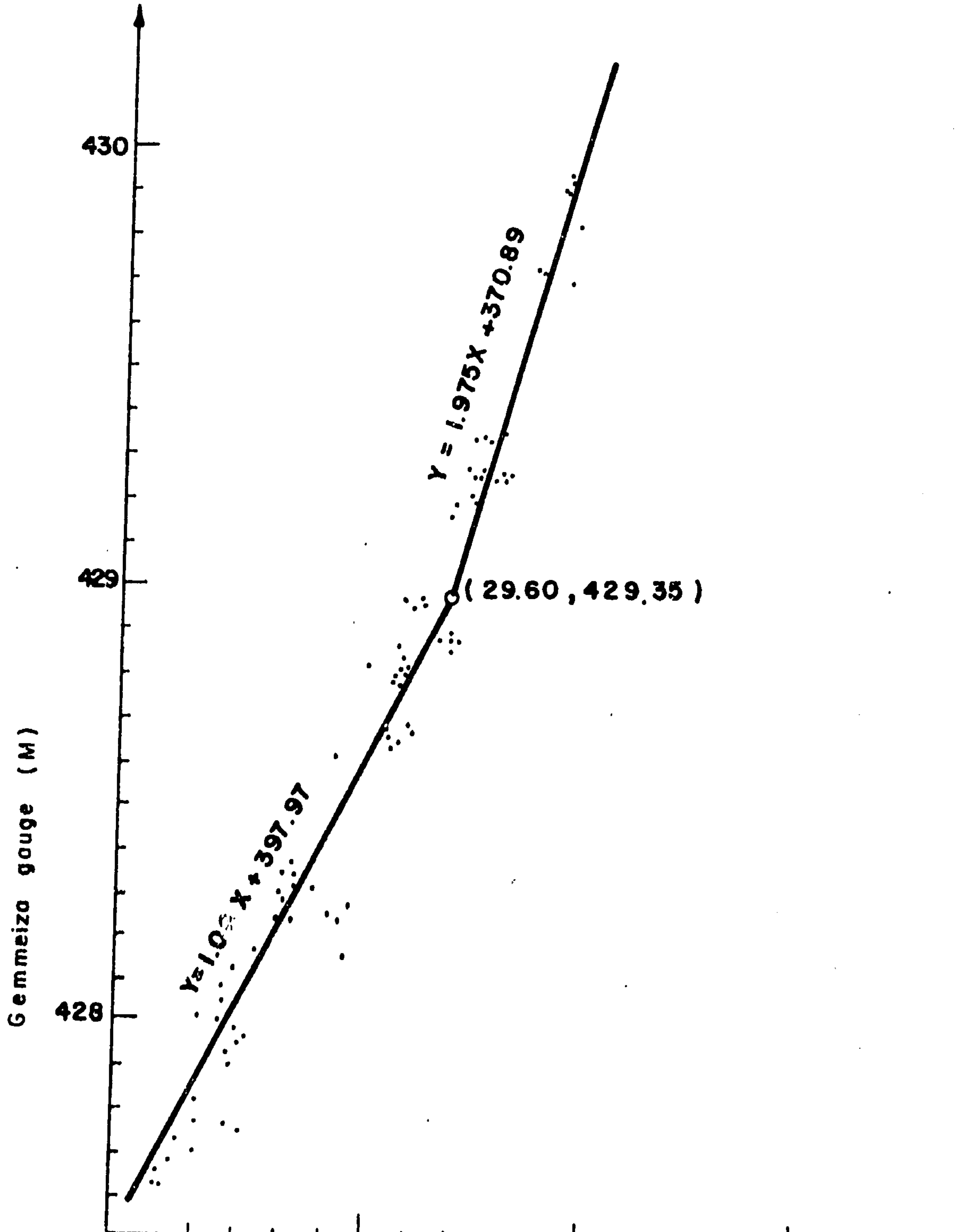

Fig.(3.8) GIGGING_GEMMEIZA GAUGES RELATIONSHIP.

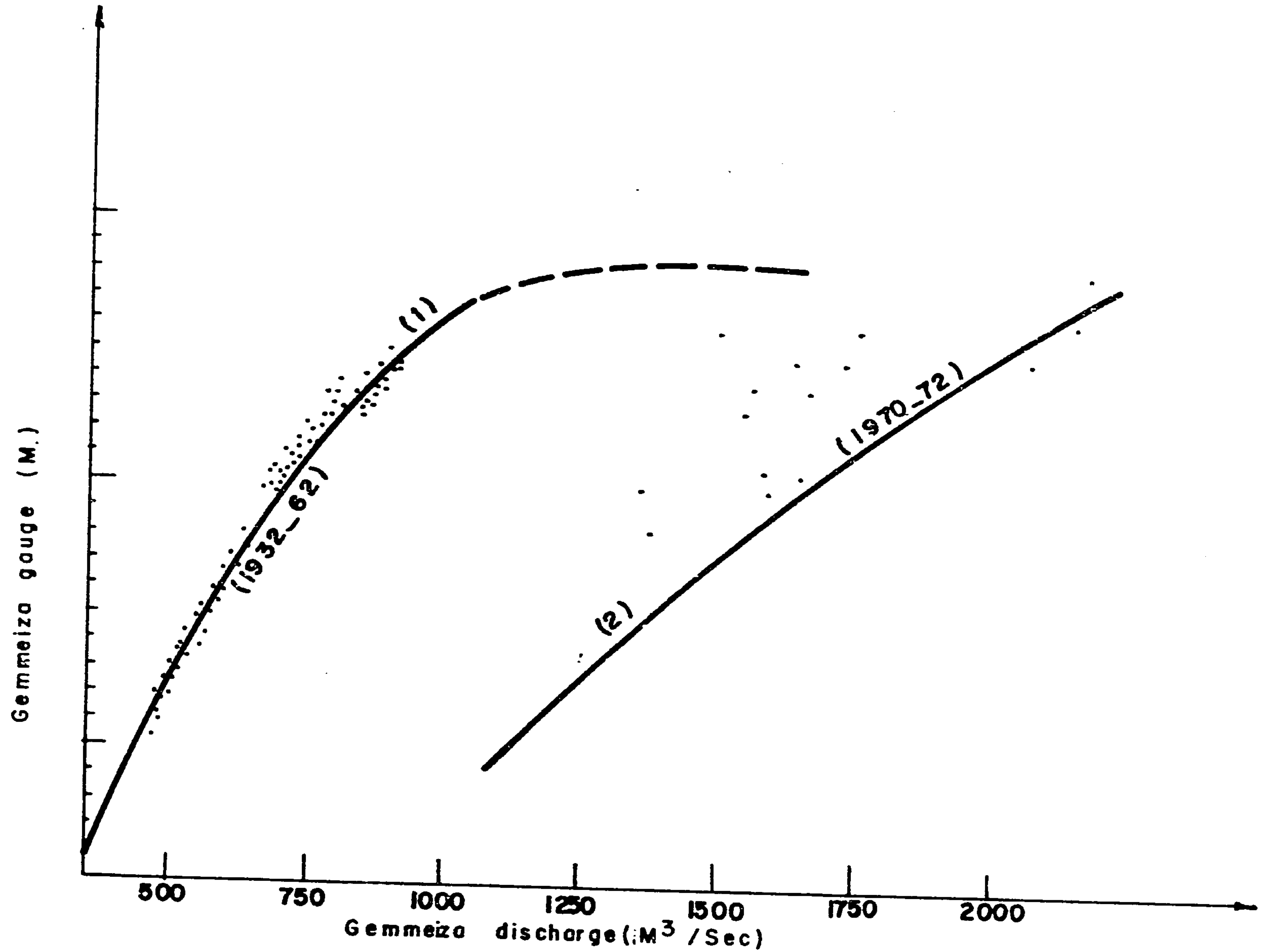

Fig.(3.9) GEMMEIZA GAUGE_DISCHARGE RELATIONSHIPS.

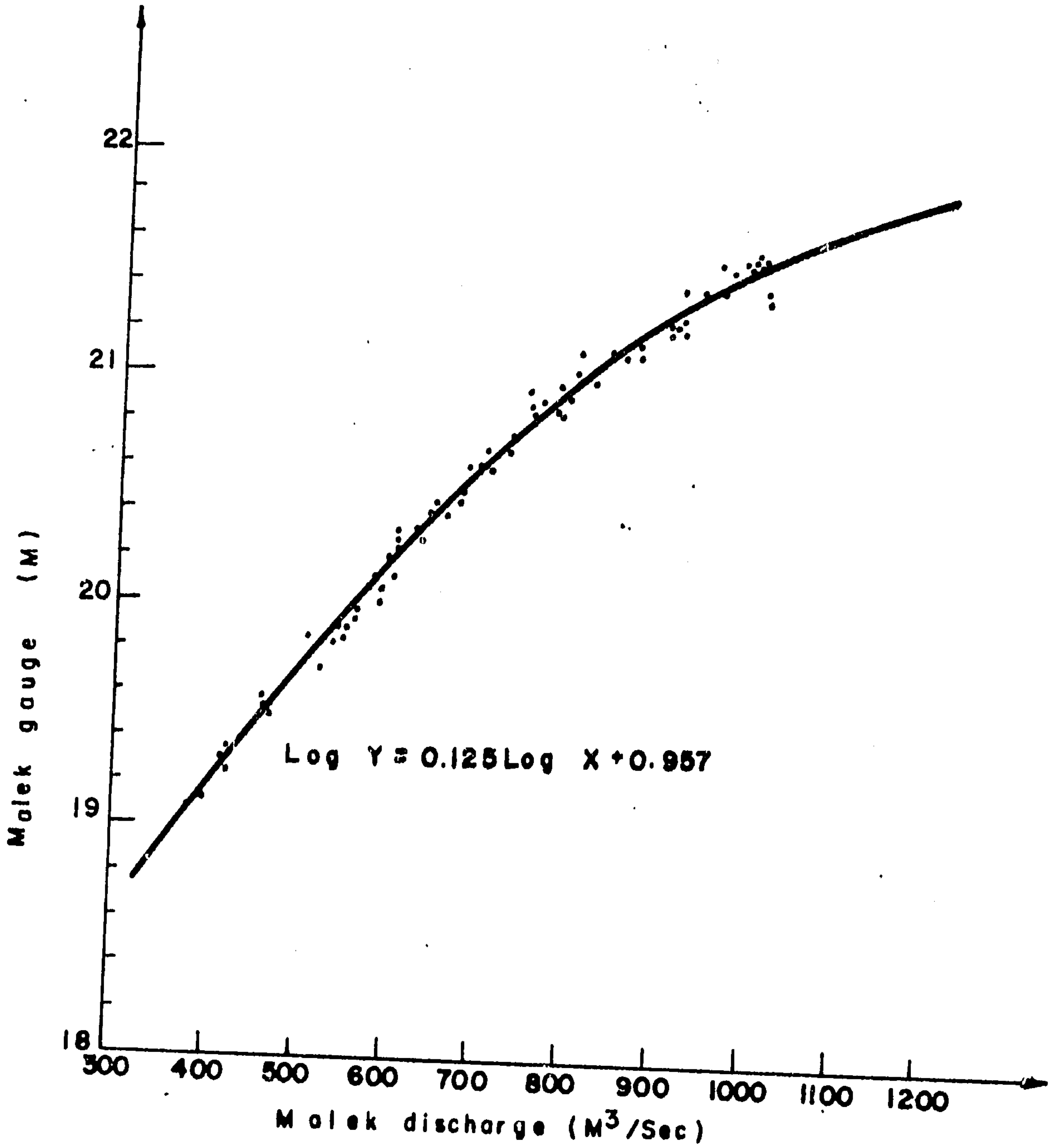

Fig. (3.10) MALEK GAUGE - DISCHARGE RELATIONSHIP.

6. BOR:

The rating curve for Bor station is plotted as shown in Fig. (3.11). Using the limited available data, no conclusions could be made from this rating curve because of the shortage of the available data and the absence of any salient features.

7. REFERENCE POLE 114 (R.P. 114):

The gauge-discharge relationship at R.P. 114 is illustrated by the two parallel straight lines presented in Fig. (3.12). The lower line is applicable for the recorded period up to 1968, while the upper line is valid for the period 1969-1972. The change in the gauge-discharge relationship may be attributed to the fact that in 1968 a settlement of about 0.4 meter in the gauge had taken place. This settlement could be read from Fig. (3.12) as the vertical displacement of the original line upwards, which amounted to 0.398 meters.

8. LAKE PAPIU:

The flow was measured at two sites upstream and downstream Papiu. There was no stable relationship between the gauge and the discharge upstream Papiu. This is due to the damping effect of the Aliab system, which is discharging considerable amounts of flow with respect to the upstream Papiu discharge. This returned flow from the Aliab system causes blocking to the discharge of Bahr El-Gabel U.S. Papiu. The relationship between upstream and downstream Papiu discharges is illustrated in Fig. (3.13). Although, we could not obtain an accurate relationship between the upstream and the downstream discharges at Papiu because the plotted points were widely deviated, it can be seen that as the downstream discharges increases the upstream discharge decreases. The blocking of the flow upstream Papiu affects the discharge entering to the Atem system. The entering flow to the Atem system

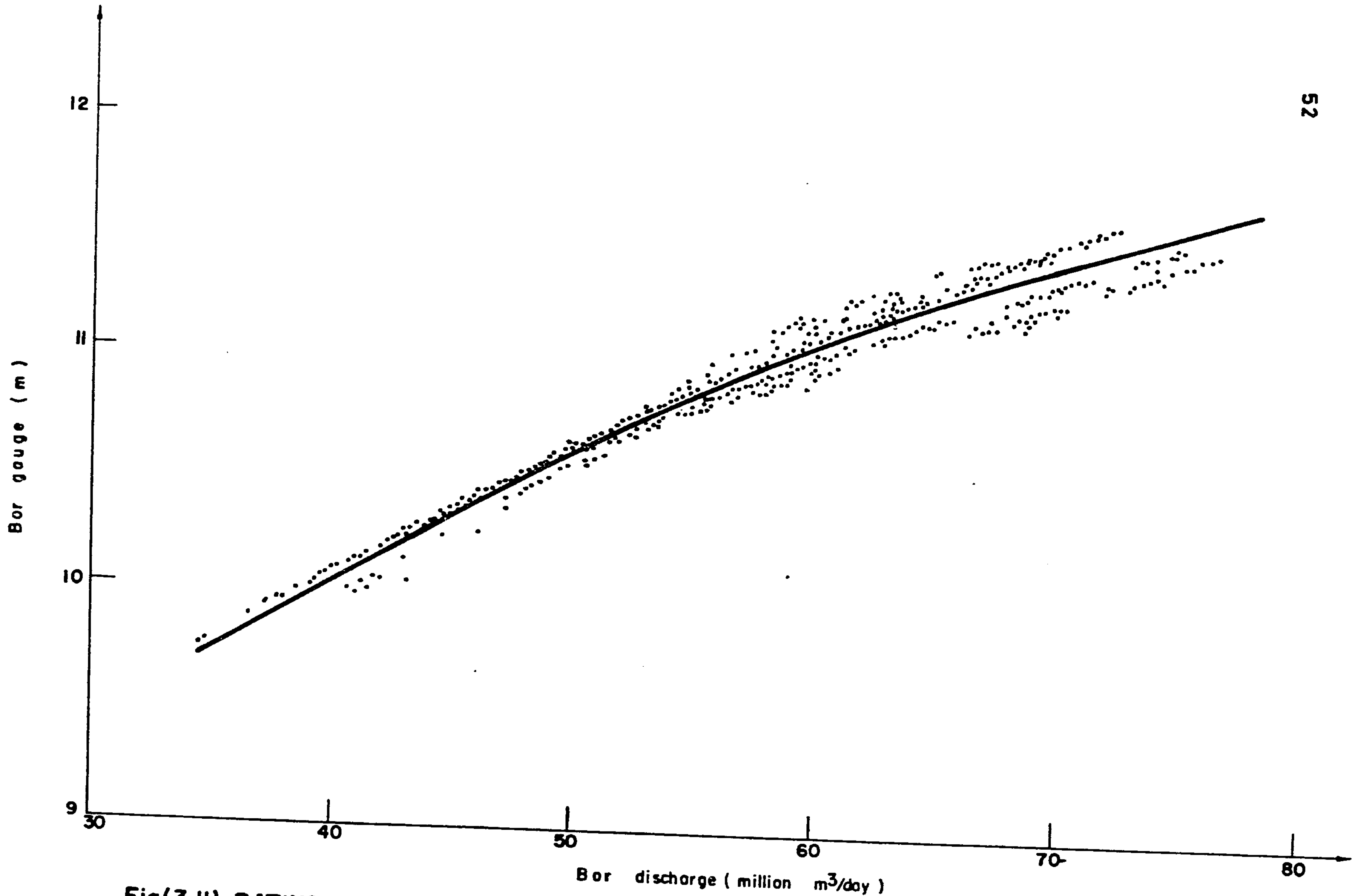

Fig.(3.11) RATING CURVE OF BAHR EL-GABEL AT BOR.

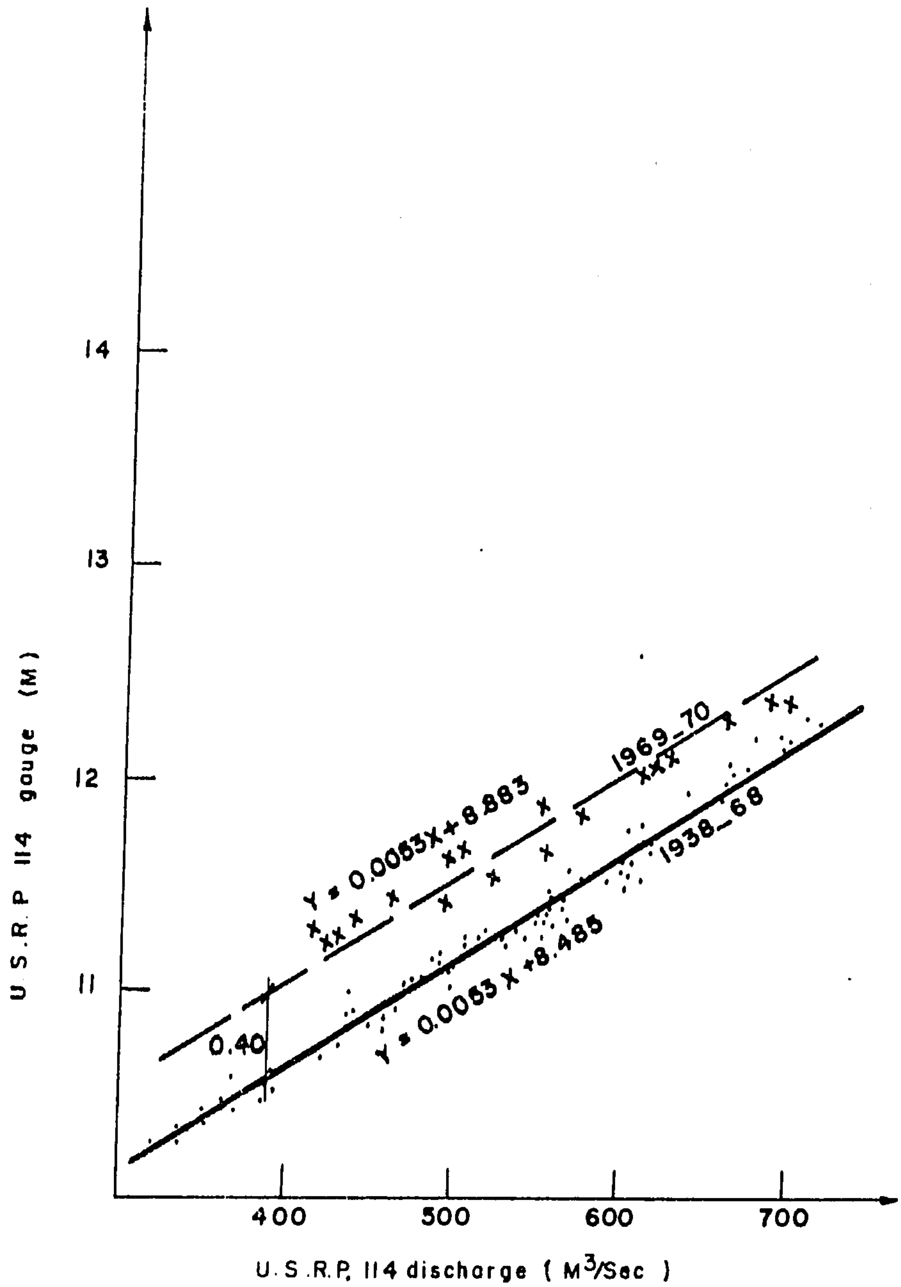

Fig(3.12)U.S.R.P. 114 GAUGE_DISCHARGE RELATIONSHIP.

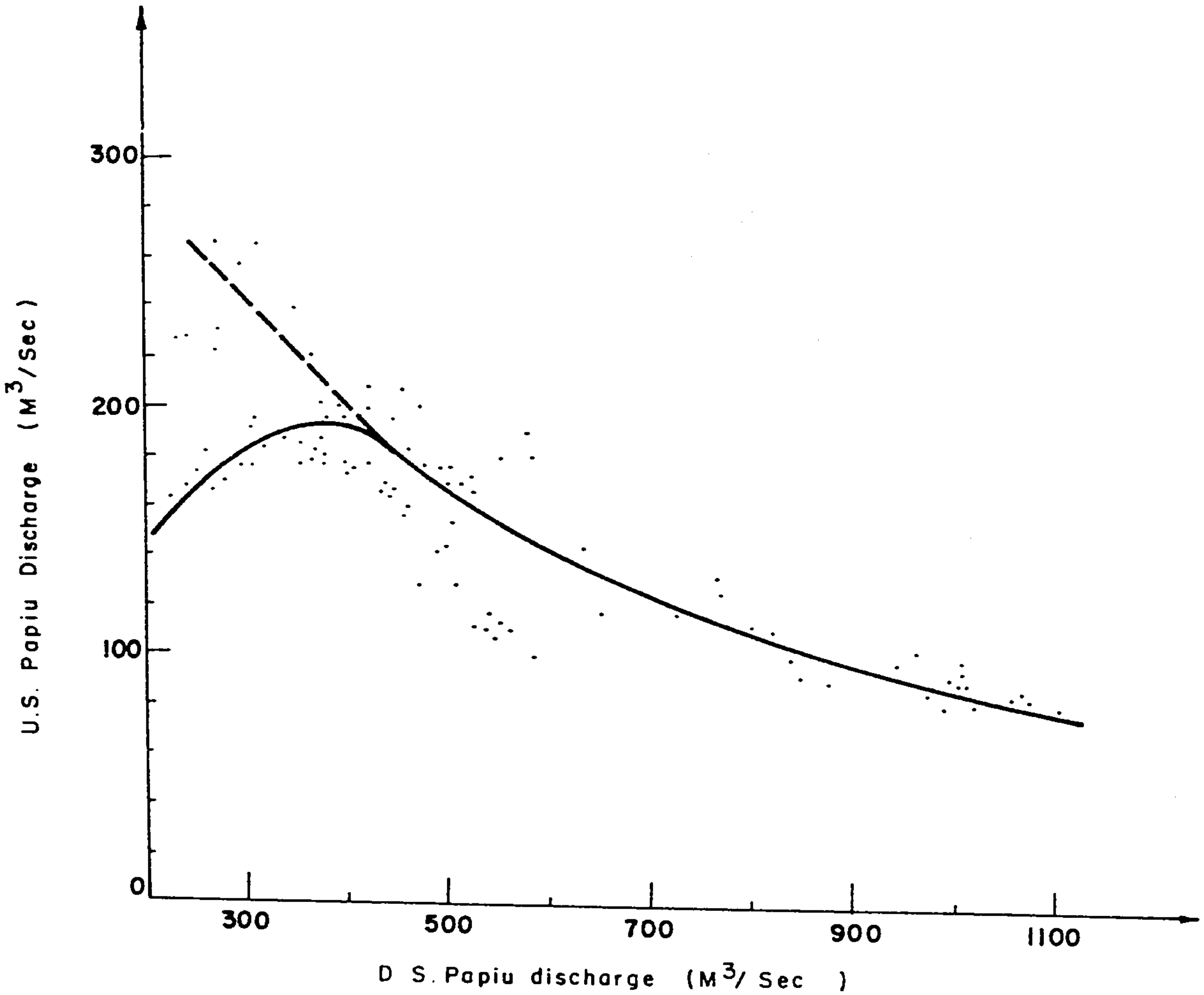

Fig(3.13) D.S PAPIU_U.S. PAPIU DISCHARGES RELATIONSHIP.

could be taken as the diffference between the measured discharge at R.P. 114 and at upstream Papiu. The discharge entering the Atem system were plotted against Papiu gauge level as shown in Fig. (3.14). From this figure, it can be seen that as Papiu gauge increases the discharge entering the Atem system increases. From the rating curve of D.S. Papiu Fig. (3.15), it could be visualized that the cross-section at D.S. Papiu is not a confined section for the gauge levels over 12.5 meters.

9. KENISA:

The gauge-discharge relationship for Kenisa sketched in Fig. (3.16) can be expressed by the equation $Y = 0.857\ X/100 + 8.4$, (X is the discharge in m^3 per second and Y is the gauge in meters). This relationship is valid for the period up to 1963. The years from 1965 up to 1967 were not recorded. The measurements that were taken during the last few years (1969-1971) were completely deviating from the previous relationship. This deviation could be caused by considerable changes in the gauge itself or in the geometry of the cross-section due to scour following the high floods period that started since 1962.

Plotting the sum of the discharges passing through the Atem branches at Jonglei versus the discharge entering the Atem system as given in Fig. (3.17), it could be concluded that there is a certain relationship between the discharges up to the 1957, namely $Y = 1.091X-45.45$, [Y as Jonglei (3) + Jonglei (4)] and X as (R.P. 114 -U.S. Papiu). This relationship does not hold for the period after 1957. This change happened because new unmeasured streams were born and started to convey some of the flow that was originally passing through Jonglei (3) and Jonglei (4) stations.

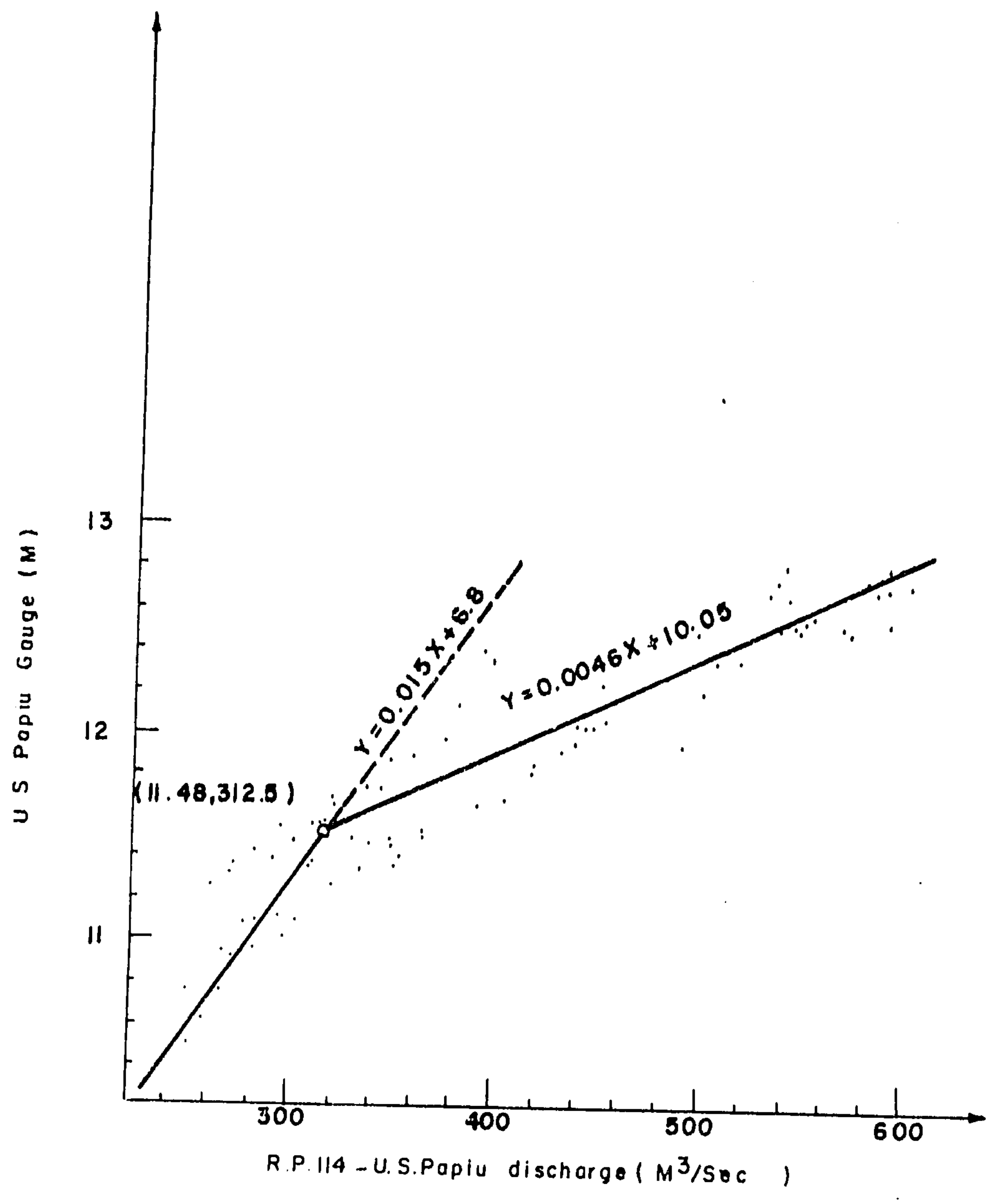

Fig.(3.14)(R.P.114 DISCHARGE – U.S.PAPIU) DISCHARGE VERSUS U.S. PAPIU GAUGE UP TO 1969.

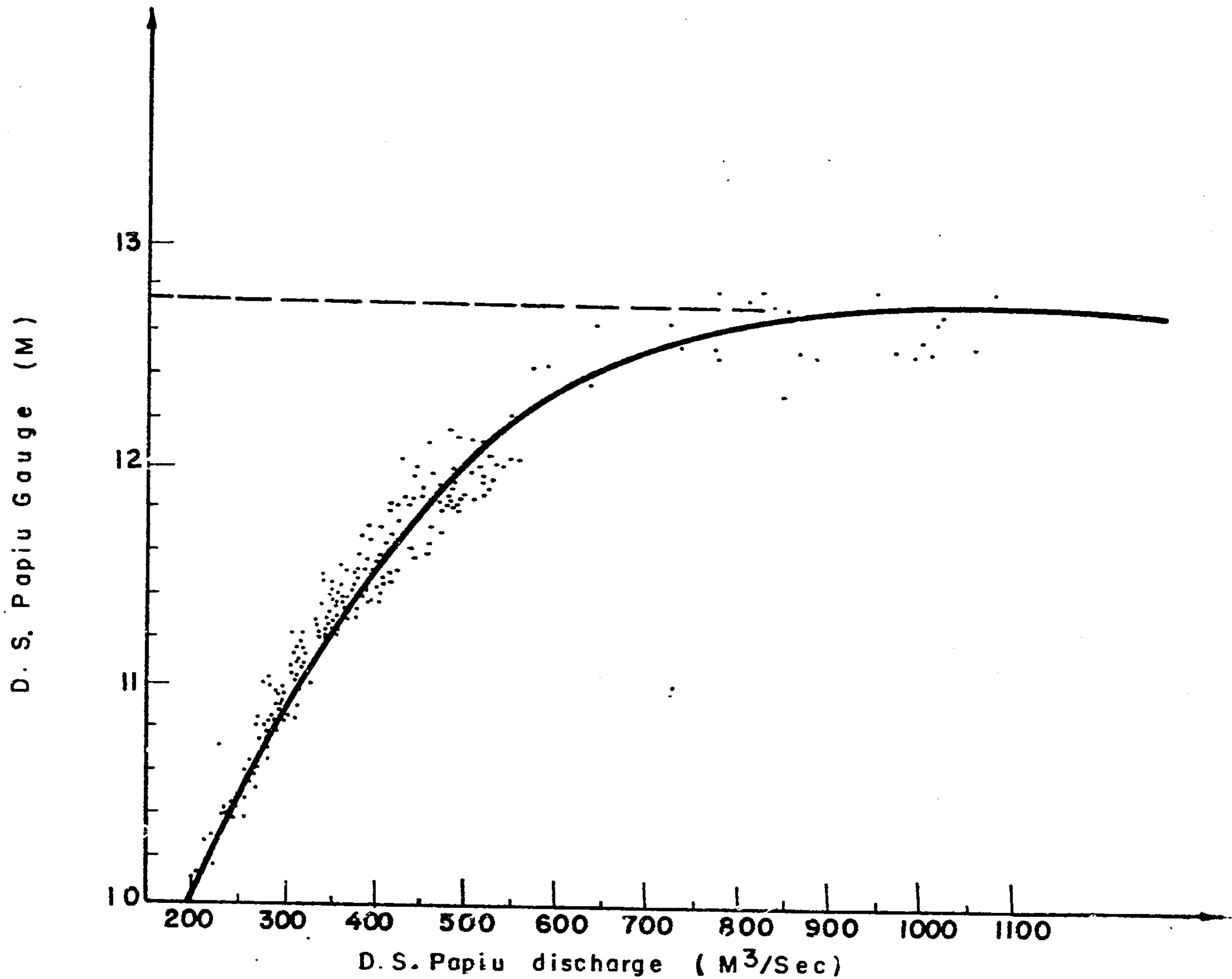

Fig.(3.15) D.S. PIPIU GAUGE_ DISCHARGE RELATIONSHIP.

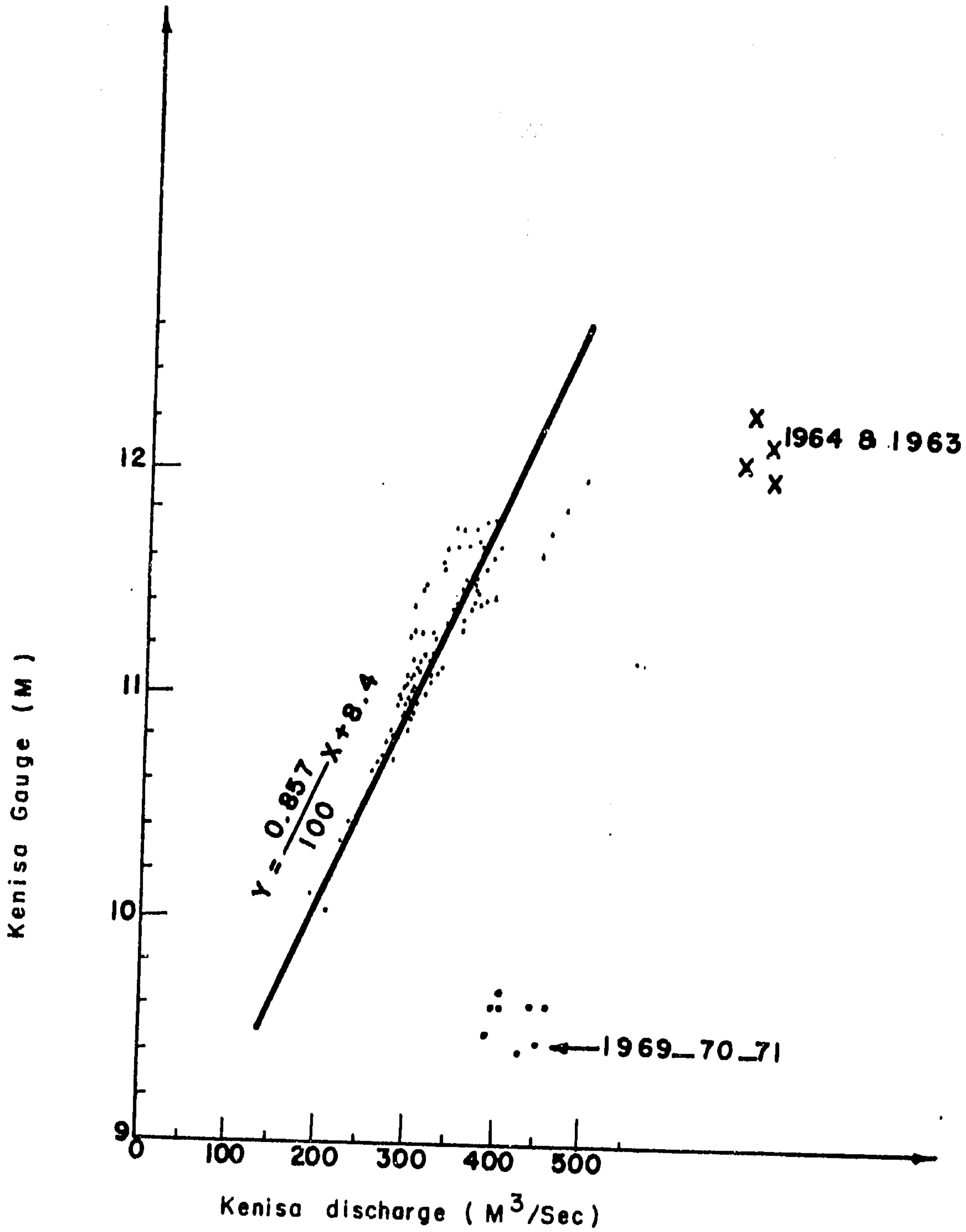

Fig.(3.16) KENISA GAUGE_DISCHARGE RELATIONSHIP.

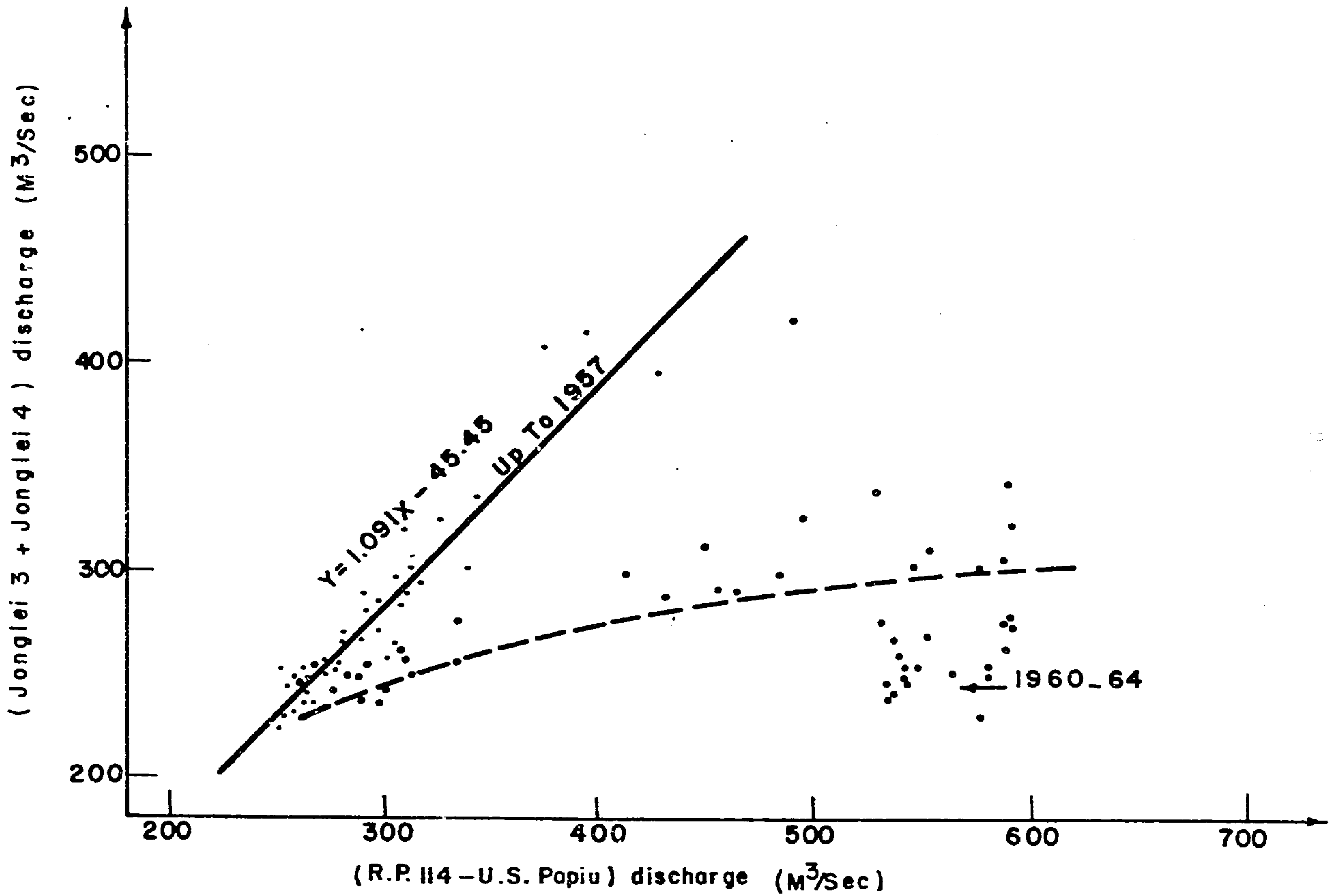

Fig.(3.17) (JONGLEI 3 + JONGLEI 4)–(R.P.114–U.S. PAPIU) DISCHARGES RELATIONSHIP UP TO 1964.

10. AWAI TAIL (1):

The discharges at two sites, upstream and downstream Awai tail were measured. The gauge levels and the discharge upstream Awai Tail (1) could not be related to each other, except for very short period of time, as shown in Fig. (3.18). The gauge-discharge relationship at downstream Awai Tail (1), Fig. (3.19) is represented by the shown relationship in the figure. From this curve, we can deduce that spilling at this section commences when the gauge level exceeds 11.60 meters.

11. DOWNSTREAM AWAI TAIL (3):

The gauge-discharge relationship for the period 1938-1968 is expressed as given in Fig. (3.20) by the relationship $Y = 0.0049X + 8.97$. The measurements of the period 1969-1972 are shown on the same figure indicating that considerable changes took place in the cross-section downstream Awai Tail (3) (X discharge in m^3 per second and Y gauge level in meter).

Attempts were made in order to correlate the gauge and the discharge data available for the reach from downstream Awai Tail (1) up to Lake No. No valuable conclusions were obtained. It is probable that the influence of some hydrological factors plays an active part in this phenomenon. These factors are:

i) The variation of the level of the stored water in Lake No.
ii) The spreading of the swamps along this reach.
iii) The existence of a back water curve developed by the Sobat river floods, which is extending up to lake No.

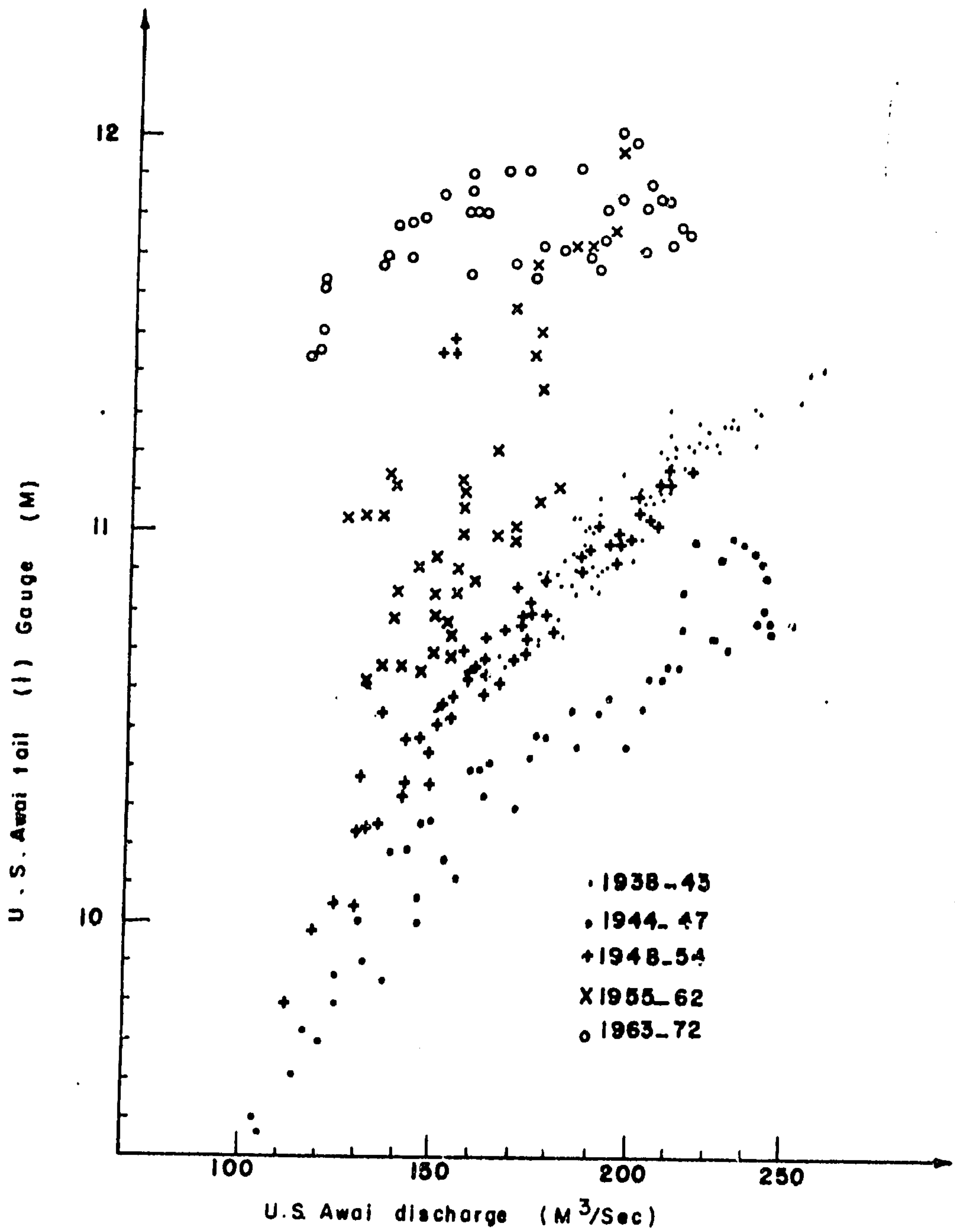

Fig(3.18) U.S. AWAI TAIL (I) GAUGE _ DISCHARGE RELATIONSHIP.

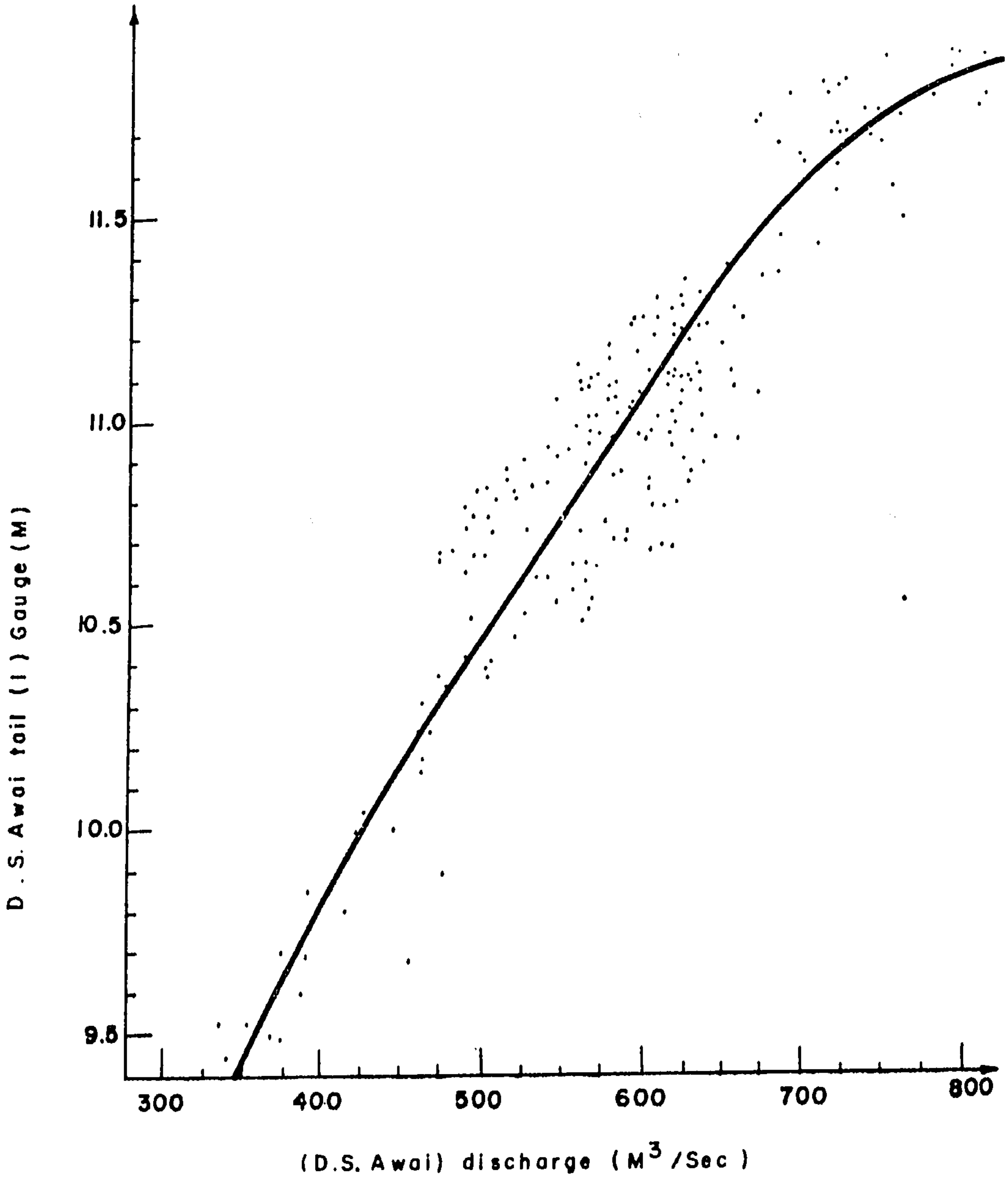

Fig. (3.19) D.S. AWAI TAIL (I) GAUGE – DISCHARGE RELATIONSHIP.

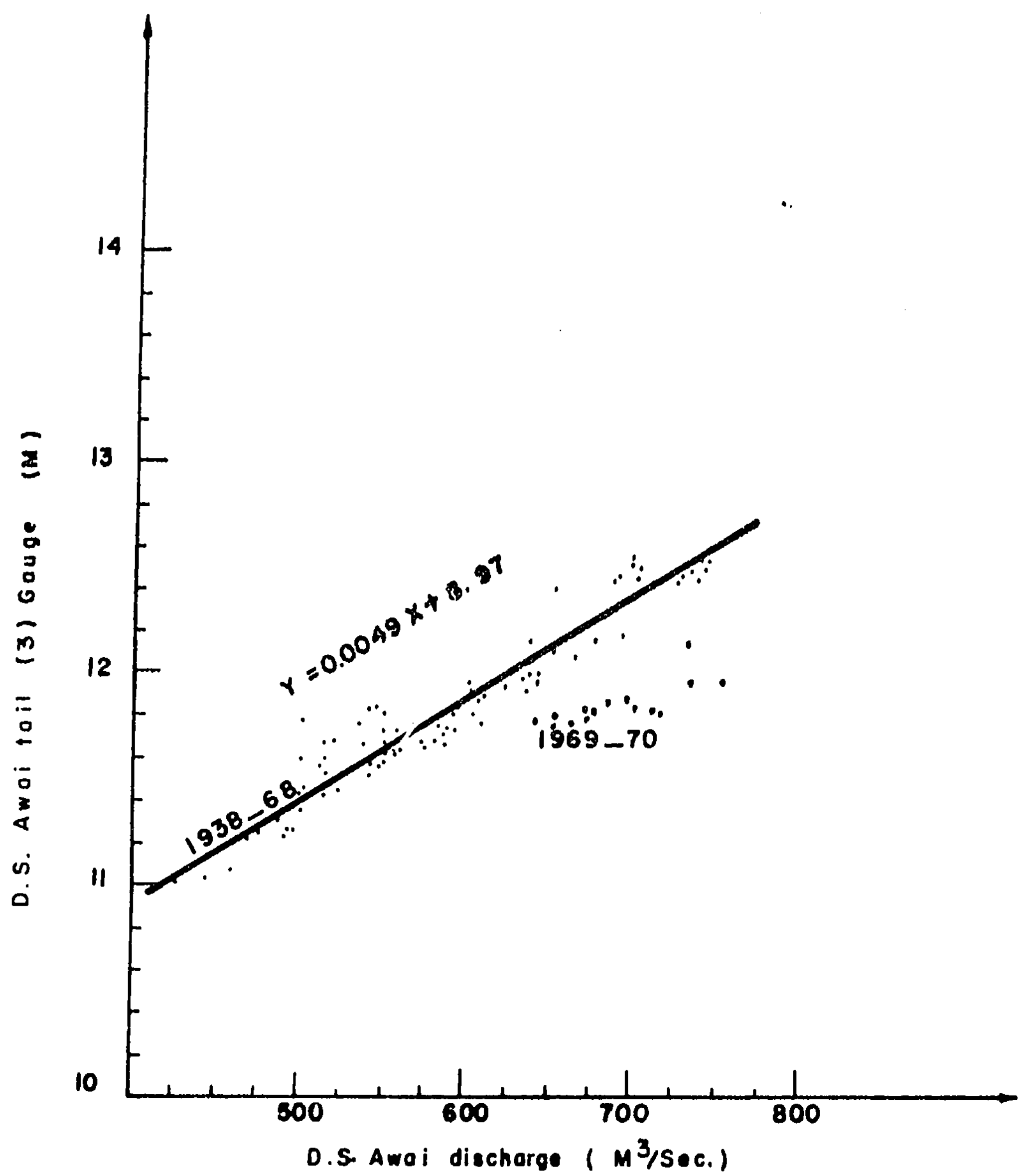

Fig.(3.20) D.S. AWAI TAIL (3) GAUGE DISCHARGE RELATIONSHIP.

CHAPTER IV

ROUTING SCHEMES FOR BAHR EL_GABEL

CHAPTER IV

ROUTING SCHEMES FOR BAHR EL-GABEL

4.1 INTRODUCTION

There are many pragmatical methods for flood routing. Examples are the method of characteristics, method of diffusion analogy, the Muskingom method and the least-squares correlation technique, refs. (2, 4 and 14). It can be said that:

i) Most of these methods require regular and precise recorded data as hourly or daily flows; this kind of data are not available for Bahr El-Gabel.

ii) The selection of the routing period depends on the lag time between stations, which cannot be defined accurately in our case of study.

iii) The hydraulic methods of routing need some data about the roughness and Chezy or Manning coefficients as well as the bed slope, which are not available.

iv) The reach of Bahr El-Gabel cannot be simulated to one confined reach in any way. This is due to the existence of several series of ponds and side channels.

Accordingly, one should conclude that the flow along Bahr El-Gabel could be routed using the direct correlation technique.

For problems in which a comparison of flows before and after the construction of control works or a comparison of various operation schedules is required, a true storage routing technique must be used, since actual data for the development of relations by statistical methods cannot be attained. For many problems, it is practicable to develop a routing technique by statistical analysis of observed data.

Using the least-squares technique has the disadvantage that it does not distinguish the variation in coefficients with the magnitude of rise. This disadvantage can be avoided by using the curve linear correlation, refs. (8-10).

4.2 SCHEMATIC REPRESENTATION OF BAHR EL-GABEL

This scheme was carried out with the aid of many maps, some of them were printed around 1930 and others were prepared during the period 1970-1975 using the aerial photogrametry and remote sensing devices, see Fig. (4.1).

The main goal during selecting this scheme was to preserve the main features of this reach. It should be realized that there are some variations from one map to another due to the hydrological nature and the geomorphology of this flat basin. Nevertheless, the selected scheme has delineated this main features. Moreover, some assumptions were made to simplify the existing complicated portions of the system, such as the series of ponds and swamps. As an example, the series of ponds known as Aliab system were represented as one channel. This channel started from the reach Terrekaka-Gemmeiza and ends at Lake Papiu. The Atem system with its different branches was represented also by one channel.

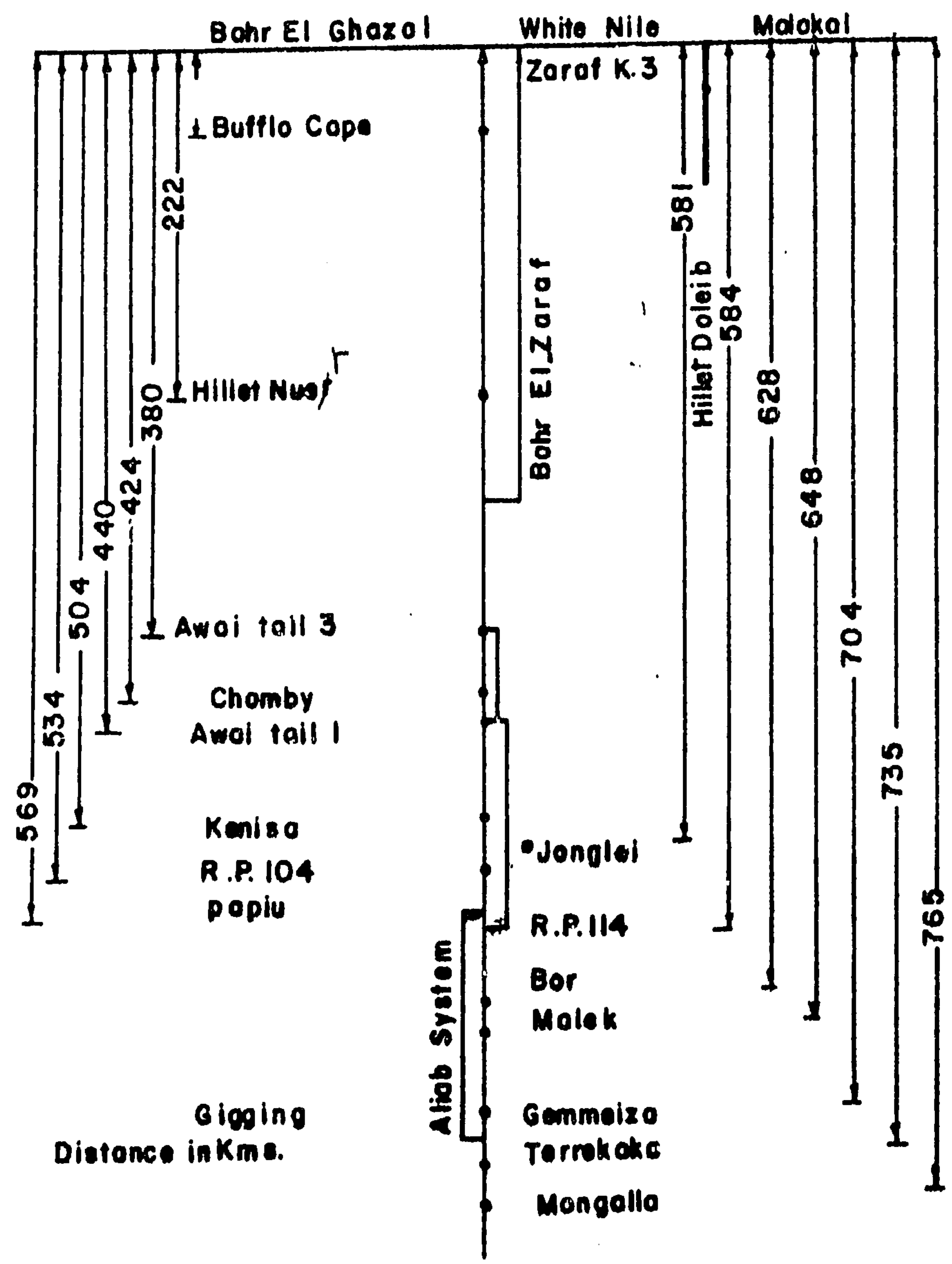

Fig.(4.1) SCHEMATIC REPRESENTATION OF BAHR EL-GABEL.

4.3 CONTROL LATITUDES AND REGRESSION EQUATIONS

In order to trace the flow passing through Bahr El-Gabel, many assumptions were taken into consideration. The flow of Bahr El-Gabel passes through six latitudes in order to reach Malakal. These latitudes were selected such that the sum of the discharges at each latitude indicates the total flow across Bahr El-Gabel, These control latitudes are representing the discharge of:

1) Mongalla.
2) Gemmeiza + Gigging.
3) Jonglei (3) + Jonglei (4) + Kenisa.
4) Downstream Awai Tail (3).
5) Bufflo Cape + Zaraf Kilo (3).
6) Malakal - Hillet Doleib.

The first latitude represents the input to Bahr El-Gabel system, while the last one models the output from this system. In order to find out the most suitable regression equation between each latitude and the successive one, attempts were carried out to fit the available discharge data to linear, exponential, logarithmic and power relationships. Therefore, the coeffecient of determination r^2 was calculated for each type of regression. This coeffecient indicates the quality of fittness achieved by the regression. Values of r^2 close to 1.0 demonstrate better fittness than values close to zero. Thus, the regression equation which had the value of r^2 close to unity, was selected to form a step in the regression between the different latitudes.

The regression equations for the whole scheme were developed for each month individually. This helped in including the seasonal effects. As, it is known, the conditions of the flow, whether it was rising or falling, storage as well as the meteorological factor affect the correlation between any two sites. Thus, the determination of the regression equations for each month avoids many complications. Another important advantage of using particular equation for each month, is to evaluate the losses or gains at that month. This was useful in the case of studying the operation of any local development project concerning any subreach.

4.4 THE FIRST ROUTING SCHEME FOR BAHR EL-GABEL

As it was mentioned before, sixty regression equations were obtained to represent the regression scheme along five reaches and six latitudes. It started from Mongalla discharge and ended by the yield at Malakal. These equations are arranged in Tables (4.1)-(4.5). Tables (4.6)-(4.7) illustrate the routed flow for the years 1959, 1952, 1937 and 1905 from Mongalla up to Malakal, by invoking this first routing scheme.

Using the developed regression scheme from Mongalla up to Malakal latitude, we can evaluate the routed flow at Malakal latitude. The corresponding estimated and measured discharges at Malakal (1905-1972) were tested as paired data. The T-test was applied for the residuals of the difference between the estimated and recorded discharges. The results of this test are presented in Table (4.8). It indicates that the regressions are not acceptable as a whole for months of January, August and September. Moreover, the other months can be accepted at low levels of significance. These results are expected due to the following reasons:

i) The tested period included an interval which was extremely high, that is from 1961 up to 1965. The records of this period were not incorporated in the regression scheme due to the abscence of sufficient and reliable data during this period.

ii) The outflow from Bahr El-Gabel is affected by Lake No conditions during August and September. This is because during these two months Lake No starts to receive the coming flood from Bahr El-Gabel. Also, at the same time, the flood of the Sobat river starts to take place. The capability of Lake No to accommodate all the coming floods, varied considerably according to the anticipated hydrological conditions.

iii) In January, Lake No starts to release the stored water, whereas the Sobat river begins its dry season.

Avoiding the extremes, the T-test was applied by using the same approach mentioned before, but covering only the period from 1905 to 1959. This elimination for the extremes changed the results of this test considerably, as it appears in Table (4.9).

4.5 THE SECOND ROUTING SCHEME FOR BAHR EL-GABEL

In order to define the expected hydrograph at Malakal after executing the proposed development projects, a simple routing scheme was developed. This scheme was formed by two main regression linear equations. The first one represents the arriving monthly flow to Jonglei latitude [Jonglei (3) + Jonglei (4) + Kenisa] as a function of the monthly flow at Mongalla, while the second models the arriving flow to Malakal station as a function of the monthly flow at Jonglei latitude and the monthly flow at Hillet Doleib. The first regression equation gave a coefficient of correlation of 0.88, [see Table (4.10)]. The first equation was used to estimate the monthly flows at Jonglei latitude for the period 1937-1959. Comparison between the recorded and the estimated monthly flows at Jonglei latitude is illustrated in Fig. (4.2). The second multi-regression equation, see Table (4.10), had correlation coefficients of 0.99 and 0.63 for Malakal against Hillet Doleid and

Jonglei latitude respectively.

The simple regression scheme was used to estimate the yearly hydrograph at Malakal for the period 1905-1972, and the normal yearly hydrograph for the same period. Comparison between the recorded and the estimated yearly hydrograph is shown in Fig. (4.3). Furthermore, the comparison between the recorded and the estimated normal yearly hydrographs is shown in Fig (4.4). From the last two figures, it could be concluded that the estimated hydrographs are not significantly different from the recorded hydrographs, and demonstrates the effectiveness of the applies routing scheme.

Table (4.1)

Regression relations between Mongalla (X) and Gigging + Gemmeiza (Y), (X and Y are monthly flows in million m^3).

Month	Regression equation	A	B	Coefficient of determination
Jan.	$Y = A * X^B$	2.55	0.87	0.94
Feb.	$Y = A * X^B$	3.78	0.82	0.90
Mar.	$Y = A * X^B$	3.96	0.81	0.89
Apr.	$Y = A * X^B$	3.39	0.83	0.93
May	$Y = A * X^B$	2.07	0.90	0.95
June	$Y = A * X^B$	2.08	0.90	0.95
July	$Y = A * e^{B.X}$	1182.51	0.000274	0.93
Aug.	$Y = A * e^{B.X}$	1237.91	0.000255	0.94
Sep.	$Y = A * X^B$	3.08	0.85	0.93
Oct.	$Y = A * X^B$	3.17	0.85	0.91
Nov.	$Y = A * X^B$	2.37	0.89	0.95
Dec.	$Y = A * X^B$	2.41	0.88	0.94

Table (4.2)

Regression relations between Gigging + Gemmeiza (X) and Jonglei latitude (Y), (X and Y are monthly flows in million m^3).

Month	Regression equation	A	B	Coefficient of determination.
Jan.	$Y = A * X^B$	3.84	0.80	0.96
Feb.	$Y = A * X^B$	3.16	0.83	0.96
Mar.	$Y = A * X^B$	3.33	0.82	0.94
Apr.	$Y = A * e^{B.X}$	581.39	0.000516	0.90
May	$Y = A * X^B$	5.70	0.74	0.69
June	$Y = A + B.X$	860.79	0.40	0.49
July	$Y = A * X^B$	7.75	0.71	0.67
Aug.	$Y = A + B.X$	605.51	0.51	0.56
Sep.	$Y = A + B.X$	576.60	0.56	0.53
Oct.	$Y = A * X^B$	9.10	0.70	0.65
Nov.	$Y = A + B.X$	450.82	0.68	0.75
Dec.	$Y = A + B.X$	497.00	0.64	0.86

Table (4.3)

Regression relations between Jonglei latitude (X) and Downstream Awai Tail 3 (Y), (X and Y are monthly flows in million m^3).

Month	Regression equation	A	B	Coefficient of determination.
Jan.	$Y = A + BX$	1050.63	0.24	0.52
Feb.	$Y = A * X^B$	58.75	0.43	0.76
Mar.	$Y = A + B \ln X$	-3543.29	672.67	0.80
Apr.	$Y = A + B \ln X$	-4600.70	813.60	0.81
May	$Y = A * X^B$	11.33	0.65	0.74
June	$Y = A + B.X$	671.16	0.42	0.54
July	$Y = A + B.X$	945.90	0.27	0.56
Aug.	$Y = A + B.X$	908.81	0.30	0.69
Sep.	$Y = A * X^B$	259.67	0.23	0.37
Oct.	$Y = A * X^B$	238.37	0.24	0.49
Nov.	$Y = A * X^B$	186.05	0.27	0.45
Dec.	$Y = A + BX$	1182.24	0.17	0.24

Table (4.4)

Regression relations between Downstream Awai Tail 3 (X) and Zaraf latitude (Y), (X and Y are monthly flows in million m^3).

Month	Regression equation	A	B	Coefficient of determination
Jan.	$Y = A * X^B$	27.67	0.52	0.43
Feb.	$Y = A + B.X$	856.99	0.22	0.23
Mar.	$Y = A * e^{B.X}$	850.56	0.000266	0.47
Apr.	$Y = A * X^B$	24.67	0.54	0.83
May	$Y = A * e^{B.X}$	519.75	0.000598	0.87
June	$Y = A * X^B$	9.97	0.66	0.65
July	$Y = A * X^B$	5.44	0.74	0.63
Aug.	$Y = A + B.X$	715.36	0.36	0.45
Sep.	$Y = A * B^X$	93.65	0.35	0.40
Oct.	$Y = A + B.X$	709.18	0.37	0.38
Nov.	$Y = A + B.X$	785.33	0.30	0.24
Dec.	$Y = A * X^B$	22.61	0.55	0.55

Table (4.5)

Regression relations between Zaraf latitude (X) and Malakal latitude (Y), (X and Y are monthly flows in million m^3).

Month	Regression equation	A	B	Coefficient of determination
Jan.	$Y = A * X^B$	0.91	1.01	0.31
Feb.	$Y = A * X^B$	3.68	0.81	0.44
Mar.	$Y = A * X^B$	3.22	0.84	0.59
Apr.	$Y = A * X^B$	4.82	0.77	0.78
May	$Y = A * X^B$	3.65	0.81	0.79
June	$Y = A * e^{B.X}$	512.30	0.000626	0.54
July	$Y = A * X^B$	21.12	0.56	0.37
Aug.	$Y = A * X^B$	2.51	0.86	0.35
Sep.	$Y = A * X^B$	2.25	0.87	0.19
Oct.	$Y = A + B.X$	55.00	0.89	0.25
Nov.	$Y = A * X^B$	0.70	1.04	0.34
Dec.	$Y = A * X^B$	0.07	1.37	0.32

Table (4.6)

Routed flow at Malakal lat. (1959, 1905).

	Jan.	Feb.	Mar.	Apr.	May	June	July	Aug.	Sep.	Oct.	Nov.	Dec.
<u>Recorded (1959):</u>												
Mongalla	1760	1490	1580	1550	2120	1910	1900	2440	2390	2220	2030	1820
Gigging + Gemm.	1698	1511	1543	1507	2040	1866	1990	2306	2291	2215	2081	1781
Jonglei lat.	1473	1376	1371	1265	1603	1606	1704	1781	1859	1999	1865	1637
D.S.A.T. 3	1403	1314	1315	1211	1372	1345	1406	1443	1466	1477	1421	1460
Zaraf lat.	1198	1146	1207	1148	1180	1157	1161	1234	1201	1255	1211	1243
Estimated Malakal lat.	1170	1106	1248	1069	1124	1057	1099	1143	1075	1172	1126	1215
Recorded Malakal lat.	1239	1097	1191	1146	1156	1075	1130	1160	1120	1140	1090	1140
<u>Recorded (1905):</u>												
Mongalla	3060	2570	2640	2580	3110	2670	2840	3040	3500	3200	3450	3500
Gigging + Gemm.	2748	2363	2339	2308	2880	2523	2574	2687	3169	3022	3337	3168
Jonglei lat.	2165	1994	1928	1912	2069	1869	2046	1975	2350	2485	2719	2524
D.S.A.T. 3	1569	1541	1545	1540	1620	1456	1498	1501	1548	1556	1573	1611
Zaraf lat.	1270	1196	1282	1298	1369	1220	1217	1255	1224	1284	1257	1312
Estimated Malakal lat.	1241	1145	1314	1203	1267	1118	1128	1160	1093	1198	1170	1309
Recorded Malakal lat.	1785	1369	1277	1080	1076	991	1050	1050	1090	1160	1130	1170

Table (4.7)

Routed flow at Malakal lat. (1952, 1937).

	Jan.	Feb.	Mar.	Apr.	May	June	July	Aug.	Sep.	Oct.	Nov.	Dec.
Recorded (1952):												
Mongalla	1870	1640	1680	1910	2400	2180	2420	3530	3180	3150	2400	2250
Gigging + Gemm.	1790	1635	1622	1792	2281	2102	2294	3045	2921	2982	2416	2147
Jonglei lat.	1537	1469	1428	1466	1741	1700	1873	2158	2212	2461	2093	1871
D.S.A.T. 3	1418	1351	1343	1338	1448	1385	1451	1556	1526	1552	1446	1500
Zaraf Lat.	1205	1154	1215	1200	1235	1180	1189	1275	1218	1283	1224	1262
Estimated Malakal lat.	1177	1112	1256	1132	1165	1072	1114	1176	1088	1197	1139	1240
Recorded Malakal lat.	1172	1029	1061	1023	1092	1034	1020	1060	1030	1080	1050	1250
Recorded (1937):												
Mongalla	1810	1630	1730	1858	2500	2250	2910	3170	2350	2650	2730	2510
Gigging + Gemm.	1740	1627	1661	1776	2366	2162	2624	2778	2259	2575	2709	2364
Jonglei lat.	1502	1462	1456	1454	1789	1725	2074	2021	1841	2221	2292	2010
D.S.A.T. 3	1410	1349	1356	1324	1474	1395	1506	1515	1463	1515	1502	1523
Zaraf lat.	1201	1153	1219	1197	1254	1186	1222	1260	1200	1269	1235	1273
Estimated Malakal lat.	1173	1112	1260	1138	1180	1076	1131	1164	1074	1184	1149	1255
Recorded Malakal lat.	1280	1129	1198	1152	1127	1067	1100	1170	1150	1240	1110	1270

Table (4.8)

Results of T-Test on the First routing scheme, [T Statistic, Two tailed test (degrees of freedom = 67)].

$H_o : M_1 = M_2$

M_1 = Recorded mean

M_2 = Estimated mean (period 1905-1972)

For Sample Size N = 68

Month	T-Statistic	Accepted at level of significance
Jan.	4.0973	rejected
Feb.	3.1919	0.001
Mar.	1.5264	0.100
Apr.	2.6138	0.010
May	1.3089	0.100
June	2.0387	0.020
July	2.3351	0.020
Aug.	4.6316	rejected
Sep.	4.1298	rejected
Oct.	3.2512	0.001
Nov.	2.8204	0.001
Dec.	2.4406	0.010

Table (4.9)

Results of T-Test on the First routing scheme excluding extreme data [T Statistics, Two-tailed test (degrees of freedom =54)].

$H_o : M_1 = M_2$

M_1 = Recorde mean

M_2 = Estimated mean

(period 1905-1959)

For Sample Size N = 55

Month	T-Statistic	Accepted at level of significance
Jan.	5.1648	rejected
Feb.	3;3548	0.001
Mar.	-1.0912	0.200
Apr.	1.2724	0.200
May	-0.9583	0.200
June	-0.9497	0.200
July	-0.3710	0.200
Aug.	4.0925	rejected
Sep.	3.5311	rejcted
Oct.	2.2458	0.020
Nov.	0.5788	0.200
Dec.	-0.0812	0.200

Table (4.10) Regression Coefficients of the second routing scheme.

Dependent variable = JONGLEI
Independent variable = MONGALA

VARIABLE	N	MEAN	VARIANCE	STANDARD DEVIATION	COEFFICIENT OF VARIATION
MONGALA	251	2068.90837	275432.22756	524.81638	25.36683
JONGLEI	251	1691.04382	95952.01007	309.76121	18.31775

CORRELATION = .883211345111

VARIABLE	REGRESSION COEFFICIENTS STD. FORMAT	REGRESSION COEFFICIENTS E-FORMAT	STANDARD ERROR REG. COEFFICIENT	T-VALUE
'CONSTANT'	612.53040	.612530397930E+03	37.43696	16.36
X^1	.52130	.521295889287E+00	.01754	29.72

Dependent variable = MALAKAL
Independent variable(s) = JONG.
SOBAT

VARIABLE	N	MEAN	VARIANCE	STANDARD DEVIATION	COEFFICIENT OF VARIATION
JONG.	264	1712.14773	107438.57506	327.77824	19.14427
SOBAT	264	1086.72917	537953.16990	733.45291	67.49178
MALAKAL	264	2236.83902	533058.75973	730.10073	32.64020

VARIABLE	REGRESSION COEFFICIENTS STD. FORMAT	REGRESSION COEFFICIENTS E-FORMAT	STANDARD ERROR REG. COEFFICIENT	T-VALUE
'CONSTANT'	1092.77368	.109277368233E+04	34.56509	31.61
JONG.	.05103	.510255306100E-01	.02328	2.19
SOBAT	.97237	.972369306888E+00	.01040	93.45

CORRELATION MATRIX	SOBAT	MALAKAL
JONG.	.6189570	.6275192
SOBAT		.9910020

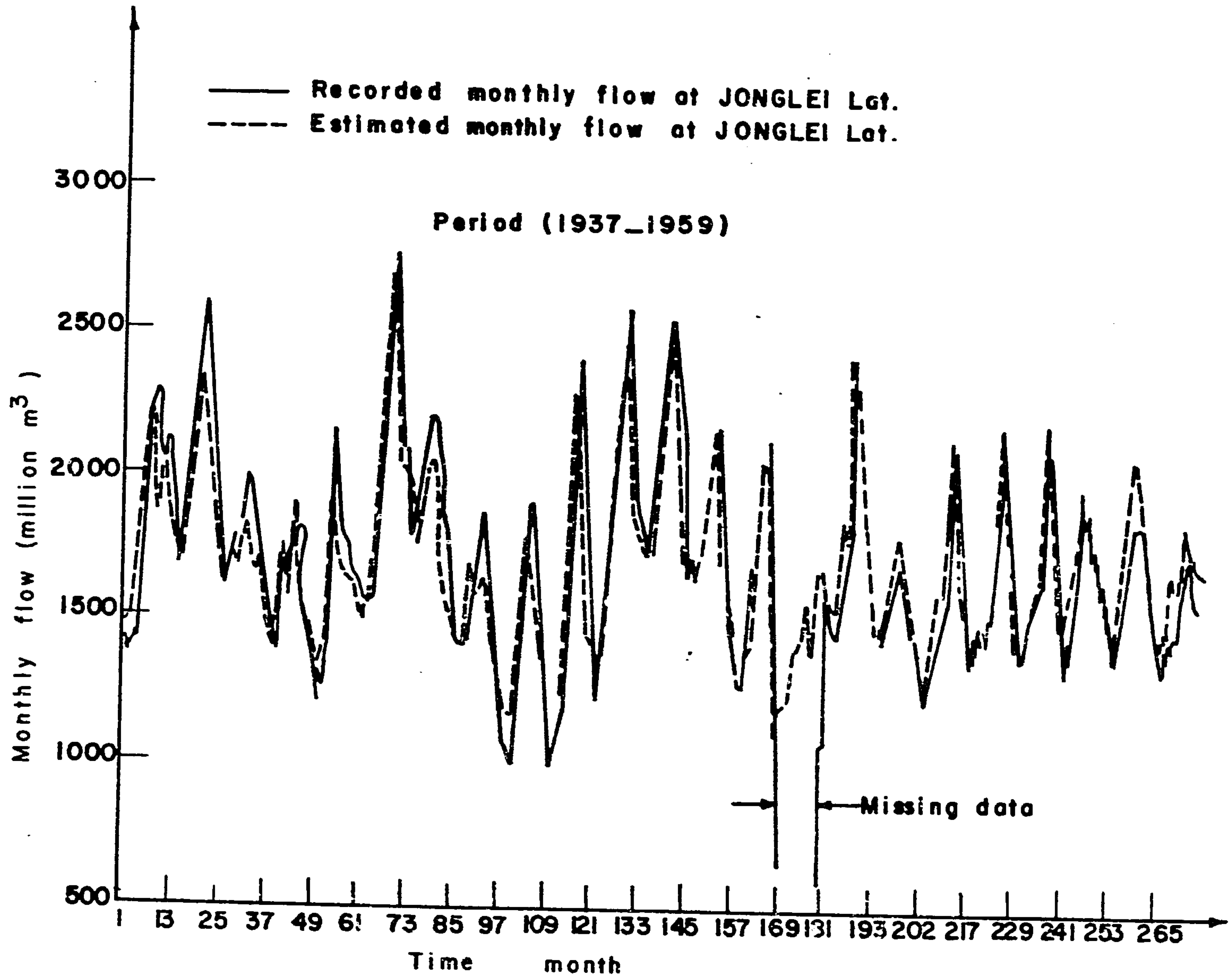

Fig.(4.2) RECORDED VERSUS ESTIMATED MONTHLY FLOWS AT STATION JONGLEI LATITUDE.

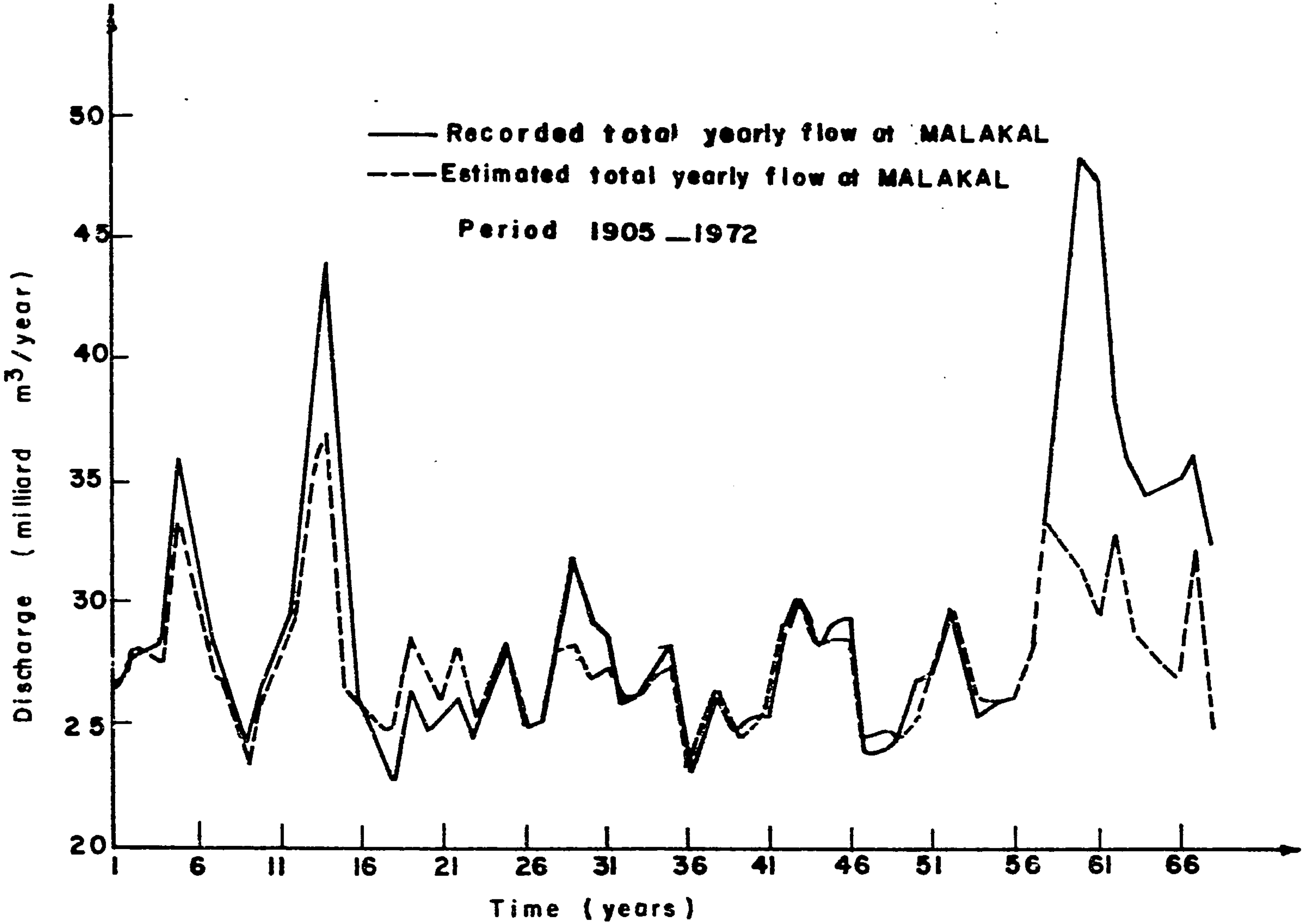

Fig. (4-3) RECORDED VERSUS ESTIMATED FLOWS AT MALAKAL INVOKING ROUTING SCHEME.

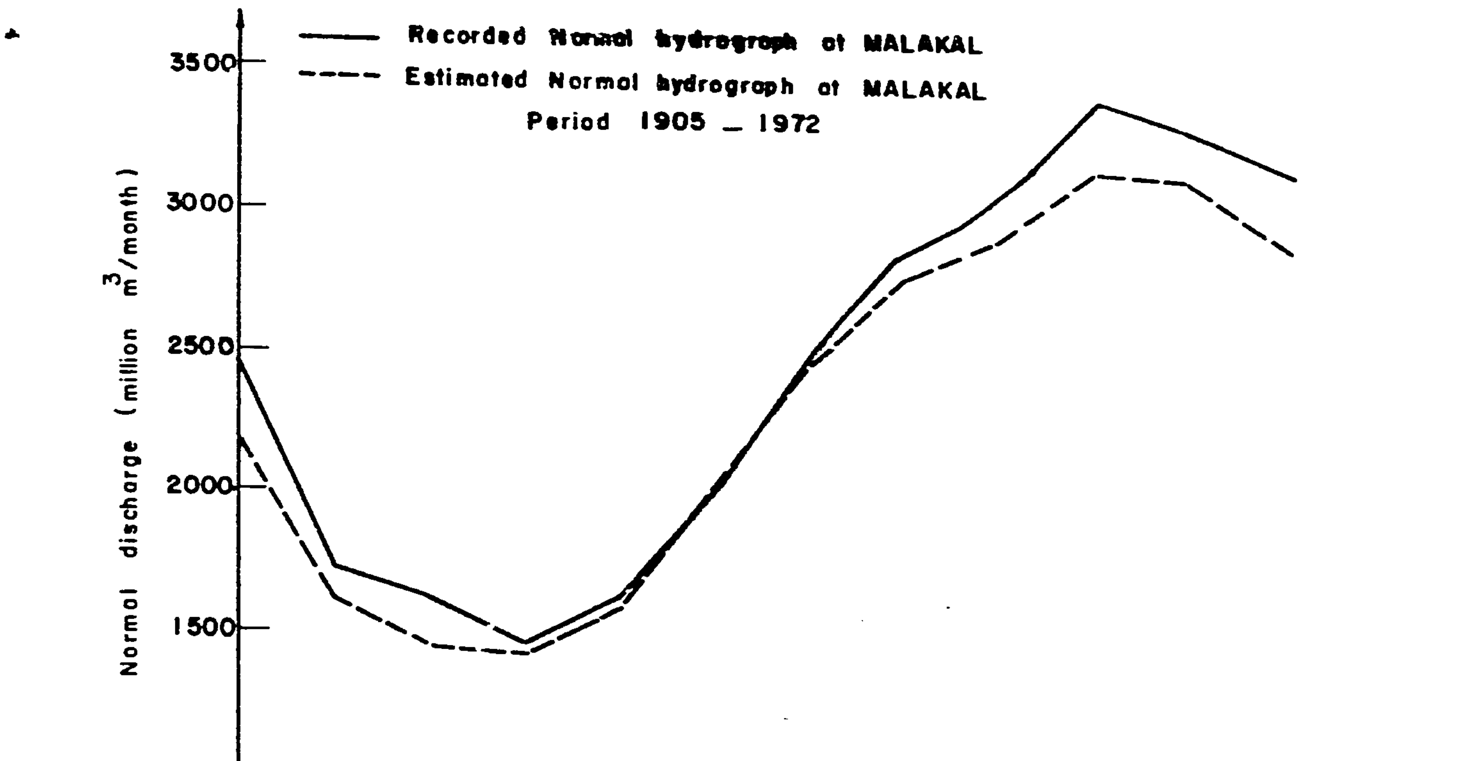

Month	Jan.	Feb.	Mar.	Apr.	May	June	July	Aug.	Sep.	Oct.	Nov.	Dec.
Estimated Mean	2194	1625	1463	1423	1599	2031	2464	2773	2931	3176	3135	2908
Recorded Mean	2474	1732	1633	1478	1642	2003	2504	2873	3074	3412	3314	3163
Mean Error	280	107	170	55	43	- 23	40	100	143	236	179	255
% Error	0.11	0.06	0.1	0.04	0.03	0.01	0.02	0.04	0.05	0.07	0.05	0.08

Recorded mean yearlyflow = 29.307 milliard m^3

Estimated mean yearly flow = 27.722 milliard m^3

Fig.(4.4) RECORDED VERSUS ESTIMATED HYDROGRAPH AT MALAKAL USING ROUTING SCHEME.

CHAPTER V

EXPECTED WATER BENEFITS OF DEVELOPMENT PROJECTS

CHAPTER V

EXPECTED WATER BENEFITS OF DEVELOPMENT PROJECTS

5.1 INTRODUCTION

Many development projects were proposed to be constructed along the area of Bahr El-Gabel. The main goal for these projects is to save as much water as possible, and to collect some water from the adjacent catchments, to be diverted to Bahr El-Gabel and Jonglei canal. In this chapter, the circumstances and the constraints of some projects are simulated utilizing the second routing scheme. The water benefits are then calculated for different operating schemes in the form of the water benefit as a total yearly amount and for the normal distribution of this benefit along the year. The recorded monthly flow data for the period 1905-1972 are used in the analysis. Some conditions were added to the second routing scheme according to the new constraints and flow conditions.

5.2 JONGLEI CANAL AND SOUTHERN COLLECTING BAHR EL-GHAZAL CANAL

Jonglei canal project was one of the earliest projects studied to reduce the Nile water losses. The expected water benefit is intended for increasing the agricultural production in Sudan and Egypt, ref. (1). The construction of Jonglei canal project started actually in 1976. The ultimate water benefit from this project will be attained in two stages. Phase I comprises the construction of a canal with a certain capacity and the auxiliary hydraulic structures, while phase II includes the enlargement of the canal together with the regulation of Equatorial lakes. The regulation of the Equatorial lakes will be performed such that it functions as over-year storage reservoirs to ensure the higher capacity of the canal. In phase I, 20 million m^3/day were to be diverted from a point on Bahr El-Gabel to the Sobat mouth near its confluence with the White Nile. In pahse II, the canal will have the capability of conveying 43 million m^3/day. The conveyance losses through the new canal will be about 5% of its inflow, ref. (5).

The plan for executing the Southern collecting canal of Bahr El-Ghazal is still under study stage. Generally, this project aims at collecting some water from the subcatchments of Bahr El-Ghazal by using intersecting collecting canal. This canal will be designed to convey discharge equivalent to 75% from the maximum recorded flow that had occured. This collecting canal is expected to join Bahr El-Gabel at Jonglei, ref.(5).

5.3 EXPECTED WATER BENEFITS

5.3.1 Expected Water Benefit From Jonglei Canal, Phases I And II

Using the second routing scheme, the recorded monthly flow at Mongalla for the period 1905-1972 were routed to Malakal according to the following cases:

Case (I): In this case, the only constraint taken was the abstraction of Jonglei canal phase I. This abstraction was assumed to be 20 million m^3/day. The expected normal monthly flow hydrograph and the recorded one were plotted in Fig. (5.1). The area enclosed

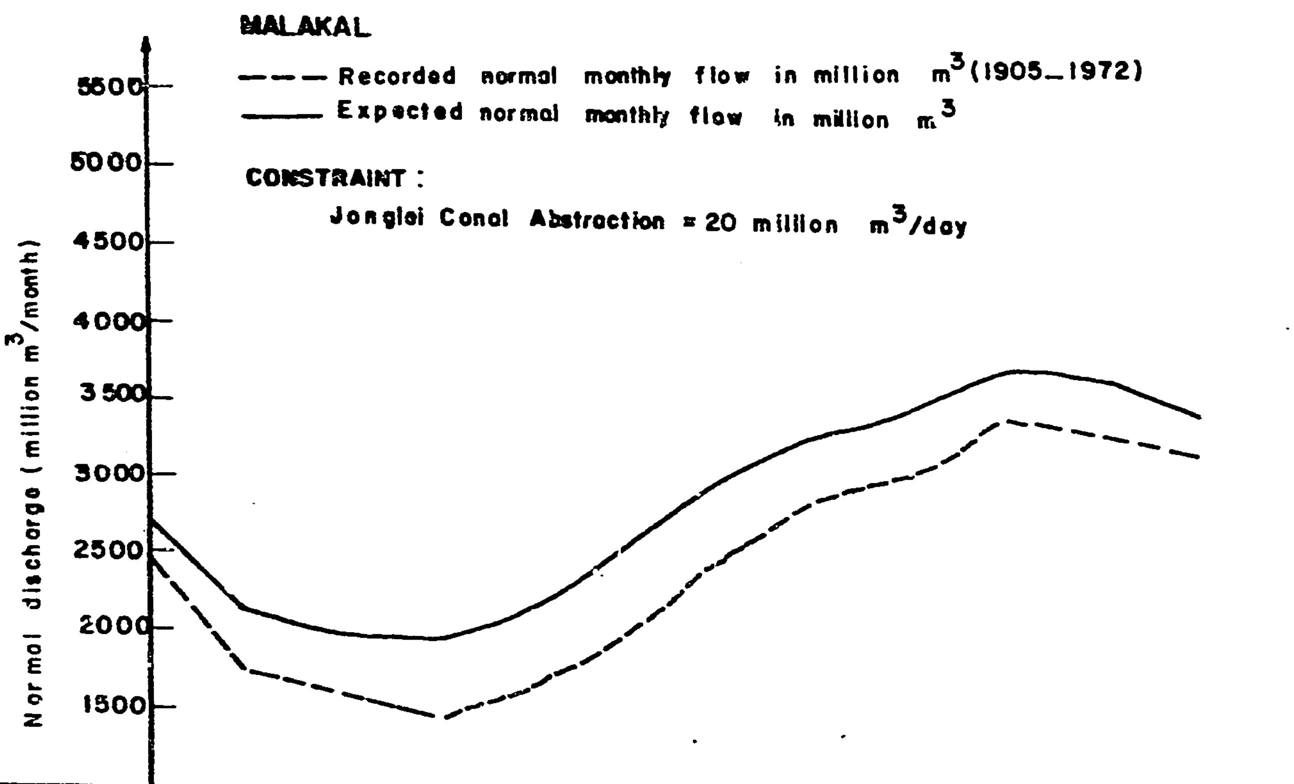

Month	Jan.	Feb.	Mar.	Apr.	May	June	July	Aug.	Sep.	Oct.	Nov.	Dec.
Expected Normal	2734	2164	2003	1963	2139	2570	3004	3312	3471	3715	3675	3447
Recorded Normal	2474	1732	1633	1478	1642	2008	2504	2873	3074	3412	3314	3163
Water Benefit	2260	432	370	485	497	562	500	439	397	303	361	284

Normal yearly water benefit = 4.89 milliard m^3/year

Fig.(5.1) EXPECTED WATER BENEFIT FROM JONGLEI CANAL, CASE I.

between the two hydrographs indicates the normal yearly water benefit. From these two hydrographs, the yearly water benefit was estimated as 4.89 milliard m^3/year.

Case (2): In this case of study, two constraints were taken into consideration. The first was that the diverted flow to Jonglei canal phase I, is 20 million m^3/day. The second was that the minimum navigation requirements in Bahr El-Gabel is 13 million m^3/day. Fig. (5.2) shows the expected normal monthly hydrograph and the expected yearly water benefit. Comparing the results obtained from case (1) and case (2), it can be concluded that fulfilling the navigation requirements has no effect on the expected water benefit.

Case (3): In this case, the diverted flow to Jonglei canal phase II is assumed to be 43 million m^3/day. The normal monthly hydrograph and the yearly water benefit for this case are illustrated in Fig. (5.3).

Case (4): Two constraints were taken into consideration. The first was the diverted flow to Jonglei canal phase II assumed to be 43 million m^3/day. The second was the navigation requirements in Bahr El-Gabel assumed as 13 million m^3/day. The normal monthly hydrograph and the yearly water benefit in this case are delineated in Fig. (5.4). From the results obtained in cases (3) and (4), it can be inferred that, the fulfillment of the navigation requirements for Jonglei canal phase II will cause the reduction of 0.7 milliard m^3/day from the expected water benefit.

MALAKAL

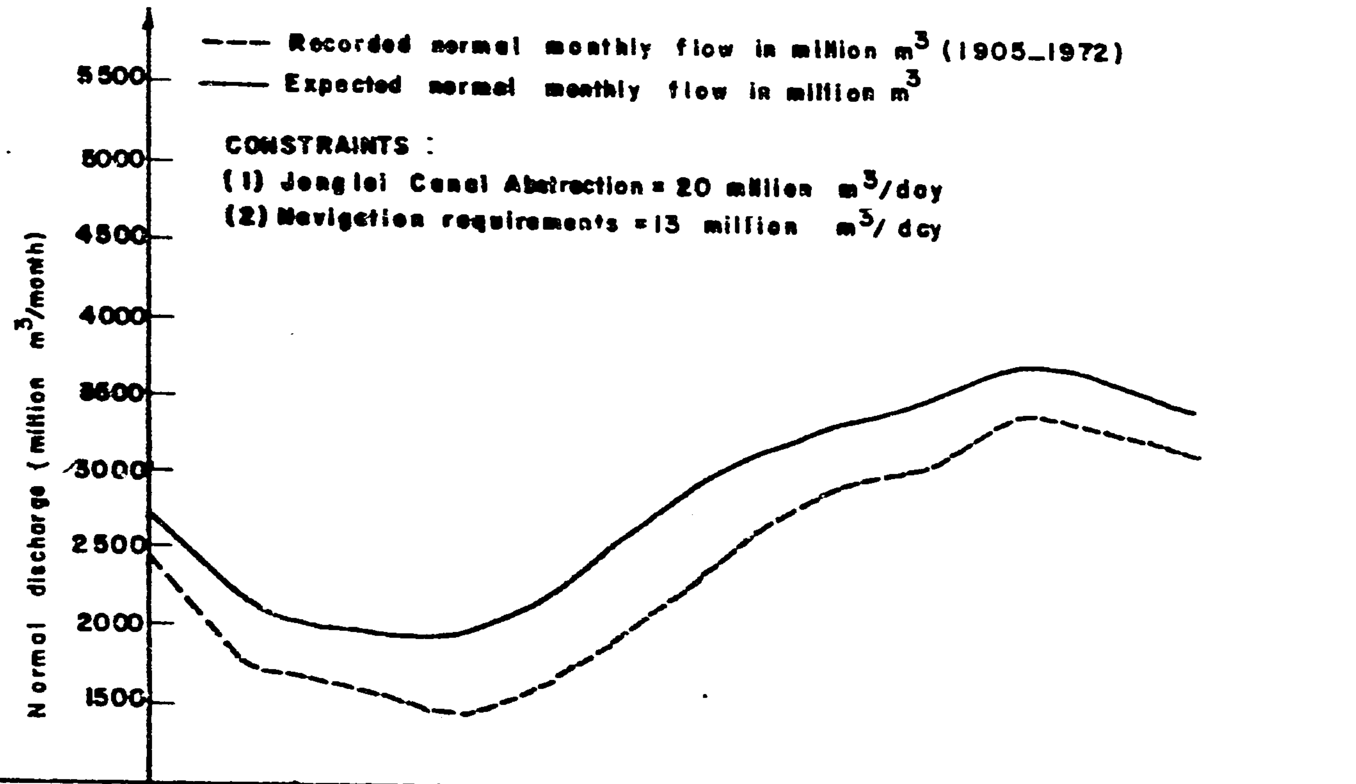

Month	Jan.	Feb.	Mar.	Apr.	May	June	July	Aug.	Sep.	Oct.	Nov.	Dec.
Expected Normal	2734	2164	2003	1963	2139	2570	3004	3312	3471	3715	3675	3447
Recorded Normal	2474	1732	1633	1478	1642	2008	2504	2874	3074	3412	3314	3163
Water Benefit	260	432	370	485	497	562	500	439	397	303	361	284

Normal yearly Water benefit = 4.89 milliard m^3/year

Fig.(5-2) EXPECTED WATER BENEFIT FROM JONGLEI CANAL, CASE 2.

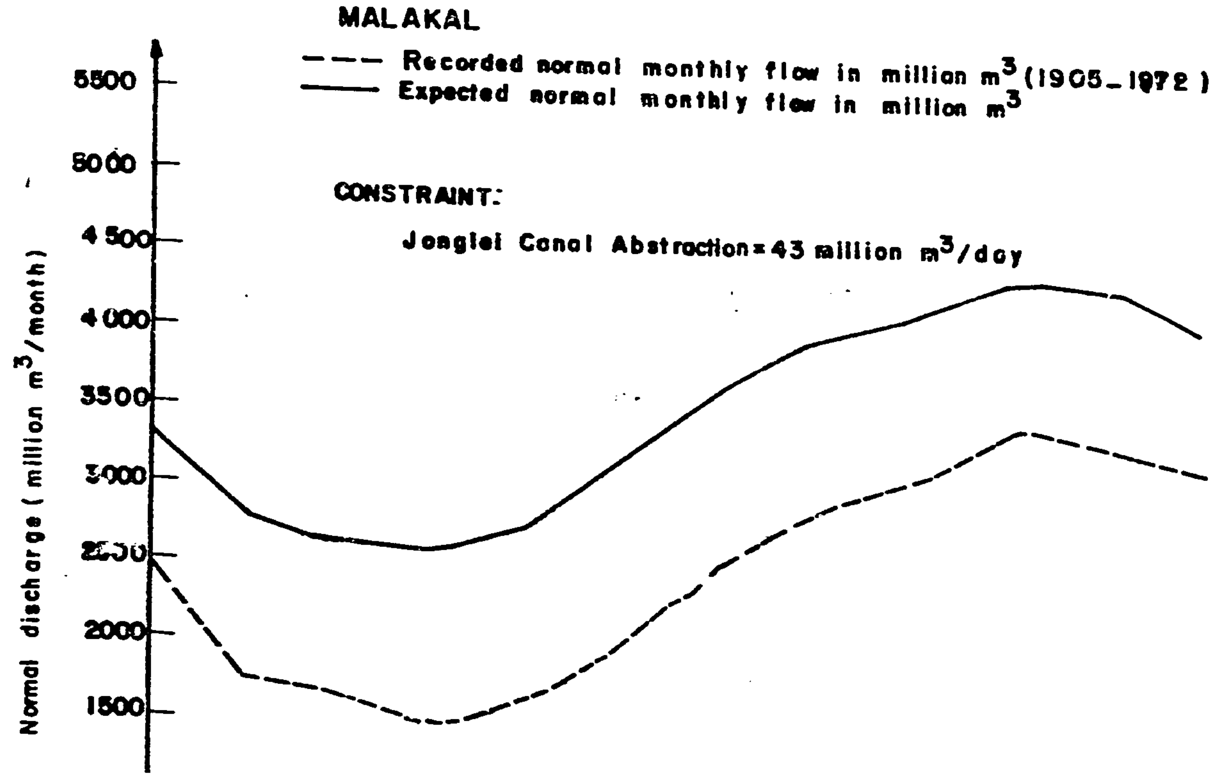

Month	Jan.	Feb.	Mar	Apr.	May	June	July	Aug.	Sep.	Oct.	Nov.	Dec.
Expected Normal	3352	2791	2626	2585	2749	3183	3611	3909	4064	4313	4280	4059
Recorded Normal	2474	1732	1633	1478	1542	2008	2504	2873	3074	3412	3314	3163
Water Benefit	878	1059	993	1107	1107	1175	1107	1036	990	901	966	896

Normal year Water benefit = 12.22 milliard m^3

Fig.(5.3) EXPECTED WATER BENEFIT FROM JONGLEI CANAL, CASE 3.

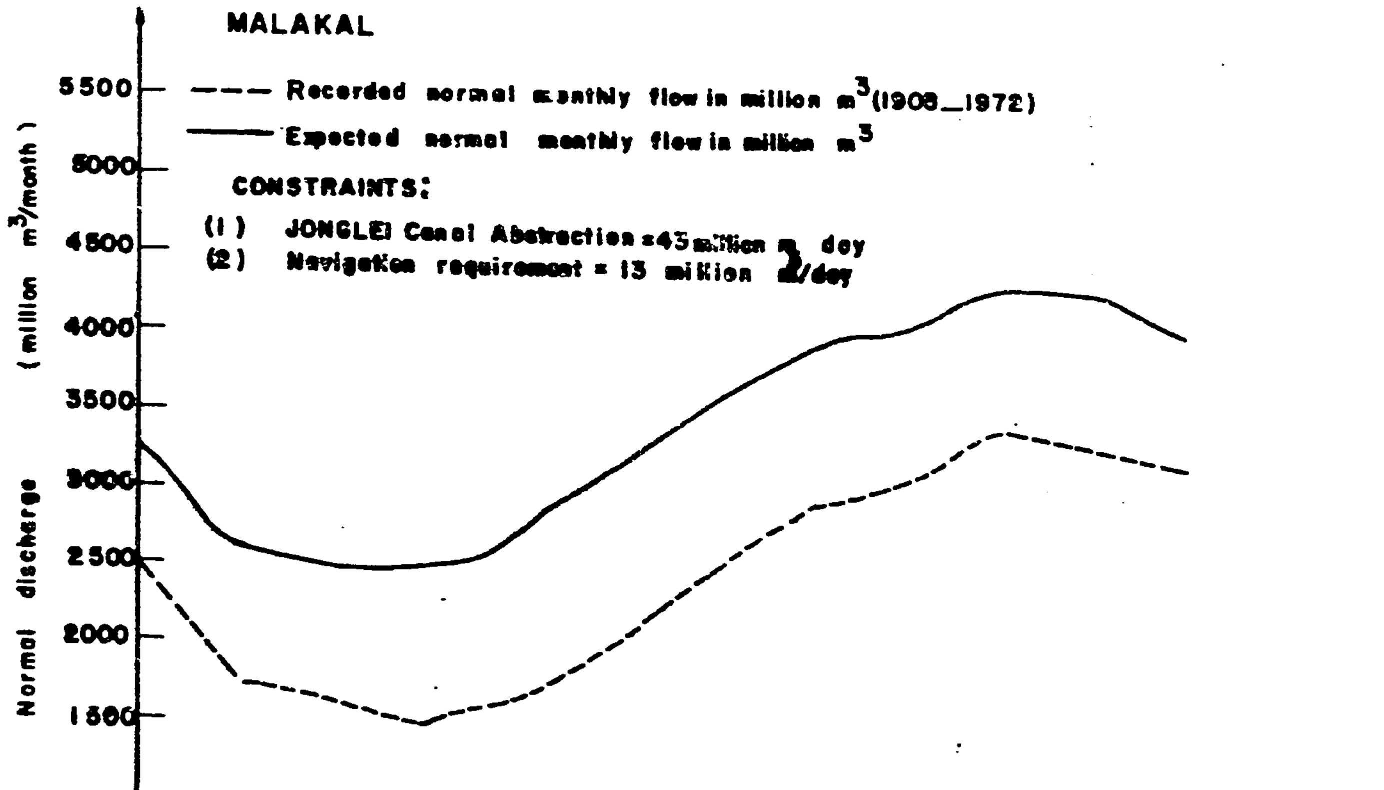

Month	Jan.	Feb.	Mar.	Apr.	May	June	July	Aug.	Sep.	Oct.	Nov.	Dec.
Expected Normal	3254	2615	2482	2266	2715	3130	3595	3921	4075	3418	4261	4006
Recorded Normal	2474	1732	1633	1478	1642	2008	2504	2873	3074	3412	3314	3163
Water Benefit	780	883	849	988	1073	1122	1091	1048	1001	906	947	843

Normal yearly Water benefit = 11.53 milliard m^3/day

Fig. (5.4) EXPECTED WATER BENEFIT OF JONGLEI CANAL, CASE. 4.

5.3.2 Expected Water Benefit For Unconditioned Jonglei Discharge:

Case (5): In this case the discharge of Bahr El-Gabel was kept within 33 million m^3/day as the maximum allowable flow downstream Jonglei. The rest of the arriving flow upstream Jonglei are diverted to Jonglei canal, regardless of the capacity of this canal. It means that the inflow to Jonglei canal is unconditional. The flow of 33 million m^3/day was representing the maximum natural flow which might pass through Bahr El-Gabel. Fig. (5.5) indicates the expected normal monthly flow and the total yearly water benefit.

5.3.3 Expected Water Benefit From Jonglei Canal Phase II And Regulating

Case (6): In this case, three constraints were taken into consideration. The first was that the diverted flow to Jonglei canal phase II is assumed to be 43 million m^3/day. The second is that the arrived flow to Mongalla is regulated and kept as a constant flow of 75 million m^3/day. The third constraint is that the navigation requirements in Bahr El-Gabel assumed to be 13 million m^3/day. The expected monthly hydrograph and the total yearly water benefit yielded under the above operating conditions were calculated as shown in Fig. (5.6).

5.3.4 Expected Water Benefit From Jonglei Canal Phase II With The Regulation Of The Lake Plateau Outflow and Executing The Southern Collecting Bahr El-Ghazal Canal

Case (7): In this case, four constraints are taken into consideration. These are the diverted flow to Jonglei canal phase II is 43 million m^3/day, the arrived flow to Mongalla is regulated and

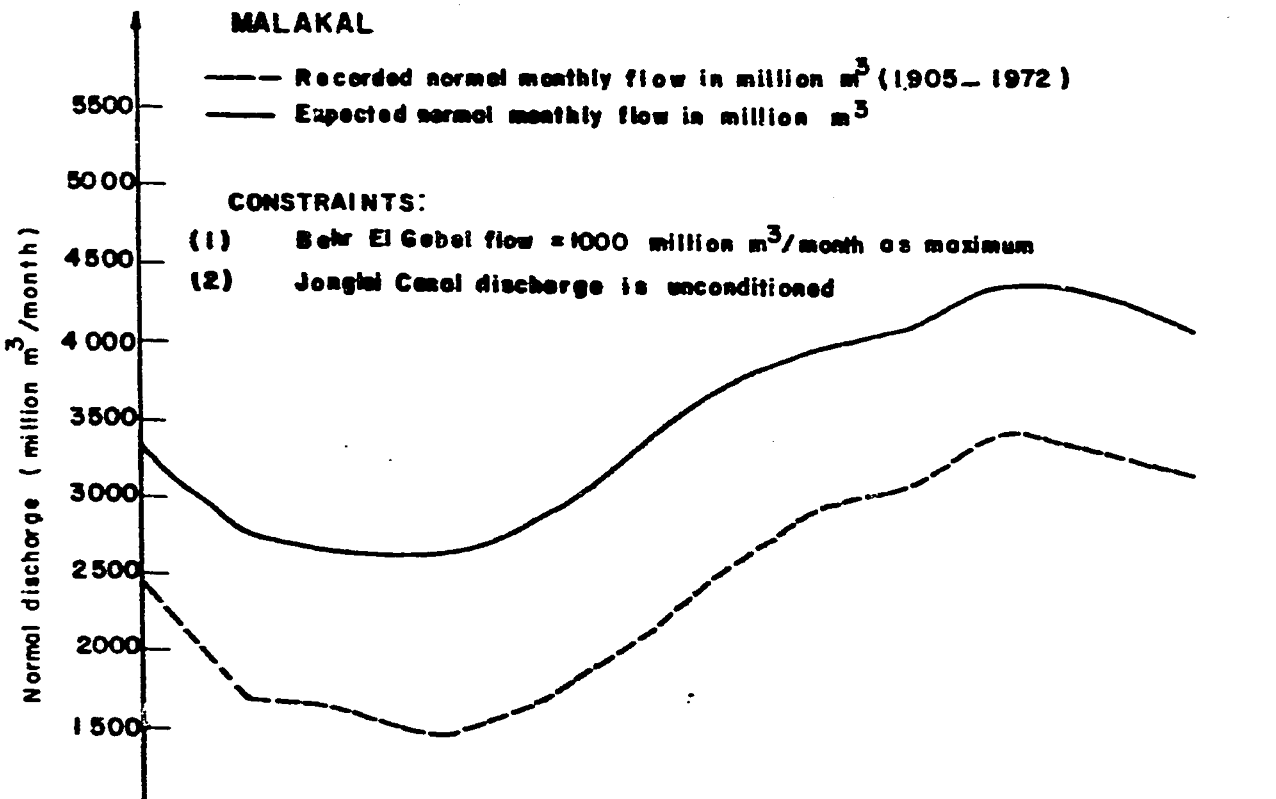

Month	Jan.	Feb	Mar.	Apr.	May	June	July	Aug.	Sep.	Oct.	Nov.	Dec.
Expected Normal	2947	2224	2124	2107	2482	2864	3413	3910	4064	4276	4102	3771
Recorded Normal	2474	1732	1633	1478	1642	2008	2504	2873	3074	3412	3314	3163
Water Benefit	473	492	491	629	840	856	909	1037	990	864	788	608

Normal yearly water benefit = 8.98 milliard m^3/year

Fig(5.5) EXPECTED WATER BENEFIT FOR UNCONDITIONED DISCHARGE IN JONGLEI CANAL, CASE 5.

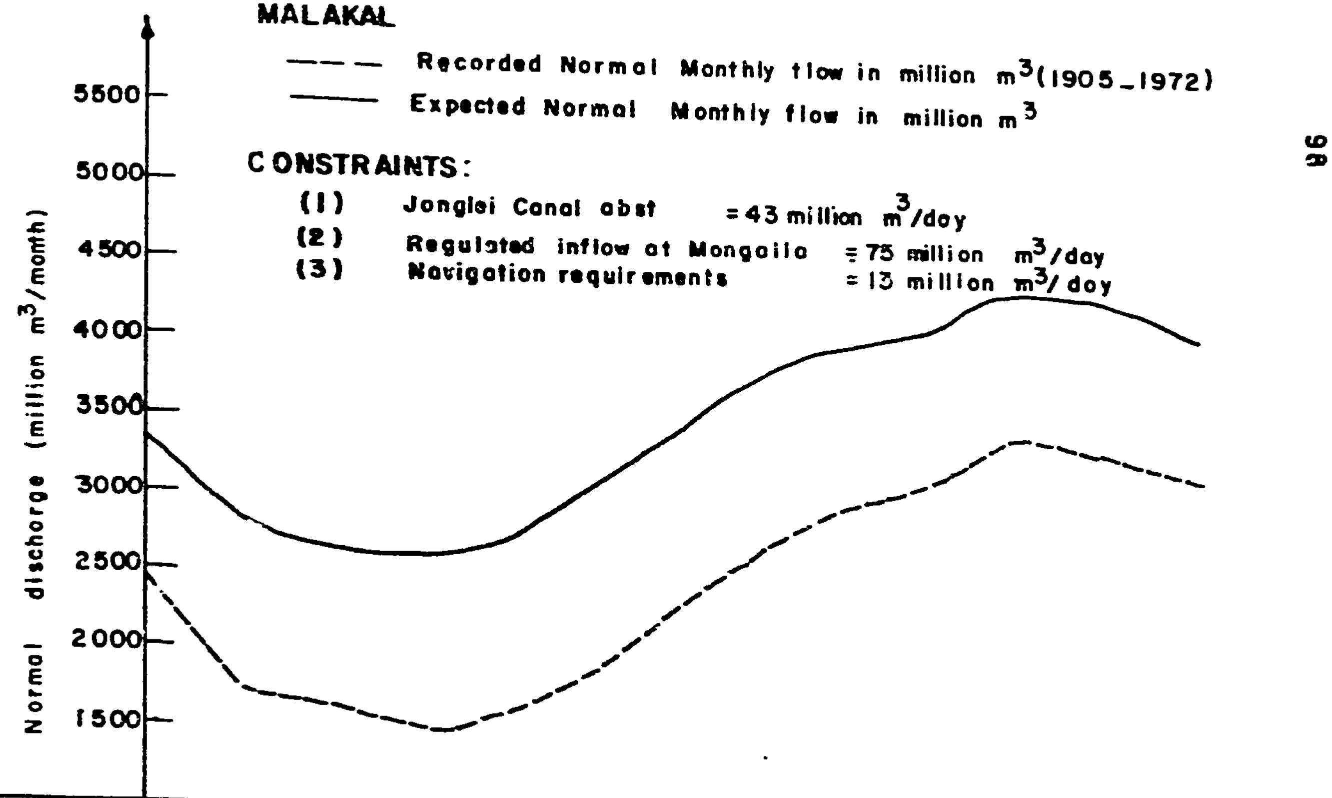

Month	Jan.	Feb.	Mar.	Apr.	May	June	July	Aug.	Sep.	Oct.	Nov.	Dec.
Expected Normal	3352	2791	2626	2585	2750	3183	3611	3909	4067	4313	4280	4059
Recorded Normal	2474	1732	1633	1478	1642	2008	2504	2873	3074	3412	3314	3163
Water Benefit	878	1059	993	1107	1108	1175	1107	1036	993	901	966	896

Normal yearly water benefit = 12.22 milliard m^3 /year

Fig. (5.6) EXPECTED WATER BENEFIT FROM JONGLEI CANAL PHASE II WITH THE REGULATION OF LAKE PLATEAU OUTFLOW, CASE 6.

kept as a constant flow equal to 75 million m^3/day, the navigation requirements in Bahr El-Gabel is 13 million m^3/day, and the expected outflow from the Southern collecting canal of Bahr El-Ghazal joining Bahr El-Gabel was assumed to be 75% from the maximum recorded monthly discharge in Bahr El-Ghazal area. The expected monthly hydrograph and the total yearly water benefit yield under all the above operating conditions are evaluated as illustrated in Fig. (5.7).

Comparing the results obtained in the cases (6) and (7), it could be concluded that, involving the Southern collecting canal of Bahr El-Ghazal in the operating scheme provides extra water benefit of about 0.16 milliard m^3/year at Malakal.

Frequency analysis for the expected water benefit has also been carried out. Three selected operating cases have been tested and the probability of occurance for the different expected water benefit are delineated in Figs. (5.8) to (5.10). These probabilities demonstrate the reliability of these expected water benefit, and indicate that the standard deviations of these benefits range between 2.51 - 3.36 milliard cubic-meters/annum.

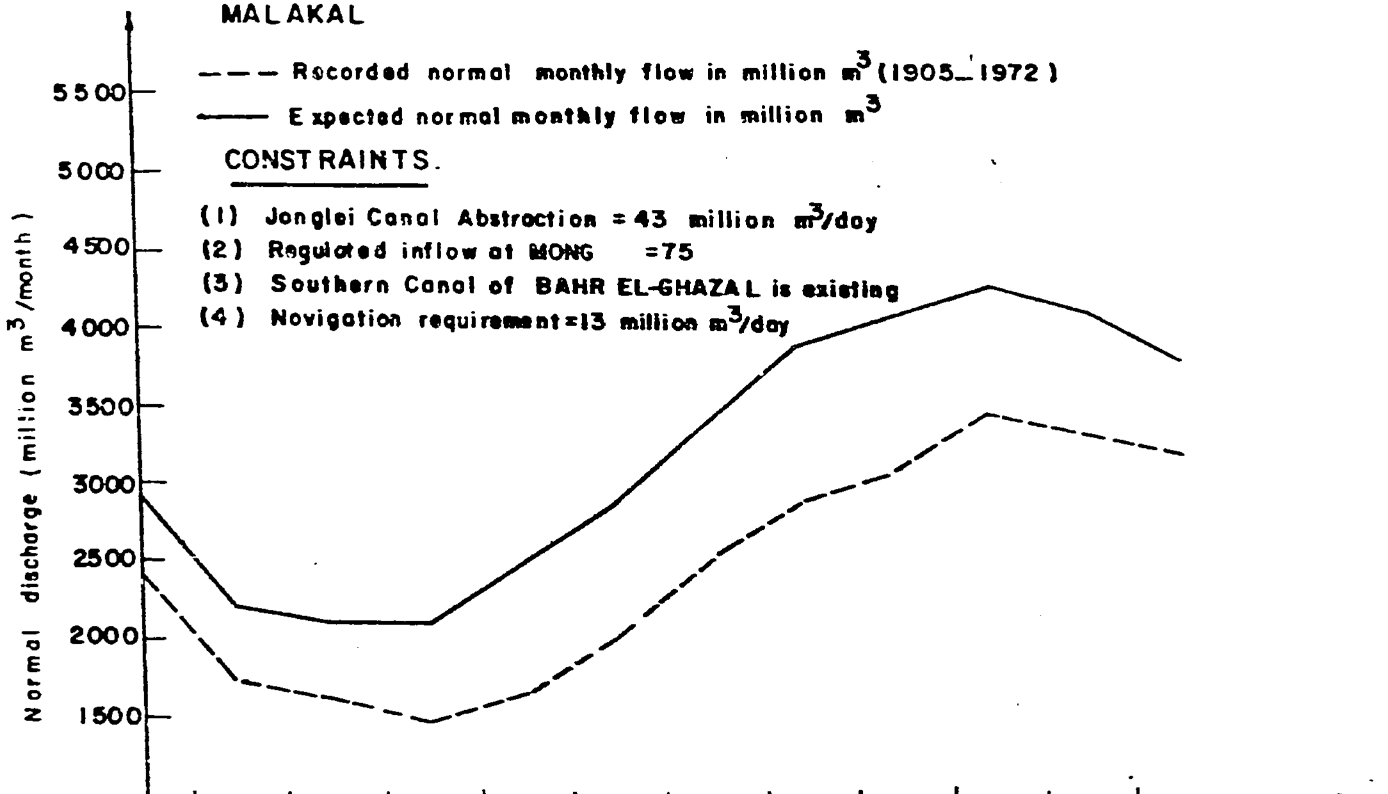

Month	Jan.	Feb.	Mar.	Apr.	May	June	July	Aug.	Sep.	Oct.	Nov.	Dec.
Expected Normal	3354	2792	2627	2586	2760	3201	3636	3935	4092	4340	4299	4064
Recorded Normal	2474	1732	1633	1478	1642	2008	2504	2873	3074	3412	3314	3163
Water Benefit	880	1060	994	1108	1118	1193	1132	1062	1018	928	985	901

Normal yearly Water benefit = 12.38 milliard m^3/year

Fig.(5.7) EXPECTED WATER BENEFIT FROM JONGLEI CANAL AND THE SOUTHERN BAHR EL_GHAZAL CANAL, CASE 7.

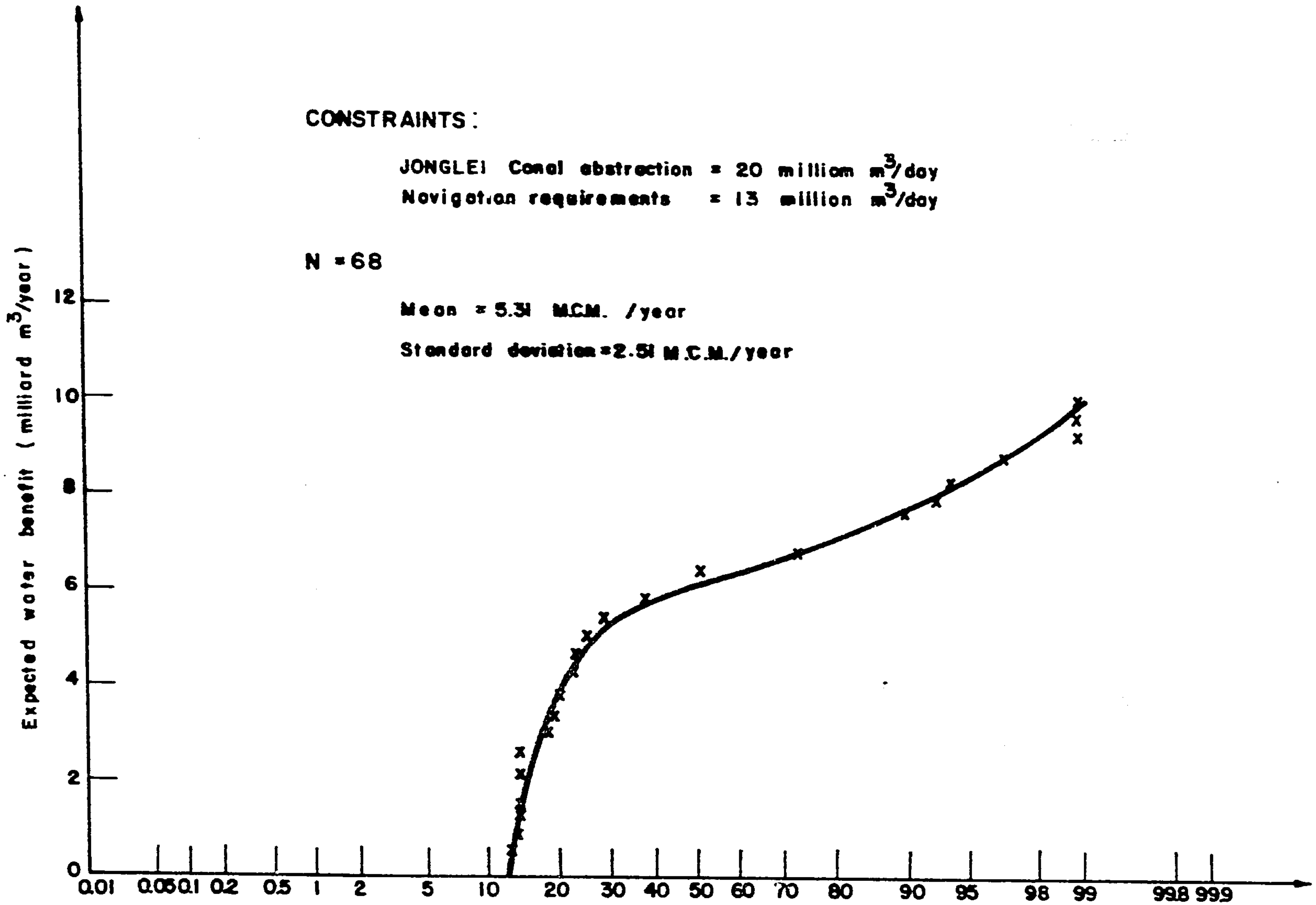

Fig. (5.8) CUMULATIVE PROBABILITY DISTRIBUTION OF EXPECTED WATER BENEFIT OF JONGLEI CANAL, CASE 2.

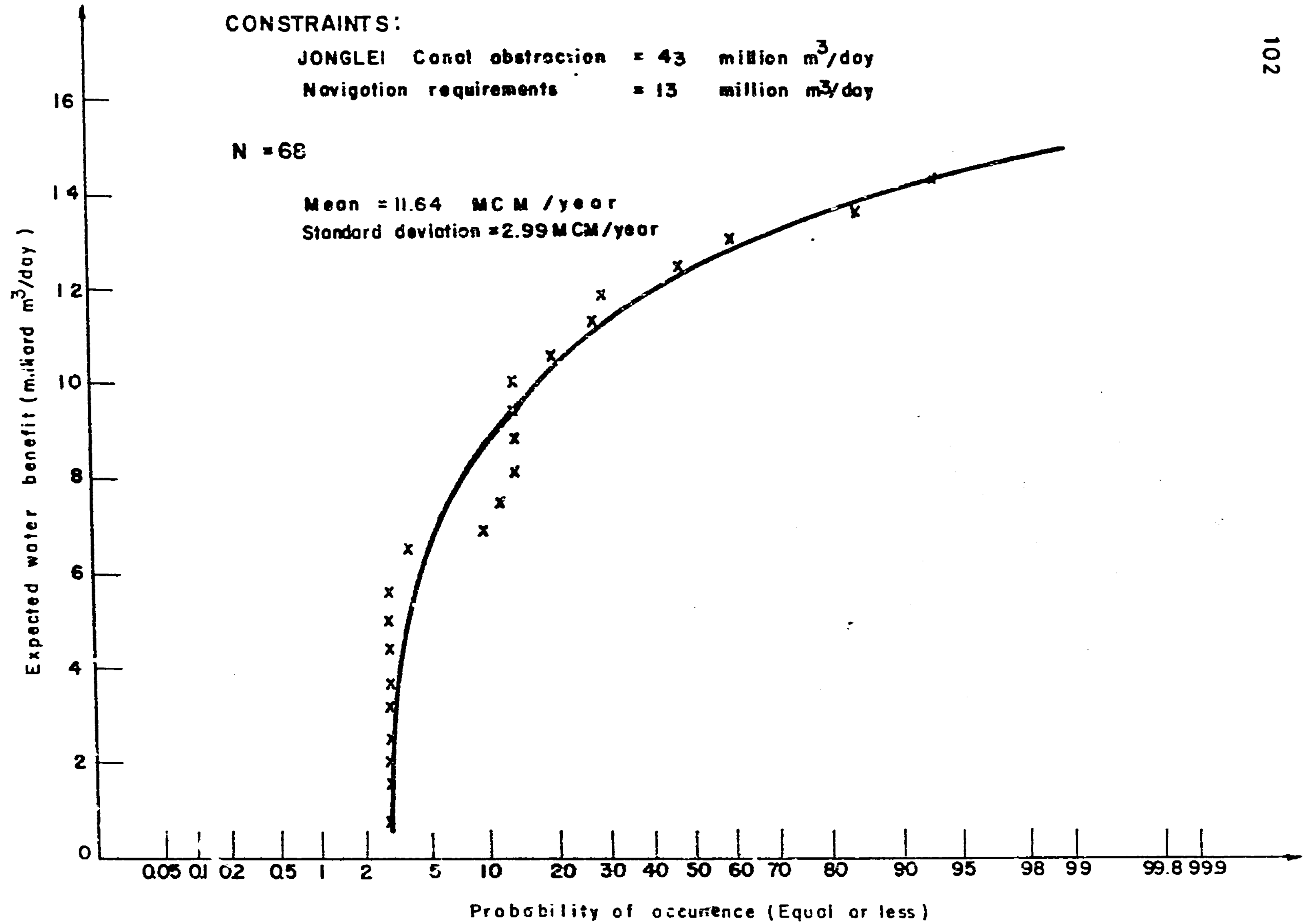

Fig.(5.9) CUMULATIVE PROBABILITY DISTRIBUTION OF EXPECTED WATER BENEFIT OF JONGLEI CANAL, CASE 4.

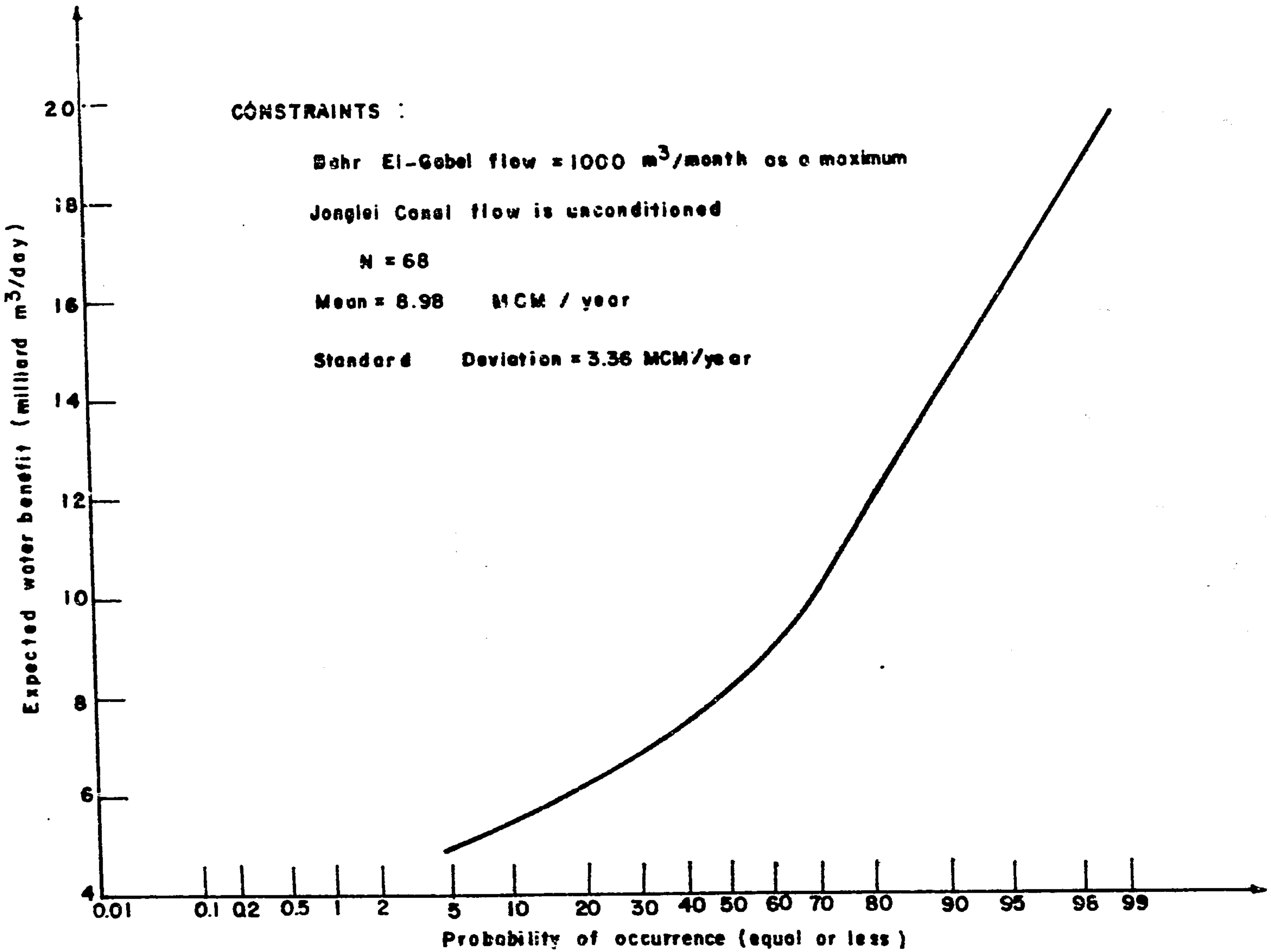

Fig.(5.10) CUMULATIVE PROBABILITY DISTRIBUTION OF EXPECTED WATER BENFIT OF JONGLEI CANAL, CASE 5.

CHAPTER VI
CONCLUDING REMARKS

CHAPTER VI

CONCLUDING REMARKS

This report has been directed towards scrutinizing the expected water benefits from project developments at Bahr El-Gabel region. These developments incorporate the Jonglei canal (phases I and II), as well as the Southern collecting Bahr El-Ghazal canal. Historical streamflow data of the region were tested using a double mass curve analysis. The test showed the consistency of the most of the data except for stations Reference Pole 114, and upstream and downstream Papiu. The inconsistency was attributed to measuring errors or the shift of the measuring guage. Routing schemes of the Bahr El-Gabel are have then been developed to be incorporated in the estimation of the expected benefits of water saving projects. These scheme have demonstrated to be adequate for such use.

Future expectations of the Bahr El-Gabel area have been investigated under several conditions and constraints. The main findings may be summarized as follows:

- The expected water benefit for the first phase of Jonglei canal will amount to 4.89 milliard m^3/year.

- Navigation requirement in the area will not influence the expected water benefit from Jonglei canal phase I.

- The expected water benefit from phase II of Jonglei canal will reach 12.33 milliard m^3/year, and may reduce to about 11.53 milliard m^3/year if navigation requirements are taken into consideration.

- The expected water benefit from Jonglei canal pahse II, when regulating the flow at Mongalla at 75 million m^3/day, will amount at 12.22 milliard m^3/day, with the navigation constraints.

- Involving the Southern collecting Bahr El-Ghazal channel with Jonglei phase II and regulated flow at Mongalla, will yield an expected water benefit of 12.38 milliard cubic-meter/annum. This reveals that the Southern Bahr El-Ghazal canal will not be effective in increasing water savings in the area.

There are still many aspects related to the future performance of the Bahr El-Gabel area. Among these topics are:

- The thorough investigation of the drainage pattern of the basin and refinement of results by introducing the effect of the many tributaries joining the main streams of Bahre El-Gabel.

- The study of infiltration rates and groundwater behaviour in the area and its effect on the future water benefits.

- The investigation of the effect of water stored in lake No on the arriving flow out of Bahr El-Gabel near station Malakal.

- The possibility of applying more sophisticated routing schemes as well as the study of the spilling capacities at different sections of the area. Such analysis may locate the points where bank elevations are needed.

REFERENCES

REFERENCES

[1] Amin, M., "Jonglei Project", Research Report, Ministry of Public Work, Cario, 1959.

[2] Bendat, J.S., and Piersol, A.G., Measurements and Analysis of Random Data, John Wiley & Sons, New York, 1966.

[3] Bras, R.L., and Cordova, J.S., Introductory Notes on Operational Hydrology, Workshop on Elements of Water Resources Systems Analysis and Planning, Cairo University, Cairo, June 1978.

[4] Christopher, C., Statistics for Technology, Chapman and Hall, London, 1975.

[5] Equatorial Nile Project, Jonglei Investigation Team, 4 volumes, Sudan Government, 1964.

[6] Hurst, H.E., et al, The Nile Basin, Cairo, 1931-1972, (Ten volumes and a number of supplements have been published at intervals comprising hydrological records and projects concerning the Nile Basin).

[7] Meteorlogical Data of Sudan, Annual Reports, up to 1972.

[8] Mobarek, I.E., Salem M.H., and Dorrah, H.T., "Stochastic Modeling of Nile Inflows to Lake Nasser", Research Report, Cairo University / MIT Technological Planning Program, Dec. 1977.

[9] Mobarek, I.E., Salem, M.H., and Dorrah, H.T., "Hydrological Studies on the River Nile", Research Report, Cario University / MIT Technological Planning Program, Cario, May 1979.

[10] Mobarek, I.E., Salem, M.H., and Dorrah, H.T., "Spilling Analysis with Applications to the River Nile", Research Report, Cairo University / MIT Technological Planning Program, Aug. 1980.

[11] Operational Navigation Charts, prepared and published by the Defence Mapping Agency Aerospcae Center, St. Louis Airforce Station, Missouri, 1977.

[12] Permanent Joint Technical Committee of the River Nile (P.J.T.C.), Annual Reports, Cairo, 1961-1971.

[13] Remote Sensing Center, "Bahr El-Gabel Area", Academy of Scientific Research and Technology, Cairo, Egypt, April 1978.

[14] Yevjevich, V.,Stochastic Process in Hydrology, Water Resources Series, Fort Collins, Colorado, 1972.

APPENDIX A

DOUBLE MASS ANALYSIS OF GAUGING STATIONS IN BAHR EL_ GABEL

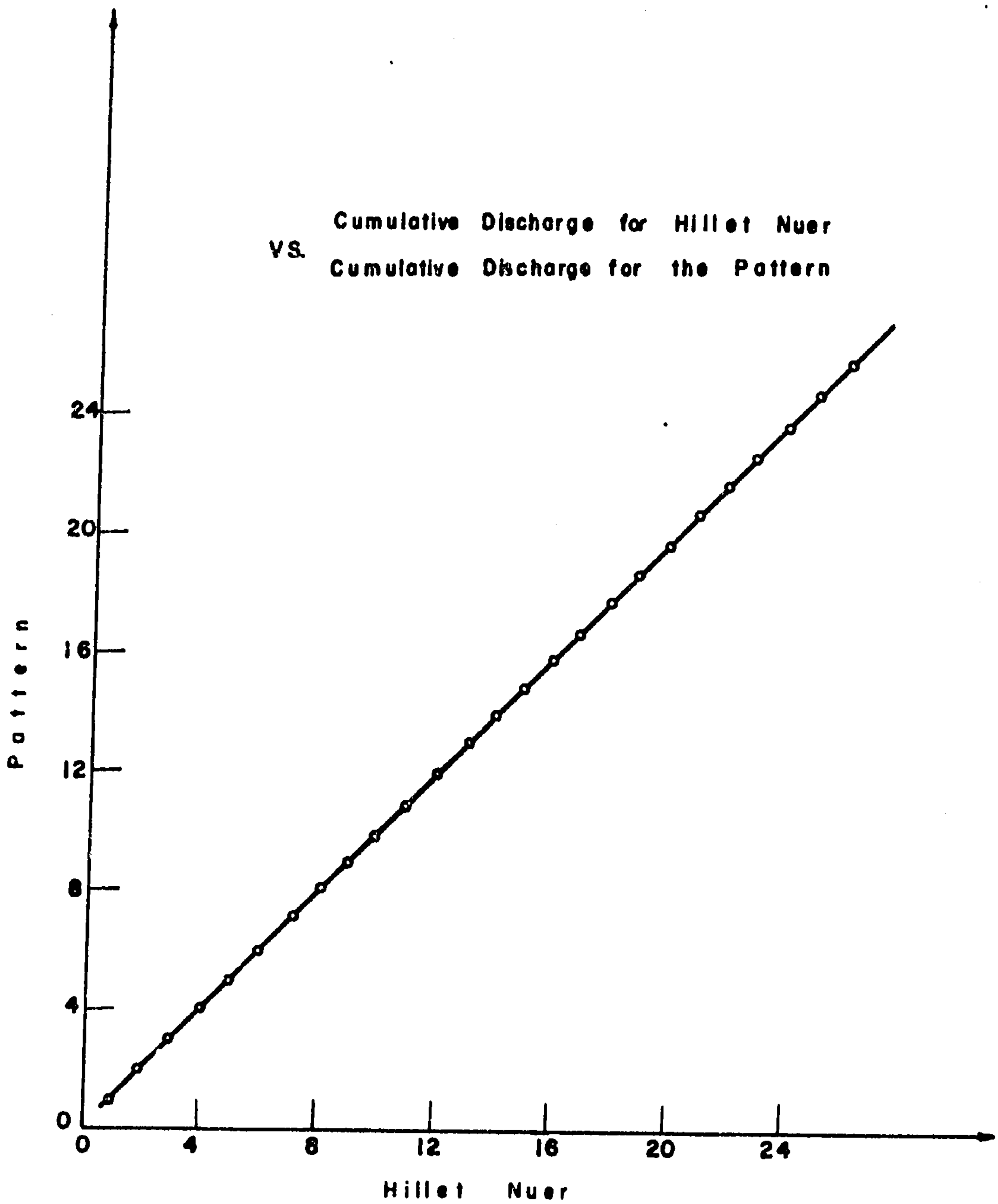

Fig (A.1) DOUBLE MASS CURVE ANALYSIS FOR STATION HILLET NUER.

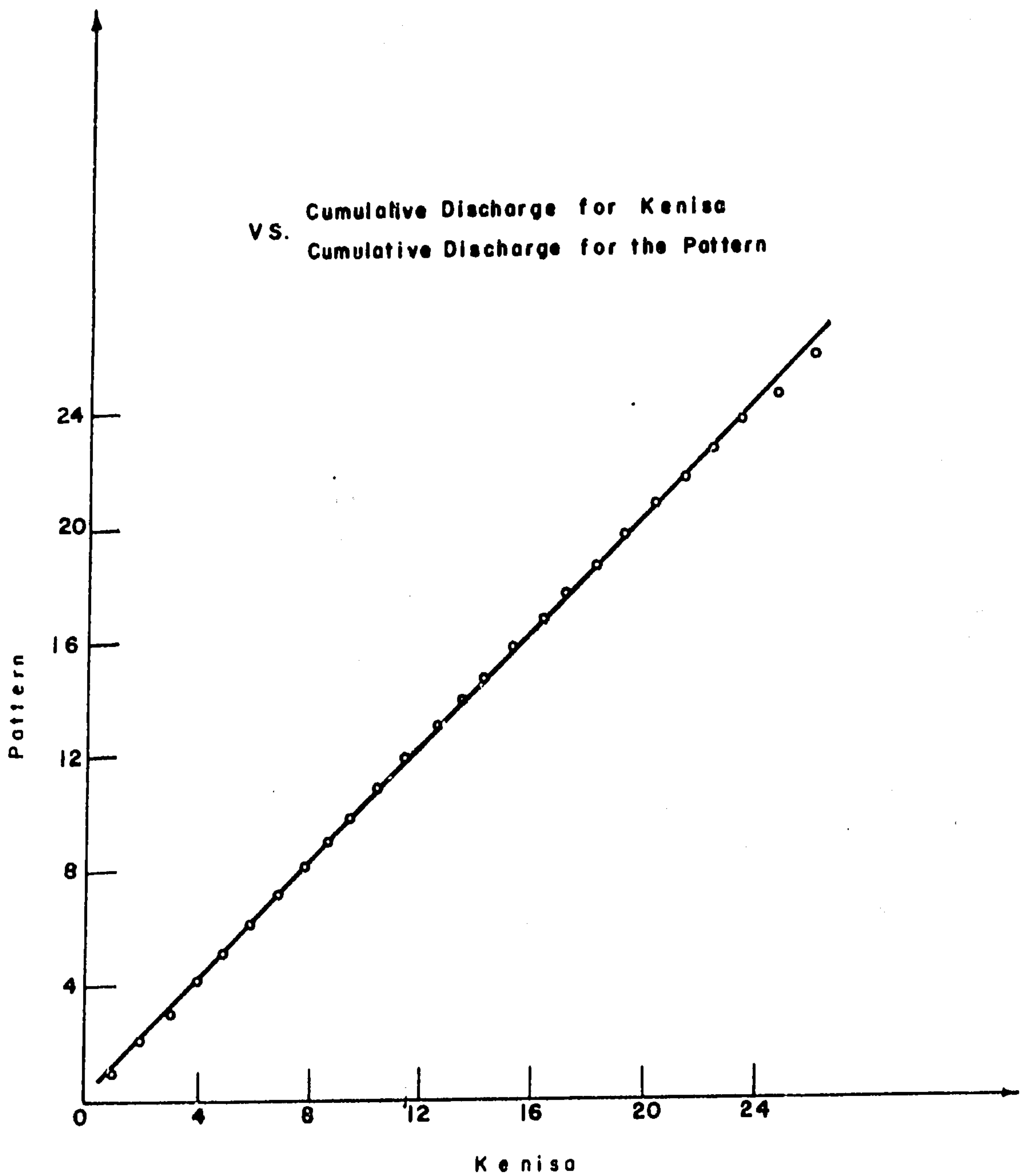

Fig. (A.2) DOUBLE MASSCURVE ANALYSIS FOR STATION KENISA.

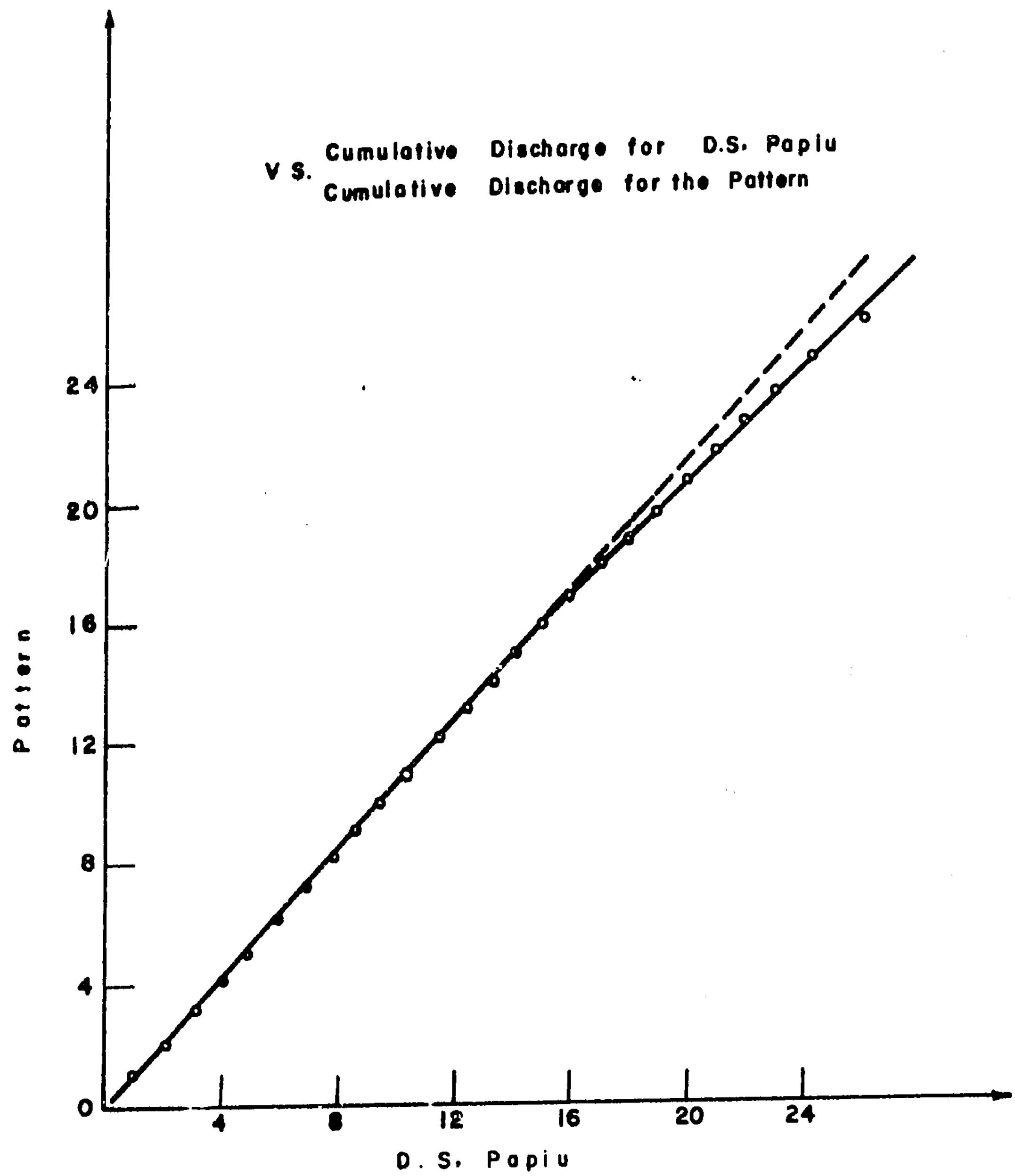

Fig(A.3) DOUBLE MASS CURVE ANALYSIS FOR STATION D. S. PAPIU.

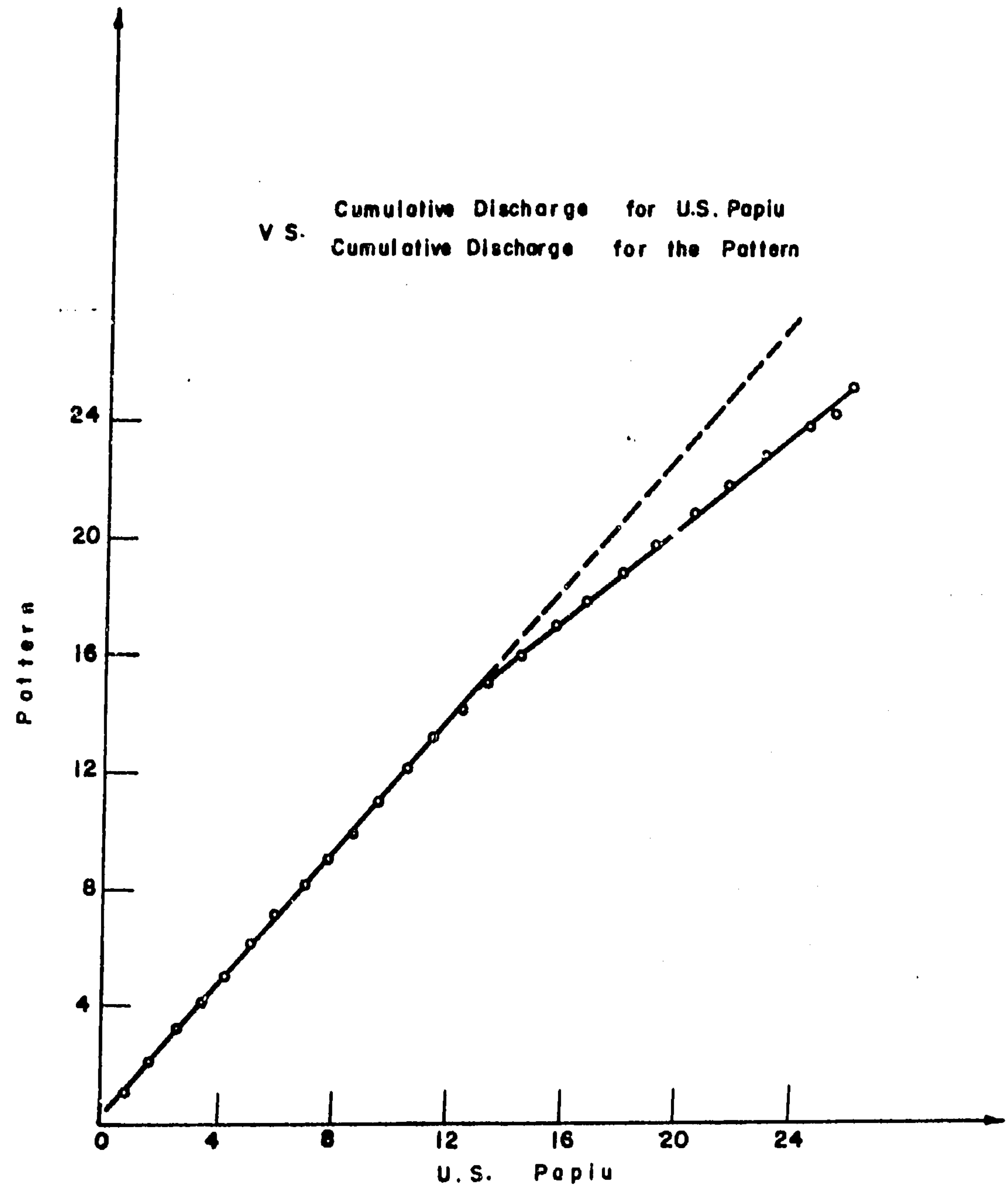

Fig. (A.4) DOUBLE MASS CURVE ANALYSIS FOR STATION U.S. PAPIU.

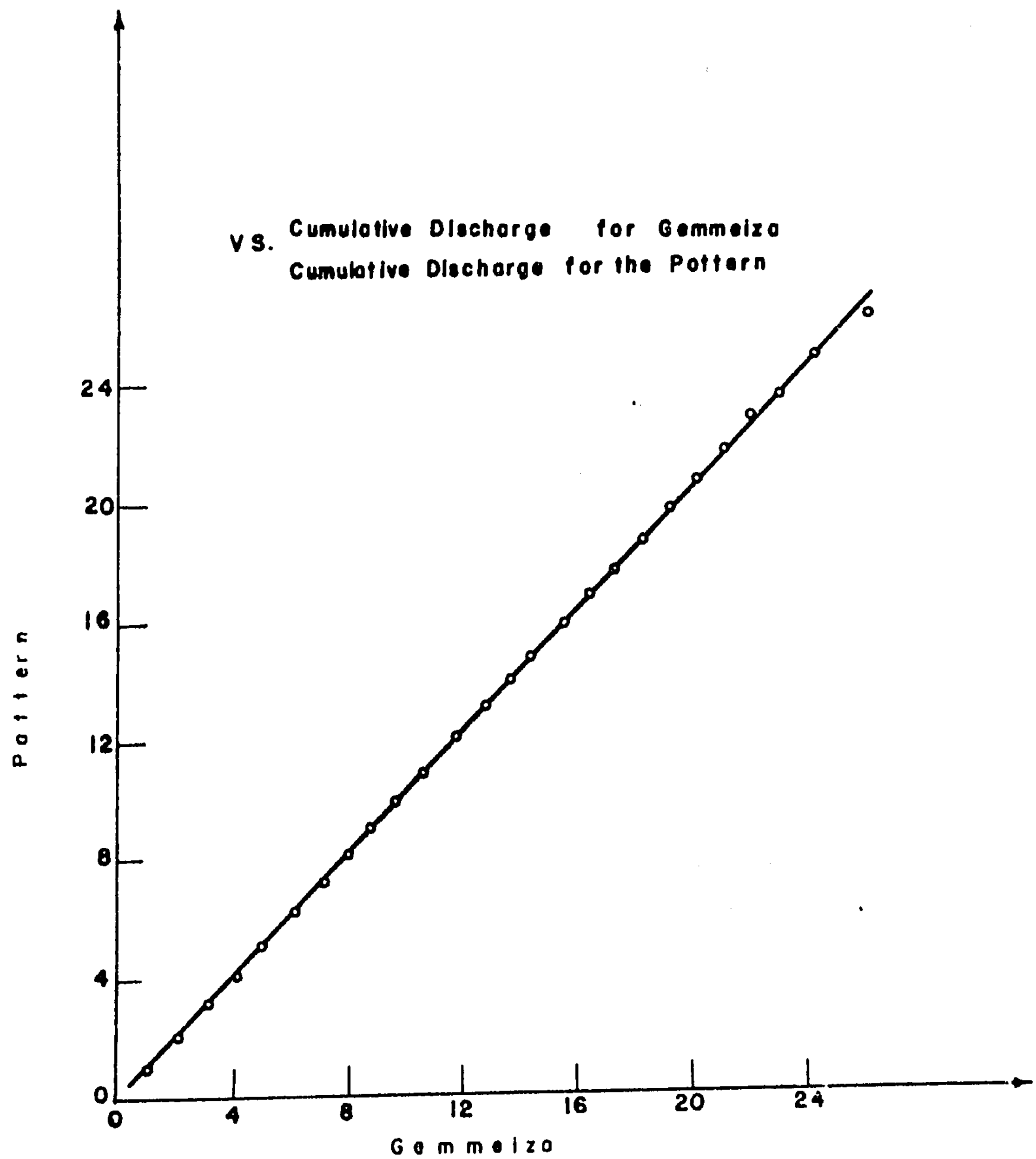

Fig.(A.5) DOUBLE MASS CURVE ANALYSIS FOR STATION GEMMEIZA.

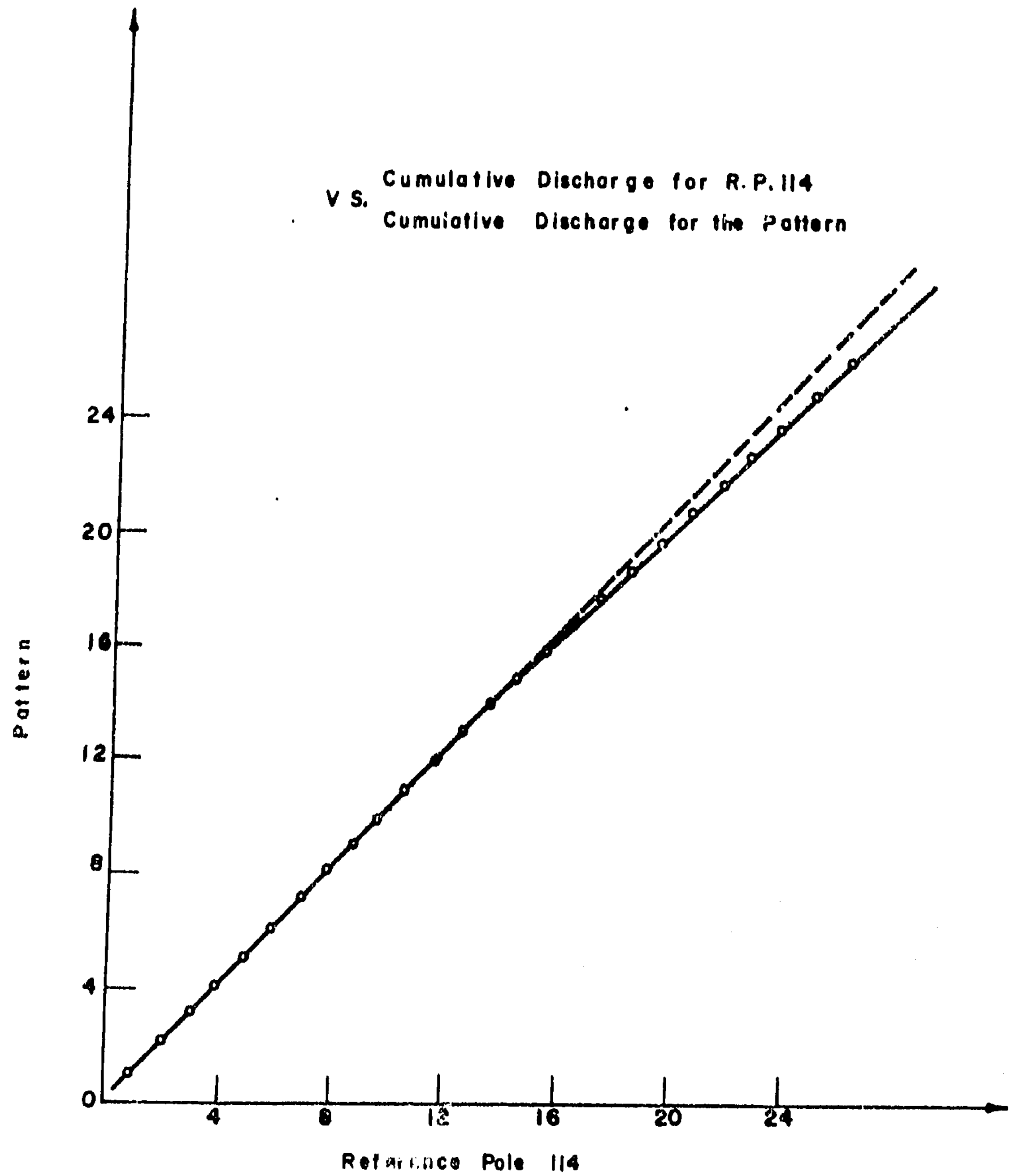

Fig.(A.6) DOUBLE MASS CURVE ANALYSIS FOR STATION REFERENCE POLE 114.

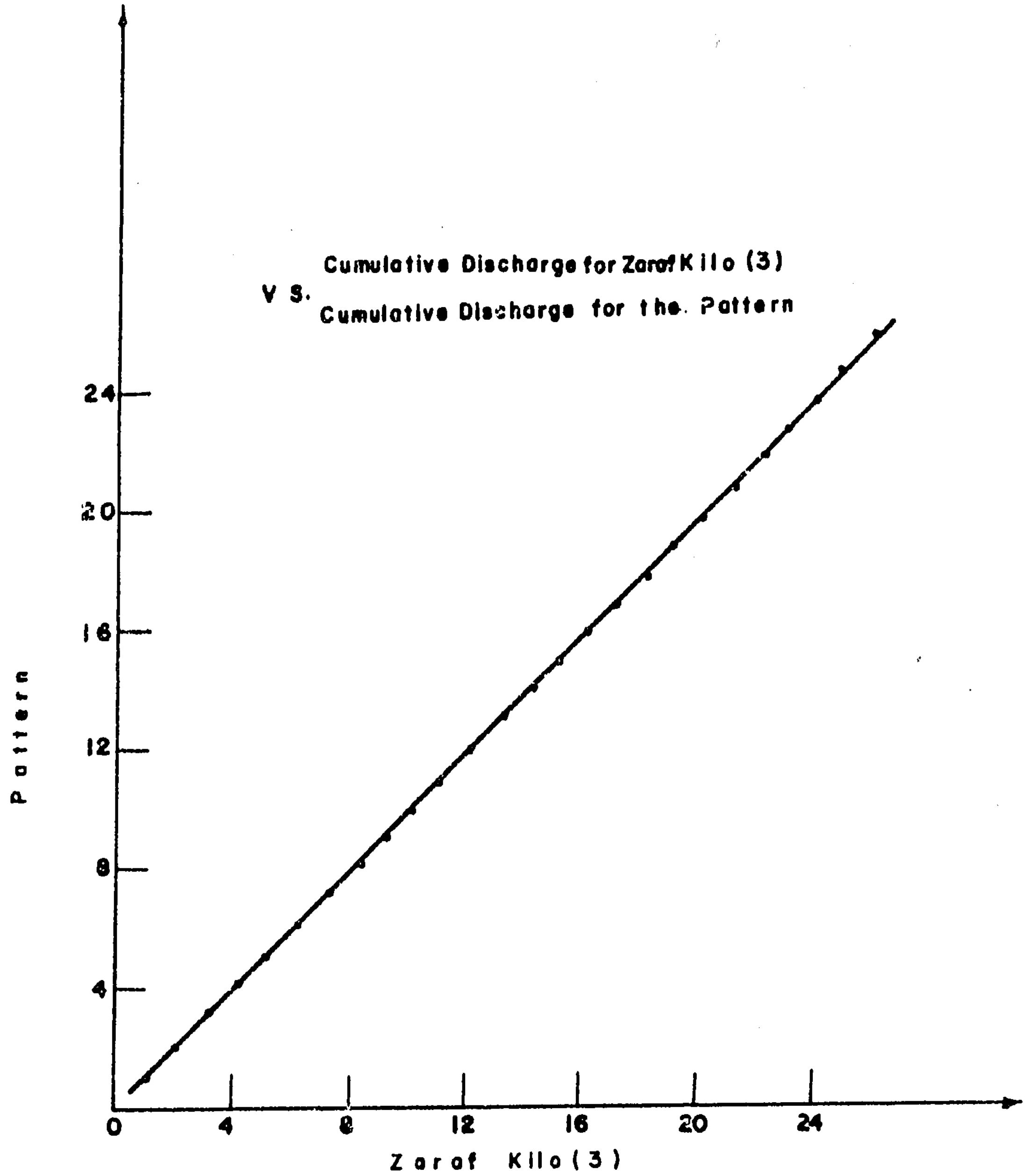

Fig.(A.7) DOUBLE MASS CURVE ANALYSIS FOR STATION ZARAF KILO 3.

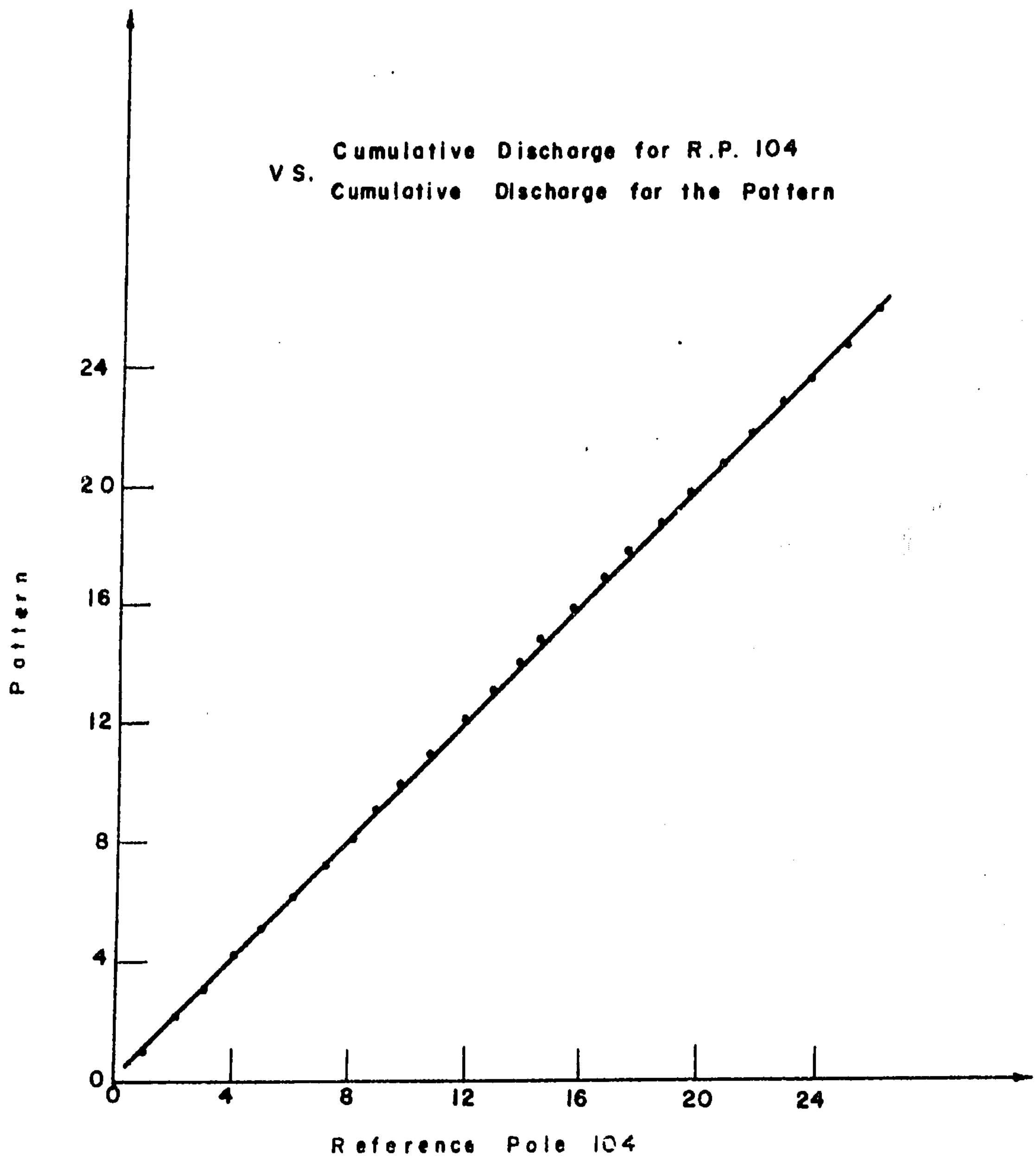

Fig.(A.8) DOUBLE MASS CURVE ANALYSIS FOR STATION REFERENCE POLE 104.

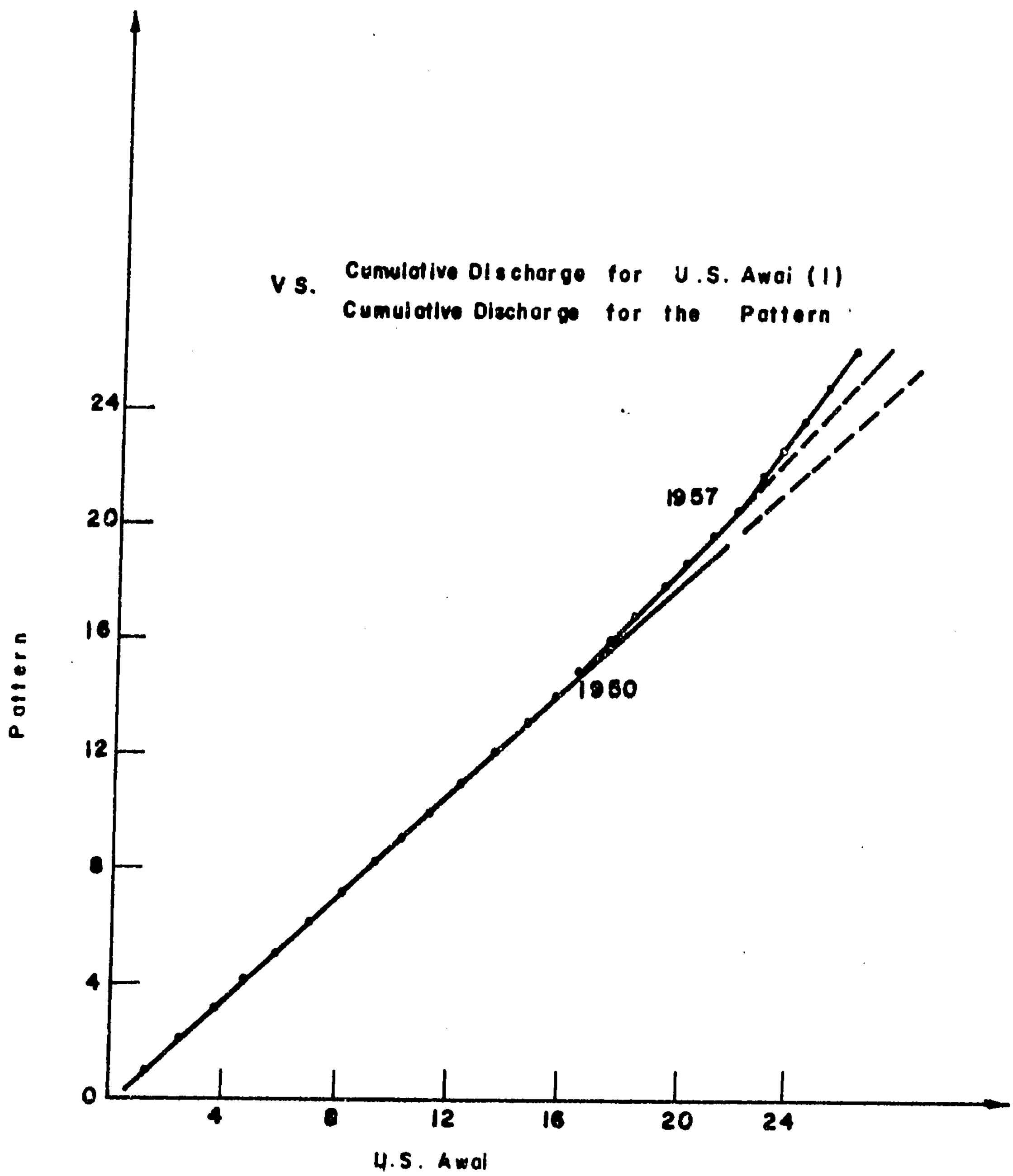

Fig. (A.9) DOUBLE MASS CURVE ANALYSIS FOR STATION U.S AWAI (I).

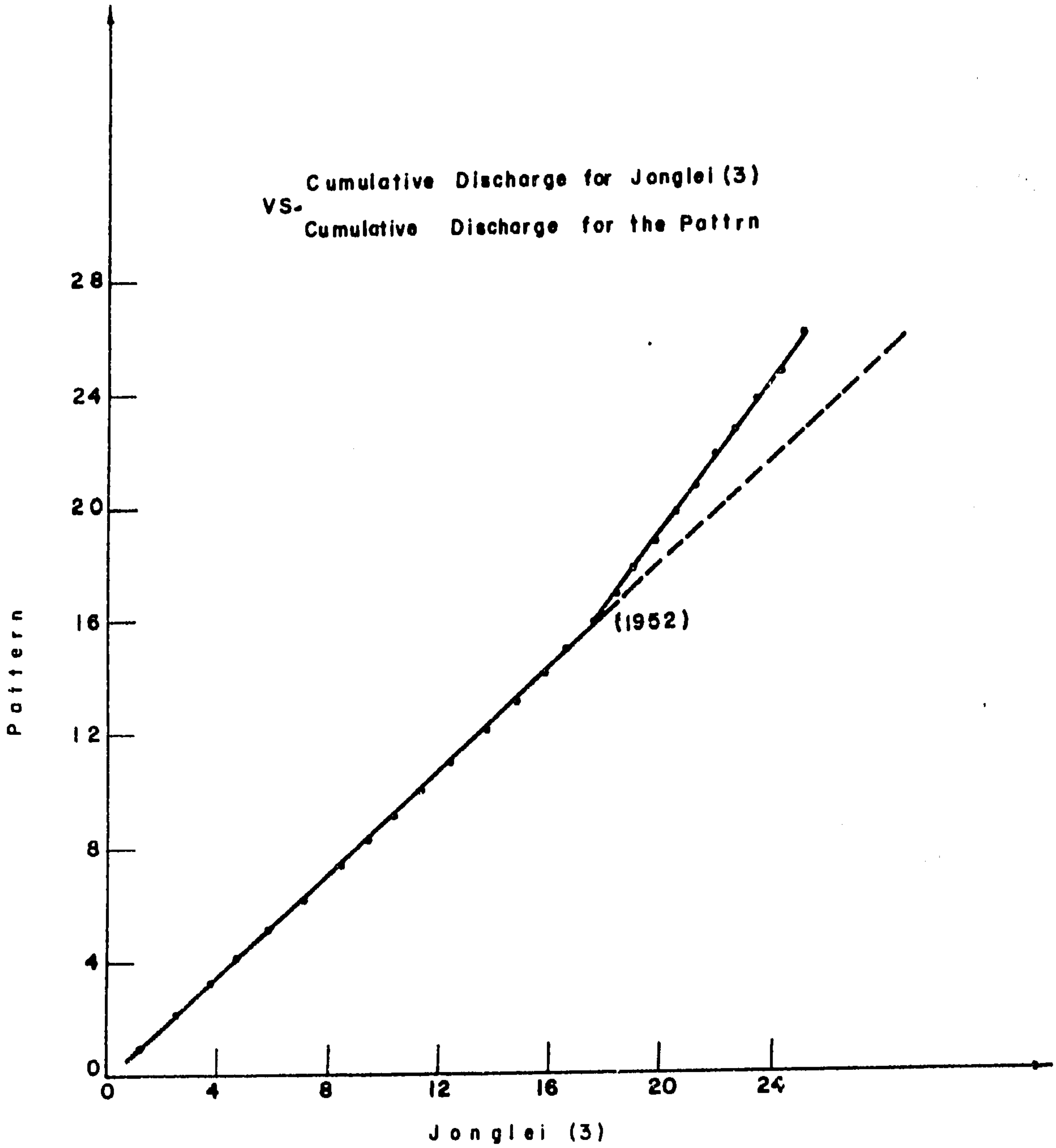

Fig.(A.10) DOUBLE MASS CURVE ANALYSIS FOR STATION JONGLEI (3).

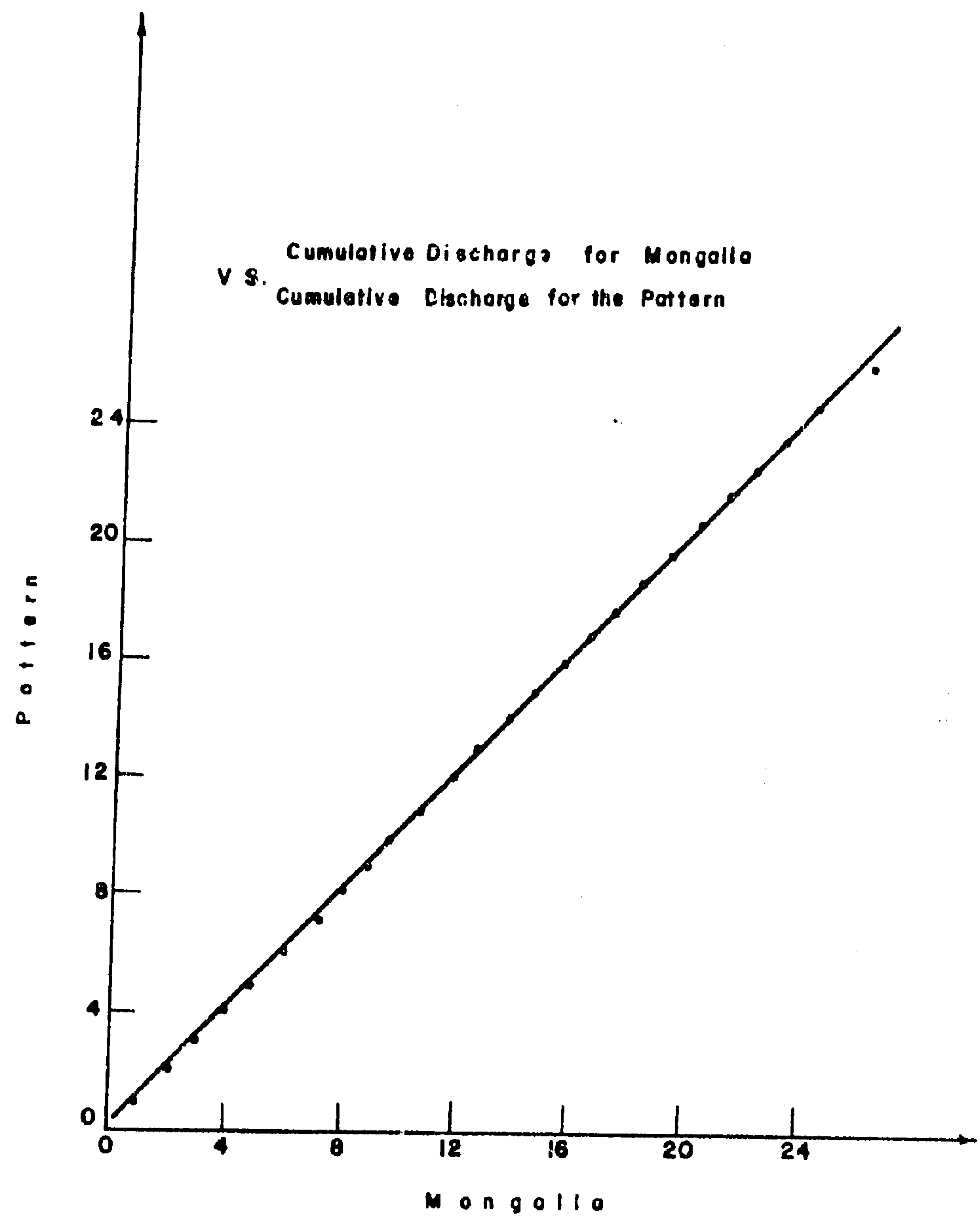

Fig. (A.II) DOUBLE MASS CURVE ANALYSIS FOR STATION MONGALLA.

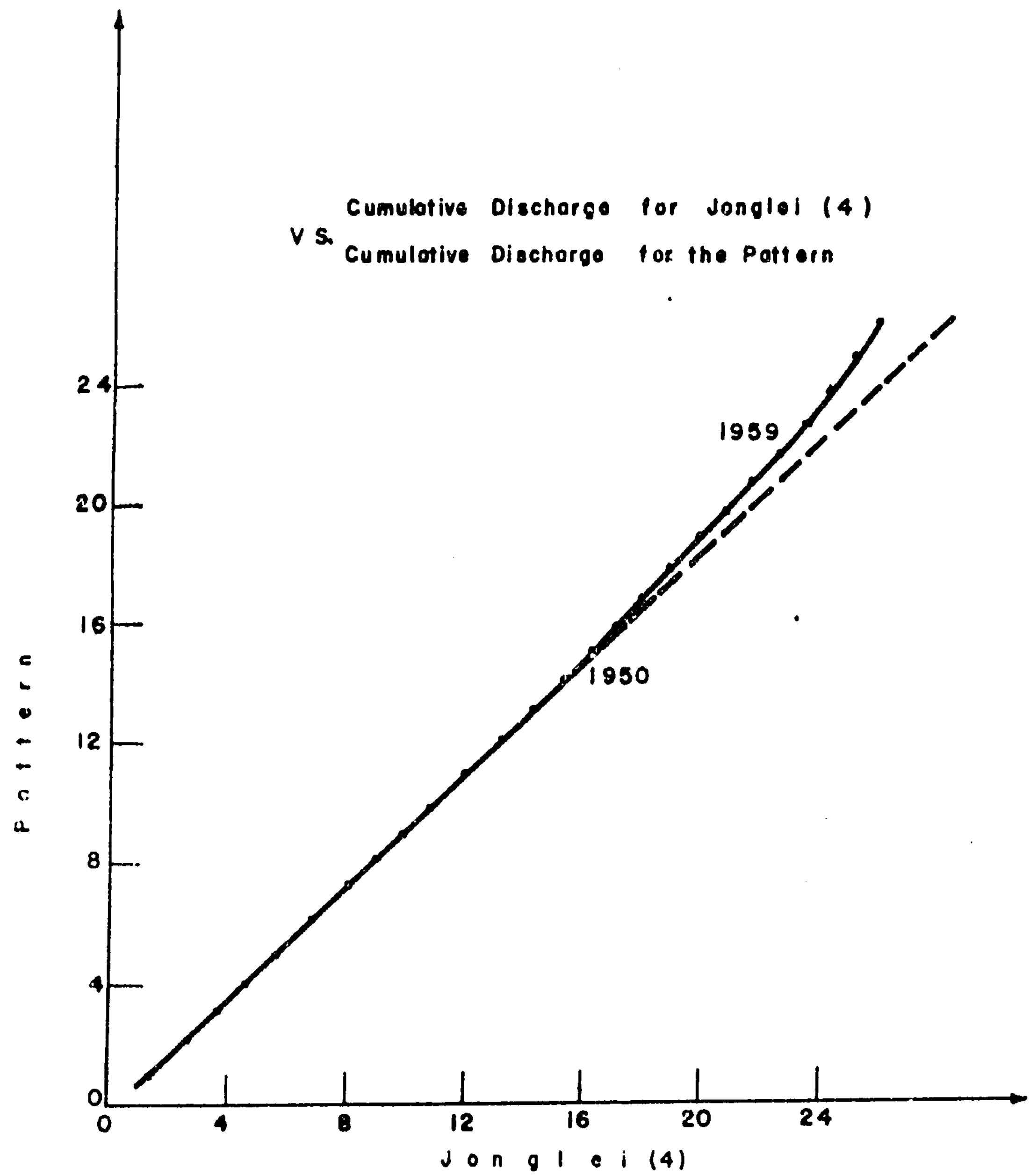

Fig. (A.12) DOUBLE MASS CURVE ANALYSIS FOR STATION JONGLEI (4).

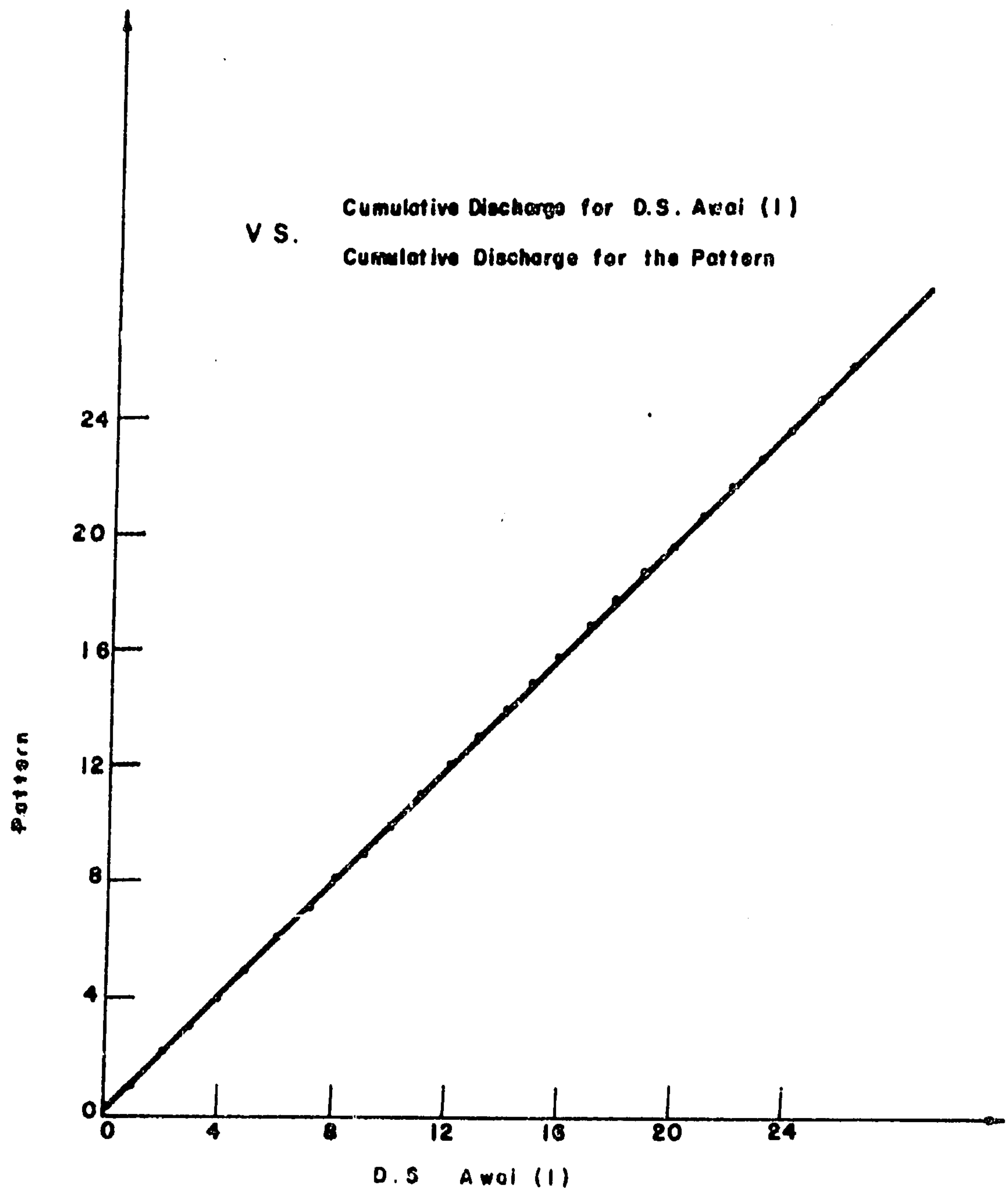

Fig.(A.13) DOUBLE MASS CURVE ANALYSIS FOR STATION D.S. AWAI (I).

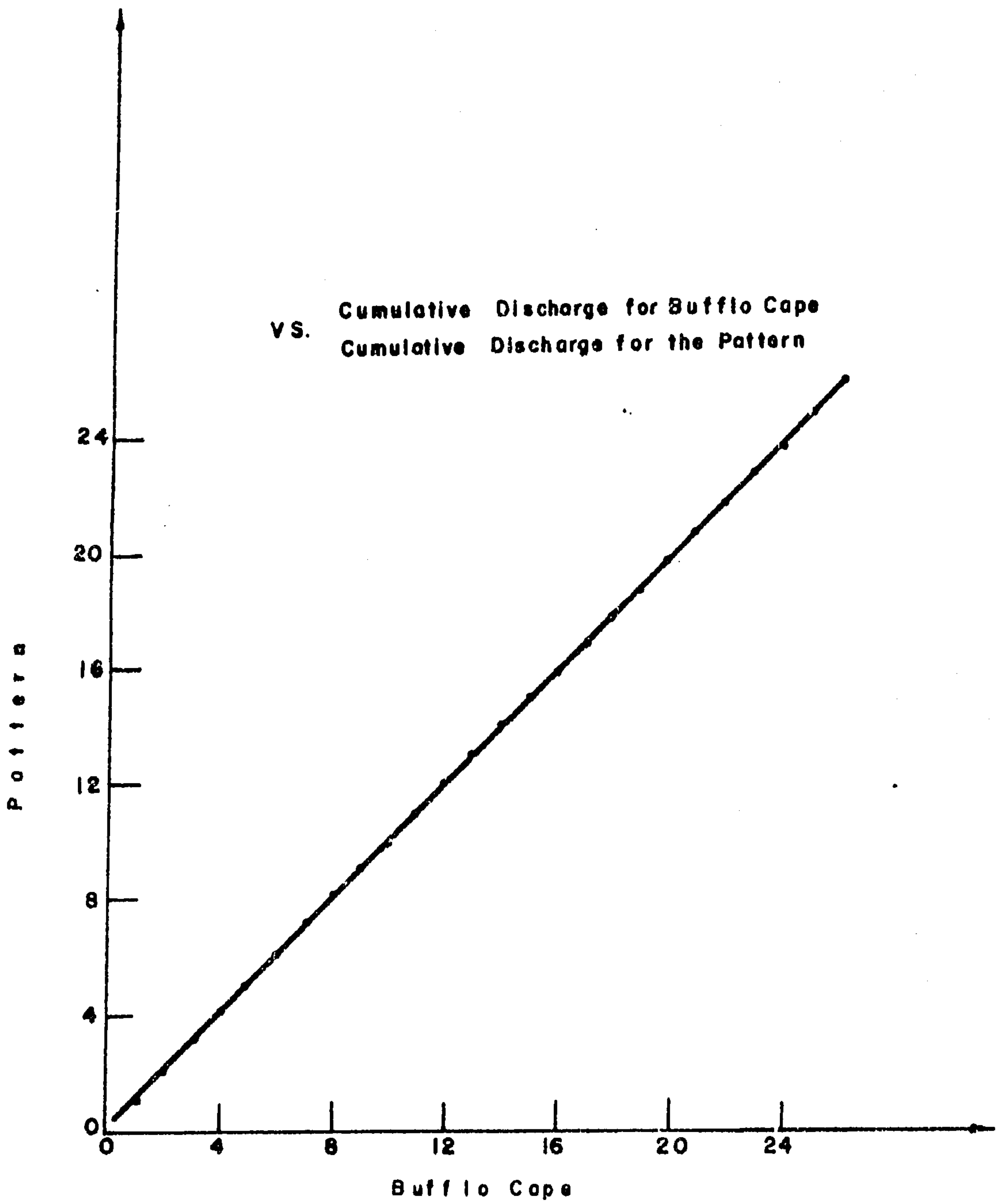

Fig. (A.14) DOUBLE MASS CU E ANALYSIS FOR STATION BUFFLO CAPE.